

**Phylogenetic Characterization of the Kinesin Superfamily
and Functional Analysis of PpKin14-Vs
in *Physcomitrella patens***

By

Zhiyuan Shen

A Thesis

Submitted to the Faculty

Of The

WORCESTER POLYTECHNIC INSTITUTE

In partial fulfillment of the requirements for the

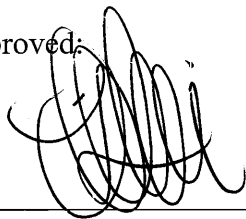
Degree of Master of Science

In

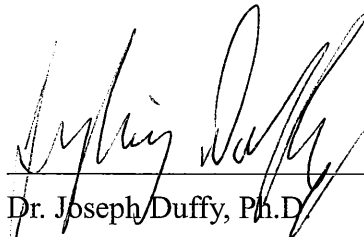
Biology & Biotechnology

Fall 2013

Approved:



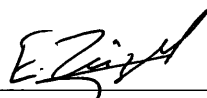
Dr. Luis Vidali, Ph.D.
Major Advisor - WPI



Dr. Joseph Duffy, Ph.D.
Committee Member & Department Head - WPI



Dr. Elizabeth Ryder, Ph.D.
Committee Member - WPI



Dr. Erkan Tüzel, Ph.D.
Committee Member - WPI

Abstract

Chloroplasts are organelles that convert light energy to chemical energy through photosynthesis. The movement of chloroplasts within the cell for the optimization of light absorption is crucial for plant survival. Cellular motor proteins and cytoskeletal tracks can facilitate transport of organelles. As an ancient superfamily of microtubule-dependent motors, kinesins participate in various cellular activities including cytokinesis, vesicle and organelle movements. Based on phylogenetic relationships and functional analysis, the kinesin superfamily has been subdivided into more than 14 families, most of which can be found in plants. With the ever increasing amount of genomic information, it is important and beneficial to systematically characterize and document kinesins within an organism. As a result of my collaborative work with other members of the Vidali lab, a detailed phylogenetic characterization of the 76 kinesins of the kinesin superfamily in the moss *Physcomitrella patens* is reported here. We found a remarkable conservation of families and subfamily classes with *Arabidopsis*, which is important for future comparative analyses of functions. Some of the families are composed of fewer members, while other families are greatly expanded in moss. To improve the comparison between species, and to simplify communication between research groups, we proposed a classification of subfamilies based on our phylogenetic analysis. As part of my efforts in studying chloroplasts motility, I investigated the function of two members of *Physcomitrella* kinesin family 14 class V proteins, Ppkin14-Va and -Vb. These two proteins are orthologs of the *Arabidopsis* KAC proteins which mediate actin-based chloroplast movement in *Arabidopsis thaliana*. In contrast, in the *Physcomitrella* both actin filaments (AFs) and microtubules (MTs) participate in chloroplast movement. Our results show that Ppkin14-Vs are important for maintaining chloroplast dispersion. They also function during chloroplast light avoidance responses via an AF-dependent, rather than MT-dependent mechanism. Although two Ppkin14-Vs do not act as MT-based motors, our phylogenetic study on moss kinesins provides an important source of information to track other potential kinesins that are predicted to move chloroplasts on MTs.

Acknowledgements

First of all, I would like to thank my advisor and committee member Dr. Luis Vidali for his consistent guidance, patience and enormous support during my graduate study. From you, Dr. Vidali, I not only learned how research is done, but also learned how to grow into a responsible, caring and humorous person. Your extraordinary passion in teaching and research will always inspire me.

I would also like to thank the rest of my graduate committee, Dr. Joseph Duffy, Dr. Elizabeth Ryder, and Dr. Erkan Tüzel, for their teaching, insightful conversations and precious suggestions toward finishing my degree. All four members on my committee, together with other faculty members from the Department of Biology and Biotechnology, have made my experience at WPI a special and rewarding one.

Without everyday support from and interactions with all previous and current members from the Vidali lab, I would not be able to present half of the work in this thesis. Special thanks go to Dr. Yen-Chun Liu who introduced me to the kinesin project reported here and who taught me research techniques and experimental designs with great patience. I would also like to thank Dr. Fabienne Furt, Angelo Robert Collatos, Jeff Bibeau, Luisanna Paulino, Erin Agar, Christopher Savoia, Xinxin Ding and Hao Sun for their support and encouragements.

I would like to thank Victoria Huntress from WPI Imaging Core for her support on the confocal microscope and the Tüzel group from WPI Physics Department, especially to Kyle Lemoi and Göker Arpağ. I would also like to thank all my peers in the Gateway Park life science building, especially to Ying Yang, Liwen Fei, Luca Issi, Alisha Perelta, Sarah Hernandez, Ally Grella, Denis Kole, Olga Kashpur, Melissa Walsh, Karen Tran, Prachi Gupta Wad, Harita Haridas, Charu Jain and Kathleen Wang. I would also like to thank my friends Wenqing Yu, Wei Wu, Zanzan Zhu, Xiaokong Yu and Wenhui Song for their support and encouragement that made my time in WPI memorable.

Last but not least, I would like to thank all my teachers and professors who enabled me to see the world on new horizons step by step. I am very thankful for the education I received from Underwood International College of Yonsei University, UC Davis and WPI. Words can never express how truly grateful and how lucky I am to have the love and support from my parents, my brother, my boyfriend and all my friends.

Table of Contents

| | |
|--|-----|
| Abstract | i |
| Acknowledgements | ii |
| Table of Contents | iii |
| List of Figures | iv |
| List of Tables | iv |
| Chapter 1 : Introduction | 1 |
| 1.1 Light Perception and Signal Transduction..... | 2 |
| 1.2 Motion System | 4 |
| 1.3 Methods and Approaches in Studying Chloroplast Movement | 7 |
| 1.4 Kinesin Superfamily | 8 |
| 1.5 Moss <i>Physcomitrella patens</i> as a Model Organism..... | 10 |
| Chapter 2 : Phylogenetic Analysis of the Kinesin Superfamily from <i>Physcomitrella patens</i> | 12 |
| Abstract | 13 |
| 2.1 Introduction..... | 14 |
| 2.2 Materials and Methods..... | 16 |
| 2.3 Results and Discussion | 21 |
| Acknowledgments..... | 51 |
| Chapter 3 : Functional Analysis of <i>Physcomitrella</i> Kinesin14-Vs | 52 |
| Abstract | 53 |
| 3.1 Introduction..... | 54 |
| 3.2 Material and Methods | 56 |
| 3.3 Results..... | 62 |
| 3.4 Discussion | 82 |
| Acknowledgements..... | 90 |
| Chapter 4 : Concluding Remarks | 91 |
| References..... | 94 |
| Appendix..... | 106 |
| Appendix File 1..... | 106 |
| Appendix File 2..... | 107 |

List of Figures

| | |
|---|----|
| Figure 1.1: Photoreceptors and signaling pathway for chloroplast movement..... | 3 |
| Figure 1.2: A model of chloroplast movement in <i>Arabidopsis thaliana</i> | 5 |
| Figure 2.1 : Kinesin 1s and armadillo repeat containing kinesins (ARKs). | 24 |
| Figure 2.2: Sub-region showing kinesin 2s and kinesin 4s..... | 27 |
| Figure 2.3: Gene models of kinesin 2s and 4s. | 28 |
| Figure 2.4: Kinesin 5s. | 30 |
| Figure 2.5: Sub-region showing kinesin 7s..... | 32 |
| Figure 2.6: Gene models of kinesin 7s..... | 33 |
| Figure 2.7: Sub-region showing kinesin 8s and kinesin 13s..... | 34 |
| Figure 2.8: Gene models of kinesin 8s and kinesin 13s..... | 35 |
| Figure 2.9: Kinesin 9s. | 36 |
| Figure 2.10: Sub-region showing kinesin 12s..... | 39 |
| Figure 2.11: Gene models of kinesin 12s..... | 40 |
| Figure 2.12: Sub-region showing kinesin 14s..... | 45 |
| Figure 2.13: Gene models of kinesin 14s..... | 46 |
| Figure 2.14: Sub-region showing kinesin 6s, 10s, 11s, and orphan kinesins. | 47 |
| Figure 2.15: Gene models of orphan kinesins. | 48 |
| Figure 3.1: Predicted gene models and common protein domains of PpKin14-Vs..... | 63 |
| Figure 3.2: Alignment of kinesin catalytic activities and MT-binding sites..... | 64 |
| Figure 3.3: PpKin14_Va+Vb knockdown phenotype..... | 68 |
| Figure 3.4: PpKin14-Vs mediate actin-dependent light avoidance response. | 71 |
| Figure 3.5: One phase exponential fit for chloroplast correlation coefficients..... | 72 |
| Figure 3.6: AF and MT dynamics measured by correlation coefficient decay..... | 76 |
| Figure 3.7: Two phase exponential fit for AF and MT correlation coefficients..... | 78 |
| Figure 3.8: MT dynamics measured manually by kymograph analysis. | 80 |
| Figure 3.9: Ppkin14-Vs in blue light response pathway | 87 |
| Figure 3.10: Ppkin14-Vs in the latest working model. | 88 |

List of Tables

| | |
|---|----|
| Table 2.1: Kinesin families and classes in <i>Physcomitrella patens</i> | 18 |
| Table 2.2: Kinesin families and functions in <i>Physcomitrella</i> and <i>Arabidopsis</i> | 22 |
| Table 3.1: Statistical analysis of chloroplast motility under cytoskeletal drug treatment | 74 |
| Table 3.2: Statistics on background noise comparison in AFs and MTs..... | 77 |
| Table 3.3: Statistical analysis of AF and MT correlation Coefficients..... | 78 |
| Table 3.4: Statistics on MT dynamics manually measured by kymographs..... | 81 |
| Table 4.1: PpKin14-Va &-Vb function summary..... | 93 |

Chapter 1 : Introduction

Chloroplasts are responsible to convert solar energy to chemical energy, which is essential to support life on earth. Similar to many other organelles, chloroplasts are precisely controlled in size, number, and location within a plant cell (Robertson and Leech, 1995; Oikawa et al., 2003; Sakamoto et al., 2008). For photosynthesizing plants, it is particularly important to control the positioning of chloroplasts, so that they can respond in time to various external stimuli such as light, chemicals, nutrients, and water (Suetsugu and Wada, 2009). Among those responses to external stimuli, light-induced chloroplast relocation is probably the most intensively studied (Wada, 2013). There are ecological advantages for plants precisely maintaining chloroplast movement (Kasahara et al., 2002). For example, chloroplast movement allows plants to adequately adapt to the constant changes in light levels resulting from earth's rotation, weather, seasons and different overlapping patterns between leaves.

The process of chloroplast photorelocation can be described in three general steps: light perception, signal transduction, and action responses through the motion system (Sato and Kadota, 2006; Suetsugu and Wada, 2009; Wada, 2013). In cells, photoreceptors perceive light stimulation, which induces signal transduction. Eventually the intracellular motion system, including the cytoskeleton and associated factors, enables the chloroplast to move toward a certain direction. These steps will be explained in more details in the following two sections. Additionally, methods used in studying chloroplast photorelocation, the kinesin superfamily, and *Physcomitrella patens* as a model organism will be summarized in separate sections.

1.1 Light Perception and Signal Transduction

The two main responses of chloroplasts to light levels are accumulation and avoidance responses. The accumulation response is induced by very low blue light ($\sim 450\text{nm}$) levels as low as $1.5 \mu\text{mol/m}^{-2}\text{s}^{-1}$ (Wada, 2013) and results in the accumulation of chloroplasts to the illuminated region of the cell. The avoidance response, which is faster (Kagawa and Wada, 1999; Yamashita et al., 2011), results in chloroplasts leaving the illuminated site and is induced by high intensity blue light ($\sim 450\text{nm}$) (for example $100 \mu\text{mol/m}^{-2}\text{s}^{-1}$) (Wada, 2013). The avoidance response in *Arabidopsis* has been shown to be important for plant survival (Kasahara et al., 2002).

Chloroplast motility has been extensively investigated in algae and land plants (Menzel and Schliwa, 1986; Kagawa et al., 2004). As early as 1908 Senn performed systematic observations on chloroplast movement responses to light conditions (Senn, 1908). In seed plants such as *Arabidopsis thaliana*, chloroplast photorelocation is induced by blue light only, while in mosses such as *Physcomitrella patens* and in the fern, chloroplast photorelocation can be induced by both blue and red light (Suetsugu and Wada, 2007b).

Blue and red light receptors perceive blue and red light respectively and result in subsequent responses along a signal transduction pathway. They work both independently and collaboratively to mediate chloroplast photorelocation movement. Blue light receptors called phototropins, responsible for phototropism, are also responsible for chloroplast photorelocation in seed plants. Red light receptors called phytochromes are also required for chloroplast photorelocation in mosses and ferns (**Figure 1.1**). Although known as a red light receptor, phytochrome also modulates blue

light induced chloroplast movement in *Arabidopsis* (DeBlasio et al., 2003; Luesse et al., 2010).

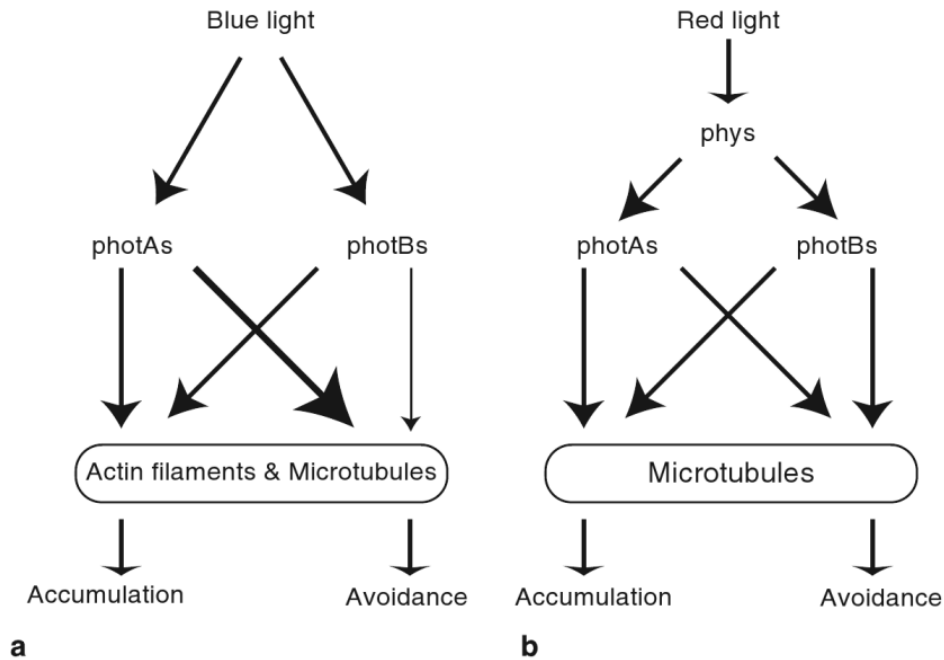


Figure 1.1: Photoreceptors and signaling pathway for chloroplast movement.

(a) In seed plants and *Physcomitrella patens*, under the blue light, both phototropinAs (photAs) and phototropinBs (photBs) mediate both accumulation and avoidance responses by utilizing both actin filaments and microtubules. photAs are essential for the avoidance response (thick arrow). (b) In *Physcomitrella patens*, under red light, four phytochromes (phys) absorb red light and utilize the phototropin-signaling pathways to mediate chloroplast movement utilizing microtubules. (Adapted from Figure 4 by Suetsugu., N. and M. Wada. (2009). Chloroplast Photorelocation Movement. The Chloroplast: Interactions with the Environment. A. S. S. H. Aronsson. Heidelberg, Germany, Springer. 13.)

There are two phototropins in *Arabidopsis* and in the fern *Adiantum capillus-veneris*, phot1 and phot2, the function of which is highly conserved across plant species. Both phot1 and phot 2 are required for the blue-light induced accumulation response, but phot2 is solely responsible for avoidance responses (Doi et al., 2004; Kagawa et al., 2004; Doi et al., 2006; Tsuboi et al., 2007; Kodama et al., 2008; Luesse et al., 2010). There are four phototropins classified into two groups (photA1, photA2, photB1 and photB2) in *Physcomitrella patens*. Both groups function in blue light induced response in

the moss, although photAs contribute more (Kasahara et al., 2004). Interestingly, phototropins in the moss can function downstream of phytochromes in response to red light because the red light response was greatly reduced in *photA2photB1photB2* triple disruptants (**Figure 1.1**) (Kasahara et al., 2004). Moreover, a chimeric photoreceptor consisting of both the phytochrome photosensory domain at the N-terminal and complete phototropin domains at the C-terminal was shown to mediate chloroplast photorelocation in the fern (Nozue et al., 1998).

In contrary to the extensive studies on photoreceptors, little is known about details in signal transduction pathways in chloroplast photorelocation. All we know so far is that the stimulation signal gets passed on to specific cytoskeletal components that will mediate the motion (**Figure 1.1**).

1.2 Motion System

The cytoskeleton contributes to cellular organization and structure, as well as intracellular traffic. The plant cytoskeleton consists of two major components: microtubules (MTs) and actin filaments (AFs). Both MTs and AFs are polymeric chain structures composed of globular protein subunits. In most cells of flowering plants, there are two kinds of AF structures, longitudinal arrays of thick actin bundles and randomly oriented thin AFs that extend from the bundles (Kandasamy and Meagher, 1999). In moss cells, AFs do not form as many bundles; instead, thin and very dynamic filaments are visible below the plasma membrane (Vidali et al., 2009). AFs, rather than MTs, have been shown to mediate chloroplast relocation in most plants studied so far, including seed plants and bryophytes. However, chloroplast movements in the moss *Physcomitrella patens* depend on both the AFs and MTs (Sato et al., 2001). These two cytoskeletal elements in moss can

potentially cooperate to fine-tune various light responses.

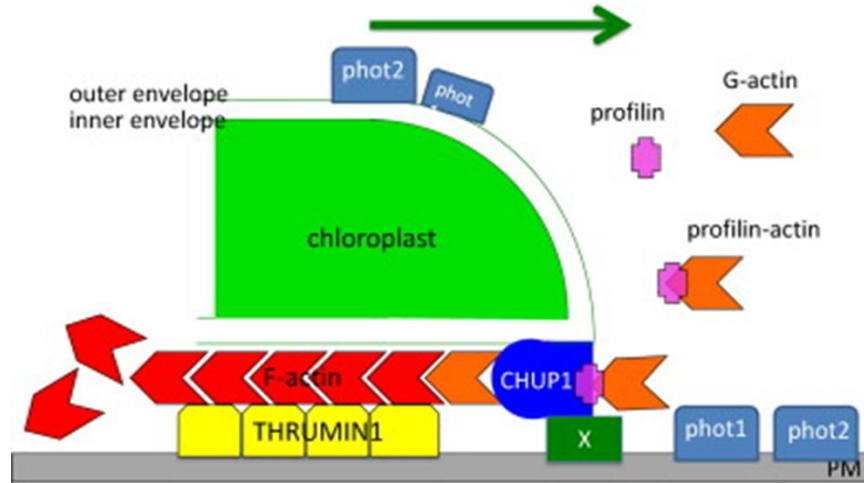


Figure 1.2: A model of chloroplast movement in *Arabidopsis thaliana*.

Model adapted from the latest chloroplast movement model in *Arabidopsis* (Wada, 2013). Both phot1 and phot2, which mediate the accumulation response, are localized at the plasma membrane (PM). phot2 on the chloroplast envelope likely mediates the avoidance response, because the amount of phot2 on the chloroplast envelope is very high comparing to that of phot1. Further, avoidance response was induced only when chloroplasts were illuminated with high light. CHUP1 binds to the chloroplast envelope via its N-terminus and may also be anchored to the plasma membrane through an unknown membrane-bound protein, X. CHUP1 recruits profilactin (profilin/actin complex) and polymerizes F-actin by inserting G-actin between itself and an existing F-actin filament. THRUMIN1 at the plasma membrane bundles the resulting F-actin filaments and fixes them to the plasma membrane as an anchor. Consequently, CHUP1 and the chloroplast are pushed by the inserted G-actin, generating the motive force for chloroplast photorelocation movement. Cp-actin filaments are depolymerized at the pointed end of actin filaments. The green arrow shows the direction of chloroplast movement.

In both *Arabidopsis* and *Physcomitrella*, actin-based motility was shown to be mediated by what appears to be short actin bundles that form at the moving front of the chloroplast (**Figure 1.2**) (Kadota et al., 2009; Yamashita et al., 2011; Wada, 2013). In *Arabidopsis* these bundles are believed to be formed by an actin bundling protein (THRUMIN1) that creates actin bundles at the illuminated region of the cell (Whippo et al., 2011). Additional proteins, such as Chloroplast Unusual Positional Protein 1 (CHUP1) (Oikawa et al., 2008; Usami et al., 2012) and other unknown proteins, possibly including two kinesin-like proteins (Suetsugu et al., 2010a), function to attach the

chloroplast to the plasma membrane. This actin-mediated mechanism is not well understood, but it does not seem to depend on myosin. Whether myosins are needed in chloroplast movement has been controversial, but recent studies support a myosin-independent mechanism because chloroplast photorelocation was not lost in myosin mutants in *Arabidopsis* (Suetsugu et al., 2010a).

CHUP1 mutants from both *Arabidopsis* and *Physcomitrella* result in aberrantly positioned chloroplasts and show severely impaired chloroplast photorelocation, although other organelles in the CHUP1 mutant show normal positioning, supporting an essential role of CHUP1 in chloroplast positioning and photorelocation (Kasahara et al., 2002; Oikawa et al., 2003; Oikawa et al., 2008; Usami et al., 2012). Mutant and biochemical studies in *Arabidopsis* suggest that CHUP1 has its N-terminal inserted on the chloroplast outer envelope, its C-terminal facing the cytosol, and its coiled-coil region anchored to the plasma membrane (Oikawa et al., 2008).

In addition to the above actin-mediated activities, a kinesin-like protein (KAC1) was isolated in a genetic screen for chloroplast motility in *Arabidopsis* (Suetsugu et al., 2010a). Previously, this protein had been shown to function in several cellular activities. It was demonstrated to bind to the Germinivirus movement protein (Kong and Hanley-Bowdoin, 2002), to katanin (Bouquin et al., 2003), and to the cell cycle protein CDKA1 (Geelen and Inze, 2001; Vanstraelen et al., 2004). Its function in chloroplast movement is novel to known functions of the protein. A second gene (*KAC2*) of high similarity to *KAC1* is also present in *Arabidopsis*. In the *kac1* mutant, the accumulation response was severely impaired and the avoidance response was slow. In the *kac1kac2* double mutant chloroplast photorelocation was lost and chloroplasts aggregation in the cell center was

observed. These results demonstrate that *KAC1* and *KAC2* are functionally equivalent. *KAC1* is expressed at a higher level than *KAC2*.

Another study on the orthologs of *AtKAC1* and *AtKAC2* in the ferns (*A. capillus-veneris* and *C. richardii*) and the moss *Physcomitrella* showed similar phenotypes (Suetsugu et al., 2012). In the fern *A. capillus-veneris*, knocking down *AcKAC1* using RNAi results in chloroplast aggregated at the side wall in the prothallial cell. Knocking down both *AcCHUPI* (*AcCHUPIA* and *AcCHUPIB*) genes results in the same phenotype. In addition, nuclei and mitochondria were also found with the chloroplast aggregations in the mutant. In the moss *Physcomitrella*, there are two orthologs to the *AtKACs*. Those two *PpKACs* are classified as kinesin14 class V from our recent phylogenetic study (Chapter 2) (Shen et al., 2012). They are functionally equivalent because only double knockout of *PpKACs* results in aggregated chloroplast in the center of gametophytic leaf cells and protonemal cells. *AcKAC1* C-terminal domain is not necessary for the chloroplasts to remain attached to the membrane in the fern *A. capillus-veneris*, but it is required in the case of the moss *Physcomitrella* (Suetsugu et al., 2012).

However, it is not clear where those two proteins are localized and how they function in maintaining chloroplast normal movement. Since both AFs and MTs are involved in chloroplast movement in the moss (Sato et al., 2001), it is important to elucidate through which cytoskeleton element those two kinesin-like proteins may act.

1.3 Methods and Approaches in Studying Chloroplast Movement

Eight methods to study the chloroplast movement have been summarized by a recent review (Wada, 2013). These methods are fixed-cell observation, green or white band assay, light transmittance, microbeam assay, movie analysis, Confocal Laser Scanning

Fluorescence (CLSF) microscopy, Total Internal Reflection Fluorescence (TIRF) microscopy and cryoelectron microscopy.

In addition to these observational methods, other significant advances are made possible because of the rapid development of molecular and cellular knowledge and technology. Identifying genetic-mapping-based mutants through phenotypic screening is a way that can be combined with the observational tools listed above to systematically identify genes and factors involved in the process of interest, in this case, chloroplast photorelocation (Suetsugu et al., 2010a).

RNA interference is another way of approaching the problem in a relatively fast and efficient manner compared with traditional knock-out methods. In the moss *Physcomitrella*, RNAi techniques have been well established and can rapidly generate knockdown mutants of a gene of interest (Bezanilla et al., 2003). DNAi is a similar technique to silence genes in ferns, except double-stranded DNA is used, instead of single-stranded RNA (Suetsugu et al., 2012).

1.4 Kinesin Superfamily

Organelle movement within the cell requires specific cellular motors and cytoskeletal tracks. In plant cells, microtubules (MTs) and actin filaments (AFs) are the two major components of the cytoskeleton which not only provides structural support, but also facilitates intracellular transport and cell division. Kinesins and dyneins are motors that move on MTs; myosins are the motors that move along AFs. Kinesins and myosins are found across eukaryotes, while cytoplasmic dyneins are missing in plants (Wickstead and Gull, 2007).

Kinesins and myosins share similarities in structure and movement. Their general

structure consists of head (motor), neck, and tail regions. Secondary structure topology evidence suggests that kinesins and myosins are derived from the same hypothetical common ancestor (Kull et al., 1998). Most kinesins and myosins form dimers, where the two motor heads bind to the cytoskeletal tracks and the motors move hand-over-hand toward a direction, similar to how one would climb along a rope. Both kinesin and myosin movements are powered by hydrolysis of ATP. There are also differences between them on how they function. Kinesins move along MTs while myosins move along AFs. There is a significant difference between the two kinds of motor proteins in terms of the rate-limiting step during the conversion of chemical energy to mechanical movement (Taylor, 1979; Ma and Taylor, 1995).

Specifically kinesins are an ancient superfamily of microtubule dependent motors. They participate in an extensive and diverse list of essential cellular functions, including mitosis, cytokinesis, cell polarization, cell elongation, flagellar development, and intracellular transport (Vale, 2003; Lee and Liu, 2004; Cai and Cresti, 2010; Zhu and Dixit, 2011a). Based on phylogenetic relationships, the kinesin superfamily has been subdivided into 14 families, which are represented in most eukaryotic phyla (Miki et al., 2001; Reddy and Day, 2001; Dagenbach and Endow, 2004; Lawrence et al., 2004). The functions of these families are sometimes conserved between species, but important variations in function across species have been observed. Plants possess most kinesin families including a few plant-specific families.

With the availability of an ever increasing number of genome sequences, including the moss *Physcomitrella patens*, it is important to document and compare the complete complement of kinesins present in various model organisms. This will help

develop a molecular framework to explore the function of each family using genetics, biochemistry and cell biology. Therefore we report a detailed phylogenetic characterization and classification of the 76 kinesins of the kinesin superfamily in *Physcomitrella*. This phylogenetic study on kinesins in *Physcomitrella* can also be used as a guiding map to screen potential kinesin motors that might move chloroplasts along MTs. From the phylogenetic tree we focus our scope on two kinesins from kinesin family 14 class V in *Physcomitrella* because kinesin14-V proteins in *Arabidopsis* have been shown to mediate actin-based chloroplast movement (Suetsugu et al., 2010a). To better understand the regulation of chloroplast relocation, it will be interesting to learn if the functions of the two moss kinesin14-Vs are conserved or different compared with their *Arabidopsis* homologs.

1.5 Moss *Physcomitrella patens* as a Model Organism

Used as a model organism since the last century, the moss *Physcomitrella patens* has emerged as a powerful model organism for genetics, developmental and metabolite studies, especially after its published genomic sequences and assembled genome maps (Knight and Perroud, 2001; Thornton et al., 2005; Rensing et al., 2008; Cove et al., 2009).

For instance, *Physcomitrella* can be easily cultured through vegetative propagation. It can grow on defined media with a relatively fast life cycle. Therefore it is an ideal candidate to be studied in a controlled environment to address biological questions. Its dominant haploid phase creates feasibility for both forward and reverse genetic analysis and for experimental techniques similar to those applied to microbes and yeasts. Although moss lacks vascular tissues, many signaling pathways found in

angiosperms are also present in the moss. In addition, about one-quarter of the moss genome contains unknown genes based on sequence motifs, providing the possibility of discovery for new gene functions (Cove et al., 2009). For example, the phototropins in the moss function to mediated blue light responses, which is consistent with discoveries in *Arabidopsis*; but also participate in red light responses, which is novel when compared to their function in *Arabidopsis* (Kasahara et al., 2004; Suetsugu and Wada, 2007a).

Physcomitrella can undergo highly efficient homologous recombination and RNA interference (more than 90% efficiency within 48 hours after transformation), making it an excellent system to perform functional genetic analysis (Bezanilla et al., 2003; Vidali and Bezanilla, 2012). For instance, in our study on two kinesin-like proteins, PpKin14-Va and -Vb, we use the published genome sequence information to generate a systematic view of kinesin 14s in *Physcomitrella*. Then we use targeted RNA interference in combination with an effective reporter system to specifically pinpoint the role of PpKin14Vs, which are genes of our interest.

Chapter 2 : Phylogenetic Analysis of the Kinesin Superfamily from *Physcomitrella patens*

Zhiyuan Shen, Angelo R. Collatos, Jeffrey P. Bibeau, Fabienne Furt, and Luis Vidali (2012). "Phylogenetic analysis of the Kinesin superfamily from *Physcomitrella*." *Front Plant Sci* 3: 230.

Keywords:

Phylogenetic analysis, kinesin, microtubule, moss, phragmoplast, gene knockout, intracellular motility, intracellular transport

Abstract

Kinesins are an ancient superfamily of microtubule dependent motors. They participate in an extensive and diverse list of essential cellular functions, including mitosis, cytokinesis, cell polarization, cell elongation, flagellar development, and intracellular transport. Based on phylogenetic relationships, the kinesin superfamily has been subdivided into 14 families, which are represented in most eukaryotic phyla. Plants possess most kinesin families including a few plant-specific families. With the availability of an ever increasing number of genome sequences from plants, it is important to document the complete complement of kinesins present in an organism where such information is available. This will help develop a molecular framework to explore the function of each family using genetics, biochemistry and cell biology.

The moss *Physcomitrella patens* has emerged as a powerful model organism to study gene functions in plants, which makes it a key candidate to explore complex gene families, such as the kinesin superfamily. Here we report a detailed phylogenetic characterization of the 76 kinesins in *Physcomitrella*. We found a remarkable conservation of families and subfamily classes with *Arabidopsis*, which is important for future comparative analyses of functions. Some of the families, such as kinesins 14s are composed of fewer members in moss, while other families, such as the kinesin 12s are greatly expanded. To improve the comparison between species, and to simplify communication between research groups, we propose a classification of subfamilies based on our phylogenetic analysis.

2.1 Introduction

Kinesins are a superfamily of microtubule dependent motors that are present in all eukaryotes (Richardson et al., 2006). The critical importance for cell function of this superfamily is highlighted by its existence and diversification in the last common ancestor of plants, animals, and fungi. The members of the various families of kinesins perform a multitude of functions, but they are all related by their conserved motor domain (Miki et al., 2005).

The kinesin motor domain, or head, comprises approximately 360 amino acids, and contains the ATPase and MT binding activities. The motor domain can be located either at the C-terminus, N-terminus, or in the middle of the molecule. In addition to the motor domain, most kinesins have a neck region that contains family specific features, a coiled-coil region that is important for dimerization, and a tail region that is thought to bind to specific cargo. The directionality of kinesin varies between families, and is sometimes correlated with the position of the motor. Although not all kinesin families have known directionality, in general members of the kinesin 1 and 2 families travel to the plus end of microtubules, while members of the kinesin 14 family travel toward the minus ends.

Because of the large size of the kinesin superfamily, it has been important to unify the nomenclature across phyla to allow comparative analyses of function. A standardized nomenclature was proposed by a special interest subgroup of the American Society of Cell Biology (ASCB), which has been broadly adopted (Lawrence et al., 2004). This nomenclature separates all major kinesins into 14 families. Kinesins that do not belong to any of these families are considered orphans, but most kinesins identified can easily be

assigned to a specific family. Together with the development of high throughput and next generation genomic sequencing, important efforts have taken place to use phylogenetic analysis and classification in diverse species ranging from unicellular to multicellular organisms to explore the large set of functions fulfilled by kinesins (Miki et al., 2005; Richardson et al., 2006).

In plants, kinesins have been implicated in a variety of cellular processes, including intracellular transport, spindle assembly, chromosome motility, phragmoplast assembly, MAP kinase regulation, and microtubule (MT) stability (Vale, 2003; Lee and Liu, 2004; Cai and Cresti, 2010; Zhu and Dixit, 2011a). Plants contain almost all the kinesin families. Plants also contain specific kinesin families (Richardson et al., 2006), including kinesins important for flagellar development that are only present in plants with motile sperm, such as ferns and mosses (this study). Occasionally, the function of some members of a family does not appear to be conserved with its animal and fungal counterparts.

The kinesin content has been determined in various plants. Reddy and co-workers identified 61, 52, 41 and 45 kinesins in *Arabidopsis*, poplar, and 2 cultivars of rice, respectively (Richardson et al., 2006), while the red algae *Cyanidioschizon merolae* contains only 5 kinesins and the green algae *Chlamydomonas reinhardtii* 23 (Reddy and Day, 2001; Richardson et al., 2006). However, the full set of kinesins in basal land plants has yet to be investigated.

The moss *Physcomitrella patens* is a simple plant model organism that allows precise genetic manipulations and provides easy access to cells for high resolution microscopy (Cove, 2005). This makes it an ideal model system to study the participation

of the MT cytoskeleton in many different processes. Surprisingly, only two kinesins, KINID1a and KINID1b, hereafter called Pp-KinesinOrph-IIa and Pp-KinesinOrph-IIb, have been studied in *Physcomitrella* and have been shown to be essential for the generation of interdigitated antiparallel MT in the phragmoplast (Hiwatashi et al., 2008). This highlights the need to have a complete inventory of the multitude of kinesins present in this organism to help perform future functional analysis. With an available genome sequence (Rensing et al., 2008) it is now possible to document all the kinesins present in this organism. In the present work, we perform a phylogenetic analysis of 76 kinesins from *Physcomitrella*, identified from their conserved motor domain.

2.2 Materials and Methods

Kinesin motor domain sequences were identified by BLAST against the cosmos.org version 1.6; the 6th annotation of the *Physcomitrella* first genome assembly (Rensing et al., 2008), and the protein sequences were identified from predicted gene models. A total of 76 sequences were identified (**Table 2.1**), the head domain was extracted from the sequences by alignment comparison with a template based on the kinesin 1 head domain (Uniprot: P33176).

For phylogenetic comparison, the sequences were imported into Vector NTI Advance 11.5.1 (Invitrogen), and an alignment was generated using its AlignX program. The basic algorithm from AlignX is ClustalW; we maintained the default parameters as follows: gap opening penalty: 10, gap extension penalty: 0.05, gap separation penalty range: 8, percent identity for alignment delay:40. The alignment was further improved by identifying the members of each family of kinesins using the fast neighbor distance-based algorithm from AlignX, and aligning the groups separately. The assignment to specific

families was very consistent for the majority of the sequences identified. This was done to remove possible minor errors (Appendix File 1) in the gene models, which were in general present at a low frequency. For the final alignment, the protein sequences of all the motor domains from all the families were used and the sequence for the globular tail domain of *Physcomitrella*'s myosin XIa (Uniprot:D6R266) was used as an outgroup.

Once a satisfactory alignment was completed, the alignment file was imported to Geneious [Biomatters Ltd.], where a tree was constructed using the plugin PhyML that applies the Maximum Likelihood method (Guindon et al., 2010). We maintained the default parameters as follows: substitution model: LG, proportion of invariable sites: 0-fixed, number of substitution rate categories: 1, no optimization, and a 1000 bootstrap resampling value. To help identify the various family groups, a representative member from human and all *S. pombe* and *S. cerevisiae* kinesins were included in the alignment. In addition, the complete collection of the *Arabidopsis* kinesins was included for comparison.

Our preliminary trees constructed with the neighbor joining algorithm available in AlineX from Vector NTI Advance resulted in similar topologies for most classes. Furthermore, in the majority of the families, the human representative sequence is present, providing good support to our alignment and tree building strategy. In the tree that we present here, only nodes showing more than 50% bootstrap support are indicated, and the bootstrap support is shown.

We have used a nomenclature based, when available, on the kinesin family name designated by a number (Lawrence et al., 2004), followed by a class number (indicated by roman numerals) (**Table 2.1**). To identify individual members of the classes we used

letters in the case of *Physcomitrella* and numbers in the case of *Arabidopsis* in order to avoid possible future confusion when the classes are monophyletic and no clear orthologues are present between species.

| Table 2.1: Kinesin families and classes in <i>Physcomitrella patens</i> | | |
|--|--------------------|--------------------------|
| kinesin family | Gene name | gene ID (Phypa_#) |
| kinesin ARK (n=5) | Pp-KinesinARK-a | 455498 |
| | Pp-KinesinARK-b | 453488 |
| | Pp-KinesinARK-c | 425827 |
| | Pp-KinesinARK-d | 427907 |
| | Pp-KinesinARK-LIKE | 446331 |
| kinesin 2 (n=1) | Pp-Kinesin02 | 425592 |
| kinesin 4 (n=8) | Pp-Kinesin04-Ia | 437833 |
| | Pp-Kinesin04-Ib | 438737 |
| | Pp-Kinesin04-Ic | 432365 |
| | Pp-Kinesin04-Id | 453193 |
| | Pp-Kinesin04-Ie | 441211 |
| | Pp-Kinesin04-IIa | 447296 |
| | Pp-Kinesin04-IIb | 433281 |
| | Pp-Kinesin04-IIc | 446183 |
| kinesin 5 (n=4) | Pp-Kinesin05-a | 457162 |
| | Pp-Kinesin05-b | 447260 |
| | Pp-Kinesin05-c | 425536 |
| | Pp-Kinesin05-d | 423604 |

Table 2.1. Kinesin families and classes in *Physcomitrella patens*

| kinesin family | Gene name | gene ID (Phypa_#) |
|-----------------------|------------------|--------------------------|
| kinesin 7 (n=7) | Pp-Kinesin07-Ia | 447411 |
| | Pp-Kinesin07-Ib | 437231 |
| | Pp-Kinesin07-IIa | 458197 |
| | Pp-Kinesin07-IIb | 432536 |
| | Pp-Kinesin07-IIc | 454208 |
| | Pp-Kinesin07-III | 426030 |
| | Pp-Kinesin07-IV | 452429 |
| kinesin 8 (n=3) | Pp-Kinesin08-Ia | 453903 |
| | Pp-Kinesin08-Ib | 424121 |
| | Pp-Kinesin08-Ic | 458481 |
| kinesin 9 (n=3) | Pp-Kinesin09-Ia | 458410 |
| | Pp-Kinesin09-Ib | 425498 |
| | Pp-Kinesin09-Ic | 428375 |
| kinesin 12 (n=18) | Pp-Kinesin12-Ia | 444072 |
| | Pp-Kinesin12-Ib | 440218 |
| | Pp-Kinesin12-Ic | 442090 |
| | Pp-Kinesin12-Id | 437562 |
| | Pp-Kinesin12-Ie | 434464 |
| | Pp-Kinesin12-If | 432190 |
| | Pp-Kinesin12-Ig | 432169 |
| | Pp-Kinesin12-Ih | 454564 |
| | Pp-Kinesin12-Ii | 432906 |
| | Pp-Kinesin12-Ij | 445541 |
| | Pp-Kinesin12-Ik | 422406 |
| | Pp-Kinesin12-Il | 431567 |
| | Pp-Kinesin12-Im | 453302 |
| | Pp-Kinesin12-In | 426336 |
| | Pp-Kinesin12-Io | 437642 |
| | Pp-Kinesin12-IIa | 422514 |
| | Pp-Kinesin12-IIb | 422285 |
| | Pp-Kinesin12-IIc | 440124 |
| kinesin 13 (n=3) | Pp-Kinesin13-Ia | 427794 |
| | Pp-Kinesin13-Ib | 438664 |
| | Pp-Kinesin13-Ia | 456175 |

| Table 2.1. Kinesin families and classes in <i>Physcomitrella patens</i> | | |
|--|--------------------|--------------------------|
| kinesin family | Gene name | gene ID (Phypa_#) |
| kinesin 14 (n=15) | Pp-Kinesin14-Ia | 439730 |
| | Pp-Kinesin14-Ib | 438782 |
| | Pp-Kinesin14-IIa | 430601 |
| | Pp-Kinesin14-IIb | 439319 |
| | Pp-Kinesin14-IIc | 436987 |
| | Pp-Kinesin14-IId | 441550 |
| | Pp-Kinesin14-IIIA | 459874 |
| | Pp-Kinesin14-IIIB | 424496 |
| | Pp-Kinesin14-IV | 435249 |
| | Pp-Kinesin14-Va | 437825 |
| | Pp-Kinesin14-Vb | 435597 |
| | Pp-Kinesin14-VIa | 439249 |
| | Pp-Kinesin14-VIb | 450599 |
| | Pp-Kinesin14-VIc | 428061 |
| | Pp-Kinesin14-VId | 458819 |
| kinesin orphans (n=9) | Pp-KinesinOrph-Ia | 457477 |
| | Pp-KinesinOrph-Ib | 453299 |
| | Pp-KinesinOrph-IIa | 436446 |
| | Pp-KinesinOrph-IIb | 430757 |
| | Pp-KinesinOrph-III | 441202 |
| | Pp-KinesinOrph-IVa | 431083 |
| | Pp-KinesinOrph-IVb | 451243 |
| | Pp-KinesinOrph-IVc | 437822 |
| | Pp-KinesinOrph-IVd | 453297 |

Note: The gene ID can be used to retrieve genes from www.cosmoss.org. From the pull down menu under "genome" in the homepage, select "sequence retrieval" and type in the format of "Phypa_#", for example, "Phypa_453297". This should lead you to the gene that the specific Phypa number designates.

2.3 Results and Discussion

In the following sections we report our findings on the number and class of kinesins for each subfamily and when possible discuss their predicted function based on comparison to other similar kinesins (**Table 2.2**). A clear kinesin 1 member is not present in *Physcomitrella*, but interestingly kinesin 1 members are present in *Arabidopsis* and other seed plants (Richardson et al., 2006; Zhu and Dixit, 2011a). Because of their similarity with kinesin 1s, we decided to start our report with the Armadillo Repeat containing Kinesins (ARK), and we decided to not include them in the orphan section since they are well conserved across plants and can be clearly identified as a separate group. We were also not able to unequivocally assign moss proteins to families 3, 6, 10 and 11; a more detailed discussion about this is presented in the last section concerning orphan kinesins.

ARK Kinesins

This kinesin family is characterized and classified by the armadillo repeat motifs found within the protein's C-terminal domain. Armadillo repeats are comprised of a repeating sequence of forty-two amino acids (Coates, 2003). This sequence contains three alpha helices; upon repetition these helices form a right handed super helix (Coates, 2003). Typically, these repeats are associated with cell signaling and the cytoskeleton. In *Arabidopsis*, it has been speculated that the armadillo regions bind to target proteins to aid in their MT based transport (Coates, 2003). Additionally, loss of function analysis of armadillo kinesins in *Arabidopsis* root hairs suggests that these proteins may play a significant role in AF and MT organization during polarized cell growth (Yang et al., 2007; Sakai et al., 2008).

Table 2.2: Kinesin families and functions in *Physcomitrella* and *Arabidopsis*

| Family | Function | Number in <i>Physcomitrella</i> | Number in <i>Arabidopsis</i> |
|-------------------------------|--|---------------------------------|------------------------------|
| <u>ARK</u> | | <u>5</u> | <u>3</u> |
| Class I | Polarized growth | 4 | 3 |
| ARK-LIKE(Class II) | unknown | 1 | - |
| <u>Kinesin 1</u> | <u>Vesicle trafficking</u> | - | <u>1</u> |
| <u>Kinesin 2</u> | <u>Flagella</u> | <u>1</u> | - |
| <u>Kinesin 4</u> | <u>Cellulose deposition</u> | <u>8</u> | <u>3</u> |
| Class I | | 5 | 3 |
| Class II | | 3 | - |
| <u>Kinesin 5</u> | <u>Cell division</u> | <u>4</u> | <u>4</u> |
| <u>Kinesin 7</u> | | <u>7</u> | <u>14</u> |
| Class I | Organelle Transport | 2 | 5 |
| Class II | Cytokinesis | 3 | 7 |
| Class III | Kinetochores Capture | 1 | 1 |
| Class IV | Kinetochores Capture | 1 | 1 |
| <u>Kinesin 8</u> | <u>Unknown in plants</u> | <u>3</u> | <u>2</u> |
| Class I | | 2 | 1 |
| Class II | | 1 | 1 |
| <u>Kinesin 9</u> | | <u>3</u> | - |
| <u>Kinesin 10</u> | | - | <u>2</u> |
| <u>Kinesin 12</u> | | <u>18</u> | <u>6</u> |
| Class I | Phragmoplast | 15 | 3 |
| Class II | Phragmoplast | 3 | 3 |
| <u>Kinesin 13</u> | <u>Golgi location</u> | <u>3</u> | <u>2</u> |
| <u>Kinesin 14</u> | | <u>15</u> | <u>21</u> |
| Class I | Cell division | 2 | 4 |
| Class II | Cytoskeleton linkage | 4 | 9 |
| Class III | | 2 | 3 |
| Class IV | | 1 | 2 |
| Class V | Chloroplast photorelocation | 2 | 2 |
| Class VI | Cytoskeleton Organization | 4 | 1 |
| <u>Orphan Kinesins</u> | <u>Regulatory proteins or pseudogenes</u> | <u>9</u> | <u>2</u> |
| Class I | | 2 | - |
| Class II | | 2 | 1 |
| Class III | | 1 | - |
| Class IV | | 4 | 2 |
| Total | | 76 | 60 |

Note: Proteins from family 14 class V are highlighted in green. They are involved in chloroplast movement in *Arabidopsis* and their function in *Physcomitrella* will be discussed in chapter 3.

Phylogenetic analysis based on the motor domain indicates that there are five sequences in *Physcomitrella* related to the *Arabidopsis* armadillo repeat containing kinesins (**Figure 2.1A**). Four of these sequences are closely related to each other, forming a monophyletic group and their gene models show the presence of armadillo repeats (**Figure 2.1B**); we classified these as class I. The gene model for the fifth sequence is lacking the armadillo repeats that would confirm its identity as an armadillo repeat containing kinesin (**Figure 2.1B**); we tentatively classified this single kinesin as ARK-Like since the tree topology fails to confirm this kinesins as an orthologue of the lone At-kinesin01. But it is intriguing that a very short gene model is also a landmark of this *Arabidopsis* kinesin 1. (Richardson et al., 2006)

It will be interesting to investigate if the participation of armadillo repeat containing kinesins in cell polarization that has been documented in *Arabidopsis* (Yang et al., 2007; Sakai et al., 2008), is also conserved in mosses, which provide an excellent model system to study cell polarization and tip growth. Furthermore, comparative analysis of loss of function phenotypes may help understand how this family of molecules functions in the cell.

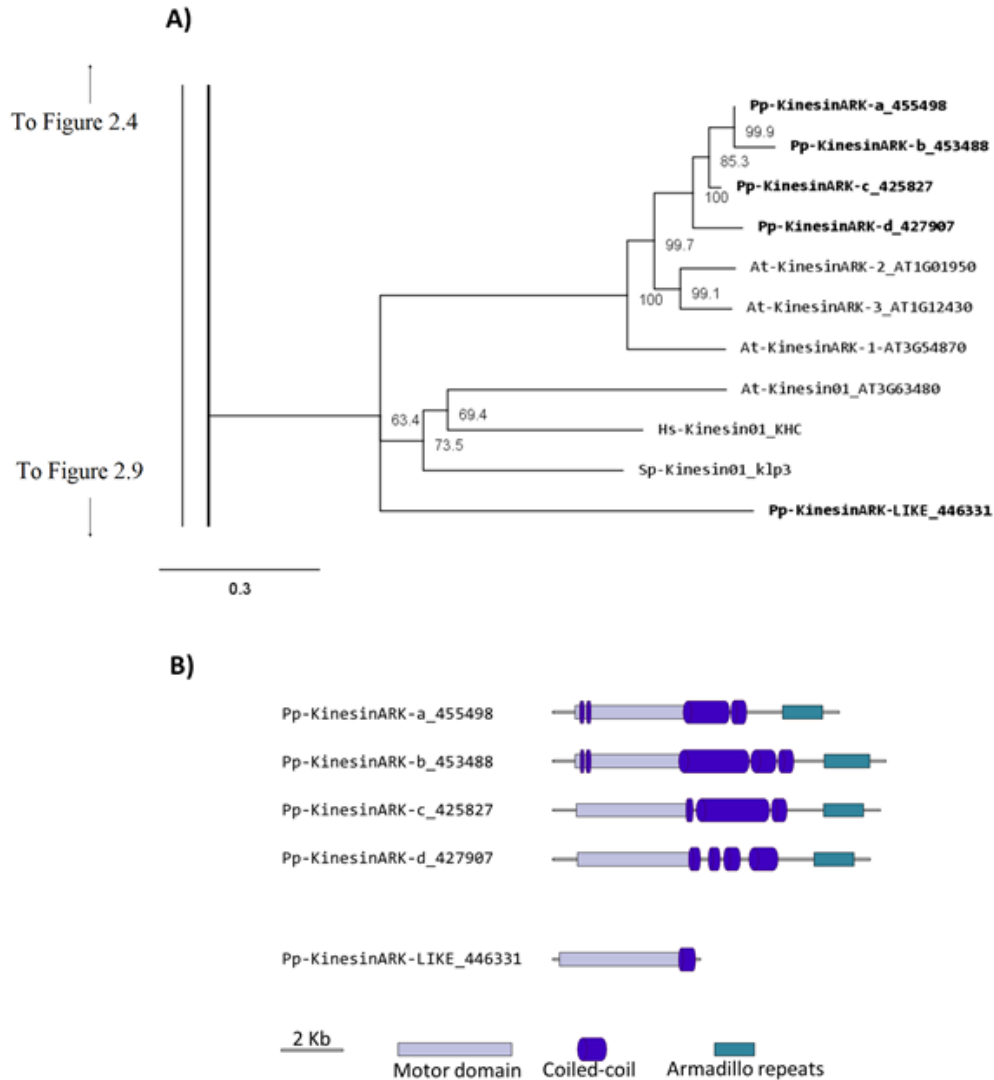


Figure 2.1 : Kinesin 1s and armadillo repeat containing kinesins (ARKs).

(A) Sub-region of the phylogenetic tree based on their motor domain showing kinesin 1s and armadillo repeat containing kinesins (ARKs). The amino acid sequences of the motor domain were aligned using ClustalW and the phylogenetic tree was constructed using the maximum likelihood method (PhyML) and a 1000 bootstrap resampling value. Numbers on the nodes show the statistical support of values above 50%. The scale shows the estimated branch length corresponding to the number of substitutions per site. The *Physcomitrella* numbers correspond to the Phypha number uniquely associated with each gene model (version 1.6) at cosmos.org. **(B)** Gene models of kinesin 1s and ARKs. Schematic diagrams showing the structure and domain architecture of kinesin 1s and armadillo repeat containing kinesins (ARKs). Domains are indicated at the bottom of the diagrams. Armadillo repeats are comprised of forty-two amino acids that can form helices which upon repetition form a right handed super helix.

Kinesin 2

Kinesin 2s have previously been shown to be involved in neuronal organelle transport (Yamazaki et al., 1995; Setou et al., 2000), meiosis in spermatogenesis (Wang et al., 2010), and intraflagellar transport (Sloboda and Howard, 2007). One of the common characteristics of kinesin 2s is their ability to create both homo and heterodimers (Rashid et al., 1995). However, in the case of *Physcomitrella patens*, there is only one kinesin 2 present (**Figure 2.2**), and therefore it will only homodimerize, unless it can associate with a different kinesin. The protein itself is relatively short, containing two short coiled coils, and one large coiled coil (**Figure 2.3A**). In *Physcomitrella* this protein is likely to participate in the *de novo* formation of flagella during spermatogenesis. Consistently, kinesin 2s are absent in *Arabidopsis* and other seed plants which do not have flagella.

Kinesin 4

This family is comprised of members that can bind to chromosomes in animals and are absent in budding and fission yeasts (Miki et al., 2005; Richardson et al., 2006). In animals, they are present in the nucleus as well as in the cytoplasm and they have been implicated in organelle and chromosomal transport (Miki et al., 2005). In plants, a member of this family was initially identified as a protein important for orienting cellulose microfibrils (FRA1). A mutation of the protein results in a fragile cell wall phenotype in *Arabidopsis* (Zhong et al., 2002); a similar mutant was also isolated in rice (Zhang et al., 2010). In addition, the rice kinesin was found to be nuclear and cytoplasmically localized, and surprisingly it functions as a DNA binding protein important for gibberillin biosynthesis and cell elongation (Li et al., 2011). Single

molecule analysis revealed that this molecule has unusually high processivity, suggesting a function in long-distance transport (Zhu and Dixit, 2011b).

Our phylogenetic analysis of kinesin 4s in *Physcomitrella* shows two well-defined classes (**Figure 2.2**), with class I clustering with the *Arabidopsis* kinesin 4s, including FRA1. Based on the available gene models, the five members of class I can be further subdivided into two classes, with Pp-kin04-Id and Pp-kin04-Ie having smaller C-terminal domains (**Figure 2.3B**). Class II is formed by three members, without counterparts in the *Arabidopsis* genome (**Figure 2.2**). This suggests the possibility that this class might carry out a function that is not present in seed plants. It would be interesting to determine whether the class I kinesin 4s have conserved a function in organizing the cell wall components in *Physcomitrella*, and whether both classes evolved similar or different functions.

It is interesting to note that there is an expanded collection of the kinesin 4s in *Physcomitrella* compared to *Arabidopsis*, the significance of this expansion remains to be elucidated.

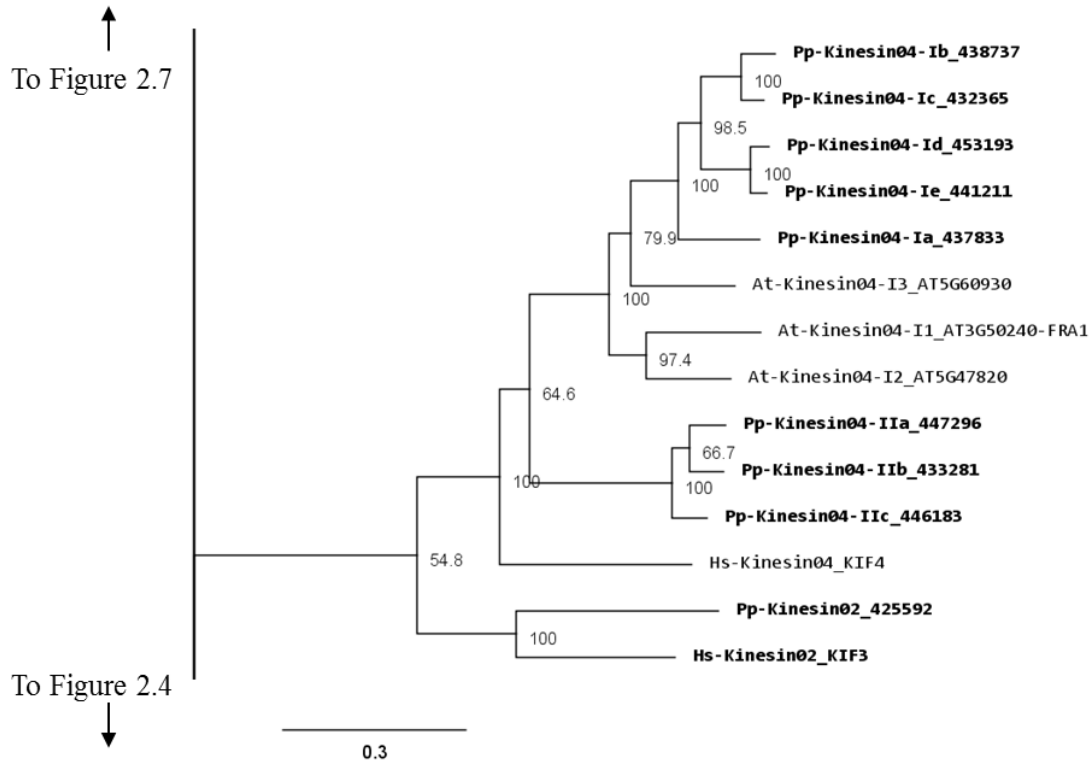


Figure 2.2: Sub-region showing kinesin 2s and kinesin 4s.

Sub-region of the phylogenetic tree based on their motor domain showing kinesin 2s and kinesin 4s. The amino acid sequences of the motor domain were aligned using ClustalW and the phylogenetic tree was constructed using the maximum likelihood method (PhyML) and a 1000 bootstrap resampling value. Numbers on the nodes show the statistical support of values above 50%. The scale shows the estimated branch length corresponding to the number of substitutions per site. The *Physcomitrella* numbers correspond to the Phypha number uniquely associated with each gene model (version 1.6) at cosmoss.org

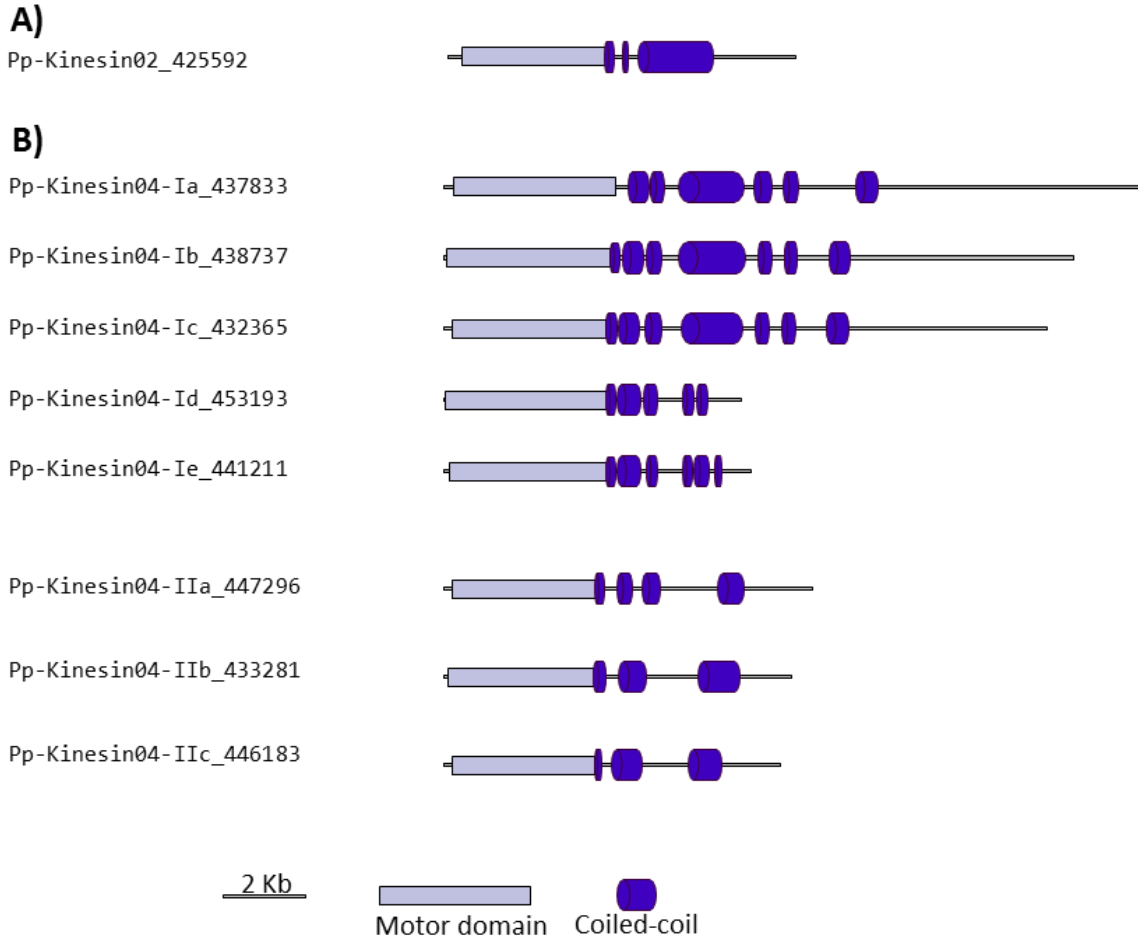


Figure 2.3: Gene models of kinesin 2s and 4s.

Schematic diagrams showing the structure and domain architecture of **A)** kinesin 2s and **B)** kinesin 4s. Domains are indicated at the bottom of the diagrams.

Kinesin 5

Kinesin 5s are tetrameric kinesins important for spindle organization and mitosis (Ferenz et al., 2010). In yeast, null mutants display division phenotypes such as delayed anaphase, larger cells, and abnormal spindle morphology (Hagan and Yanagida, 1992; Straight et al., 1998). This family spans multiple kingdoms as it is found in mammals, fungi, and plants (Miki et al., 2005; Richardson et al., 2006; Bannigan et al., 2008). Using a conditional loss of function approach, a similar but expanded function has been documented in plants, where one member of this family in *Arabidopsis* (AtKRP125c)

was found to be important for spindle and cortical MT organization (Bannigan et al., 2007).

In *Physcomitrella*, there are four kinesin 5 members, which cluster as a monophyletic group (**Figure 2.4A**). Based on their gene models, they have a very similar structure (**Figure 2.4B**). We anticipate that these kinesins will perform similar functions to their *Arabidopsis*, animal, and fungal counterparts. Nevertheless, it is interesting that a mutation in only one of the four genes of *Arabidopsis* results in an altered growth phenotype (Bannigan et al., 2007), suggesting a degree of specialization in some of the kinesin 5s in *Arabidopsis*. Future functional analyses of the four moss isoforms will help clarify whether a similar type of specialization is present or absent in *Physcomitrella*.

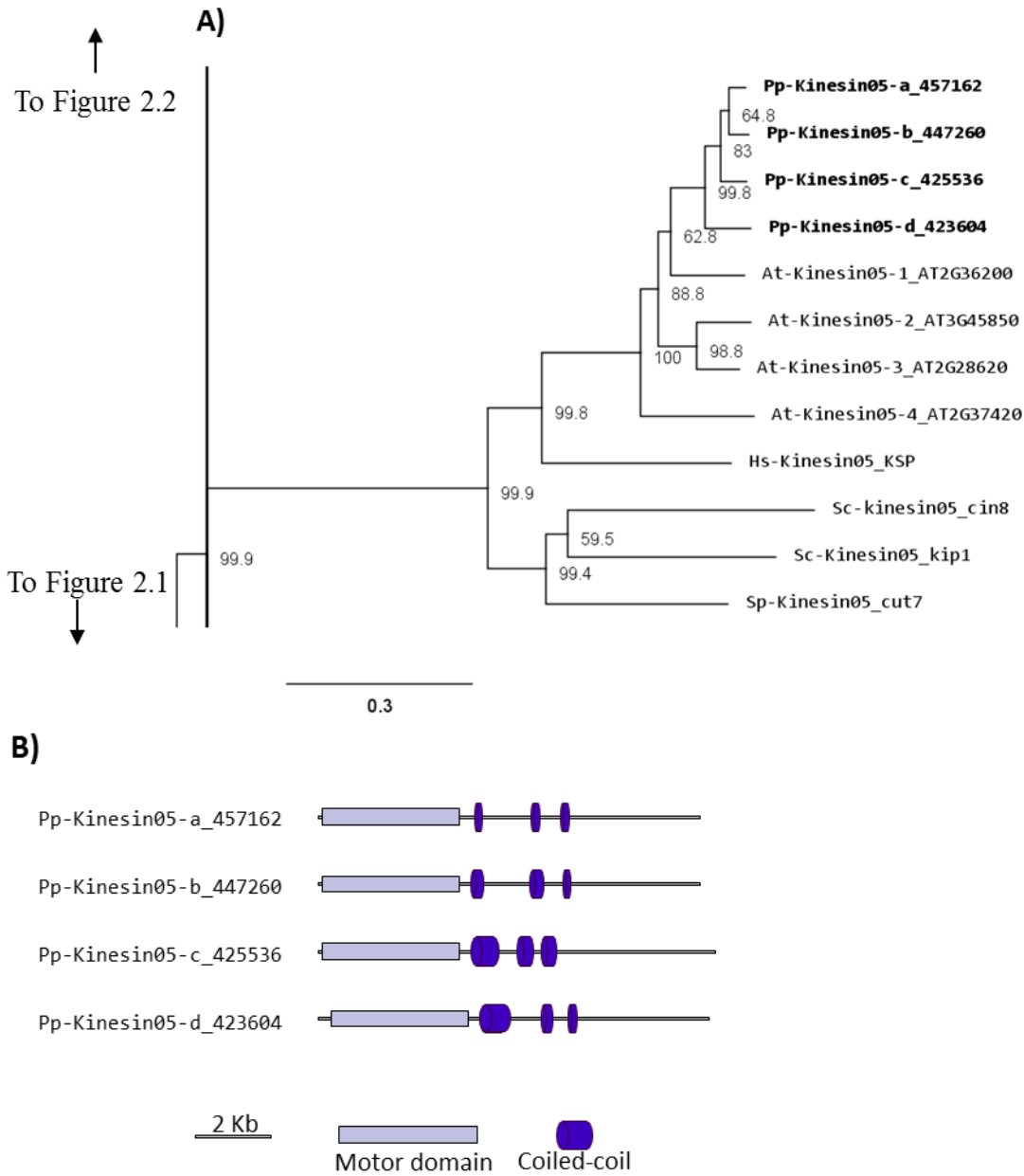


Figure 2.4: Kinesin 5s.

(A) Sub-region of the phylogenetic tree based on their motor domain showing kinesin 5s. The amino acid sequences of the motor domain were aligned using ClustalW and the phylogenetic tree was constructed using the maximum likelihood method (PhyML) and a 1000 bootstrap resampling value. Numbers on the nodes show the statistical support of values above 50%. The scale shows the estimated branch length corresponding to the number of substitutions per site. The *Physcomitrella* numbers correspond to the Phypha number uniquely associated with each gene model (version 1.6) at cosmoss.org. (B) Gene models of kinesin 5s. Schematic diagrams showing the structure and domain architecture of kinesin 5s. Domains are indicated at the bottom of the diagrams.

Kinesin 7

Members of the kinesin 7 family have been implicated in the transport of chromosomes and nuclear migration in animal and yeast (Miki et al., 2005). This family is greatly expanded in *Arabidopsis* with 14 members (Richardson et al., 2006; Zhu and Dixit, 2011a). Functional analysis of some of its members has shown a participation in cell division. For example, loss of function of AtNACK1 and AtNACK2 results in inhibition of cytokinesis (Tanaka et al., 2004; Takahashi et al., 2010); a similar phenotype was found in rice, when the expression of the single OsNACK gene is reduced in a leaky mutant (Sazuka et al., 2005). Other members of this family have a mitochondrial signaling sequence, but their function has yet to be investigated (Itoh et al., 2001).

Our phylogenetic analysis shows a smaller size for this family in *Physcomitrella* with 7 members compared with *Arabidopsis* (**Figure 2.5**); nevertheless the classes found seem to be conserved between species. We identified four classes, with class I containing the MKRP-related kinesins, that could be associated with organelles (Itoh et al., 2001). *Physcomitrella* has only two representatives for this class, compared with five for *Arabidopsis*. Class II has three representatives in *Physcomitrella*, compared with seven in *Arabidopsis*. The moss class II kinesin 7s seem to represent an independent monophyletic group with no specific clustering to the *Arabidopsis* subgroups. Unfortunately this makes it difficult to clearly define a functional orthologue to the well-characterized NACK kinesins (Tanaka et al., 2004; Takahashi et al., 2010; Sasabe et al., 2011), and further functional analysis will be needed to determine whether the moss class II kinesin 7s are also involved in cytokinesis.

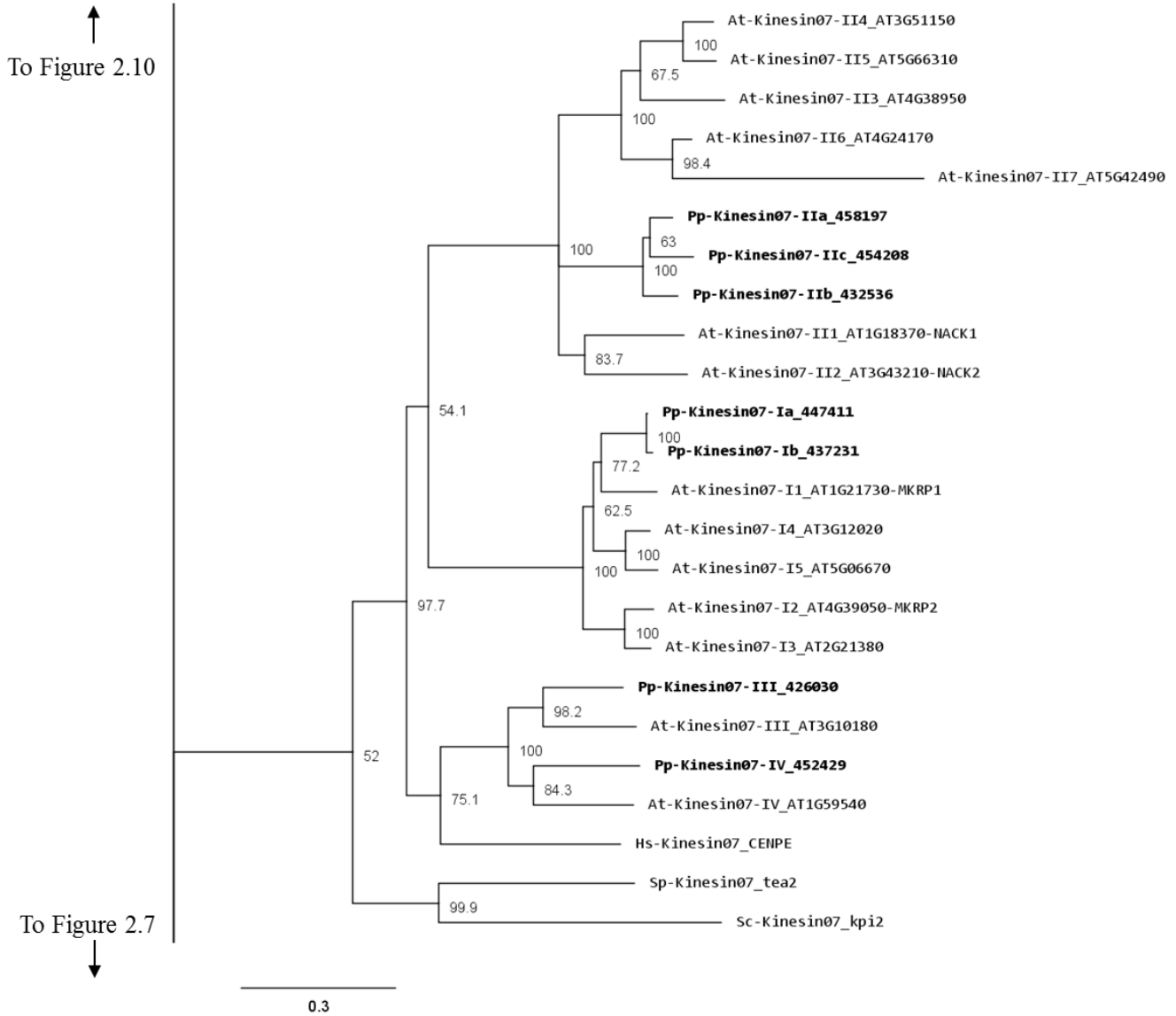


Figure 2.5: Sub-region showing kinesin 7s.

Sub-region of the phylogenetic tree based on their motor domain showing kinesin 7s. The amino acid sequences of the motor domain were aligned using ClustalW and the phylogenetic tree was constructed using the maximum likelihood method (PhyML) and a 1000 bootstrap resampling value. Numbers on the nodes show the statistical support of values above 50%. The scale shows the estimated branch length corresponding to the number of substitutions per site. The *Physcomitrella* numbers correspond to the Phypa number uniquely associated with each gene model (version 1.6) at cosmos.org.

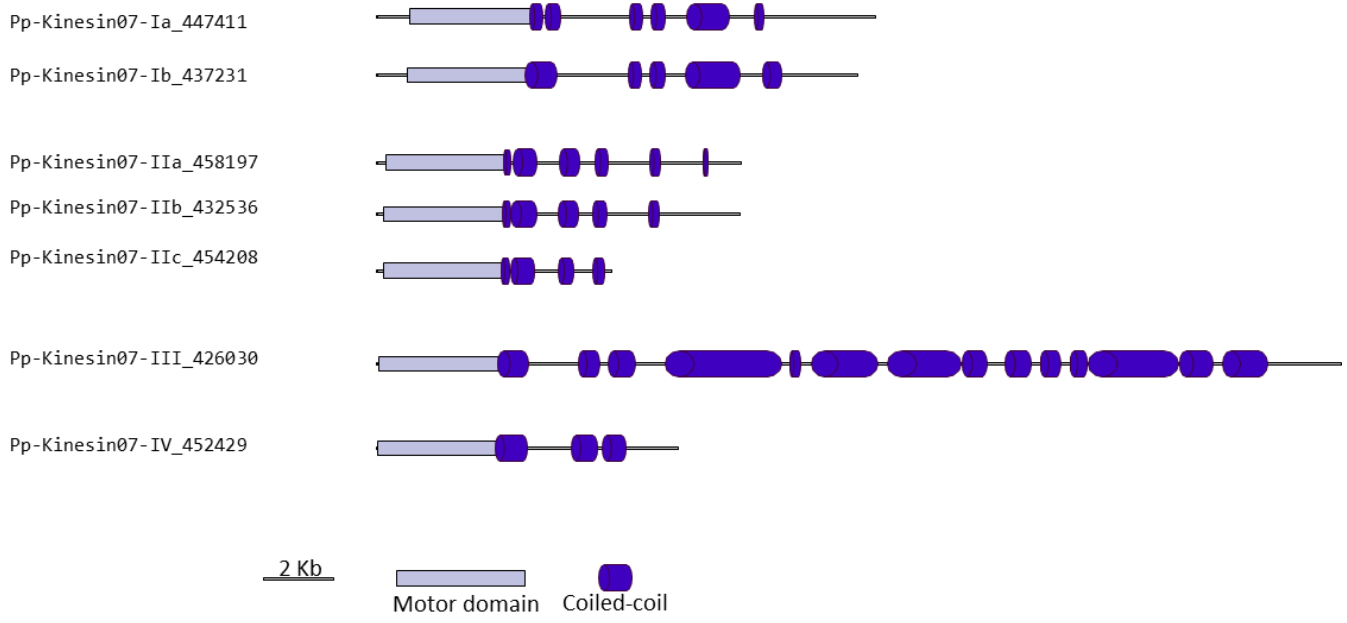


Figure 2.6: Gene models of kinesin 7s.

Schematic diagrams showing the structure and domain architecture of kinesin 7s. Domains are indicated at the bottom of the diagrams.

Classes III and IV are closely related at the motor domain level (**Figure 2.5**), but their C-terminal domains are very different, with class III containing a much longer coiled coil rich domain (**Figure 2.6**). Interestingly, orthologues exist for both classes in *Arabidopsis*, an indication that the common ancestor of mosses and vascular plants contained these two classes. These classes are more closely related to CENPE and may share some of its function on kinetochore capture (Weaver et al., 2003).

Kinesin 8

Although nothing is known about kinesin 8s in plant systems, significant research has been conducted on these kinesins in animal and fungi. Some of the group's functions include mitochondrial transport in *Drosophila*, mitotic chromosome segregation in yeast, and MT destabilization in humans (Miki et al., 2005; Peters et al., 2010). Our phylogenetic analysis indicates that there are two kinesin 8 classes for both moss and

Arabidopsis (**Figure 2.7**). Of these two, class I contains a single *Arabidopsis* kinesin and two moss kinesins; class II contains a single moss and *Arabidopsis* kinesin. The gene model for the moss class II kinesin shows an extended N-terminal domain (**Figure 2.8A**). Because of their similarity to other kinesin 8 members from animals and fungi, we anticipate these kinesins will have a conserved function. Nevertheless, the existence of two orthologue genes in plants suggests that diversification of function was already present, to some degree, in the last common ancestor of bryophytes and vascular plants.

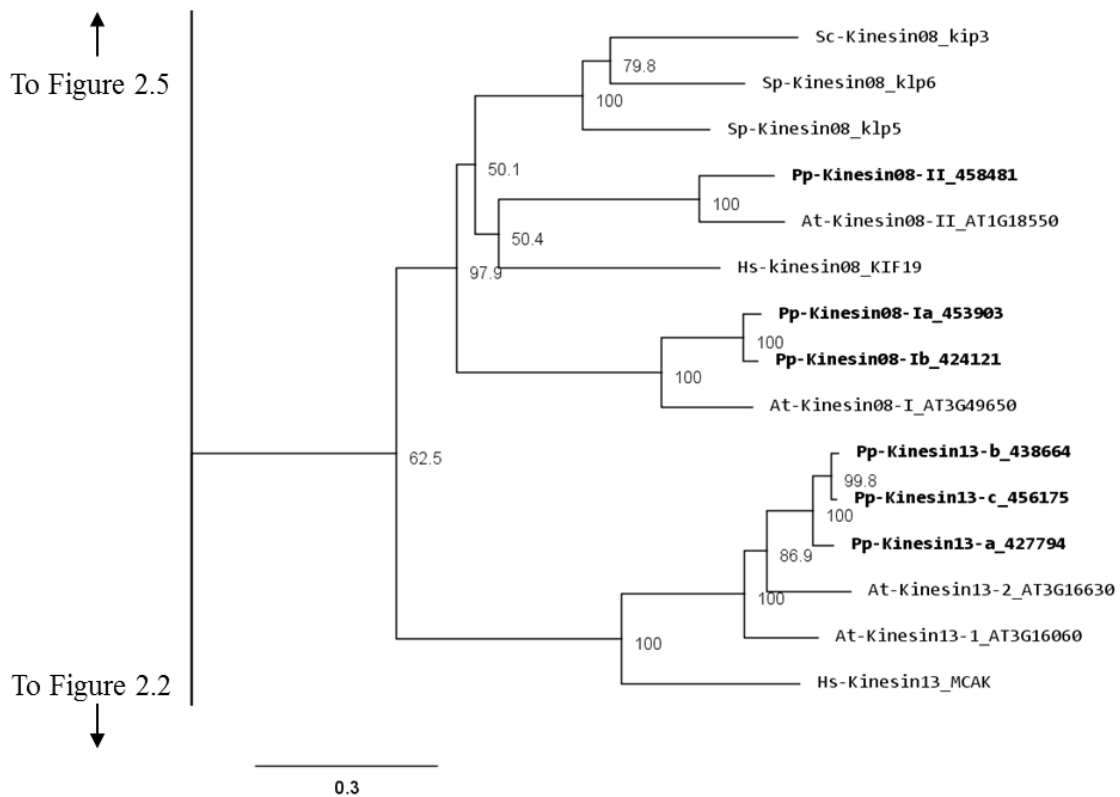


Figure 2.7: Sub-region showing kinesin 8s and kinesin 13s.

Sub-region of the phylogenetic tree based on their motor domain showing kinesin 8s and kinesin 13s. The amino acid sequences of the motor domain were aligned using ClustalW and the phylogenetic tree was constructed using the maximum likelihood method (PhyML) and a 1000 bootstrap resampling value. Numbers on the nodes show the statistical support of values above 50%. The scale shows the estimated branch length corresponding to the number of substitutions per site. The *Physcomitrella* numbers correspond to the Phypa number uniquely associated with each gene model (version 1.6) at cosmos.org.

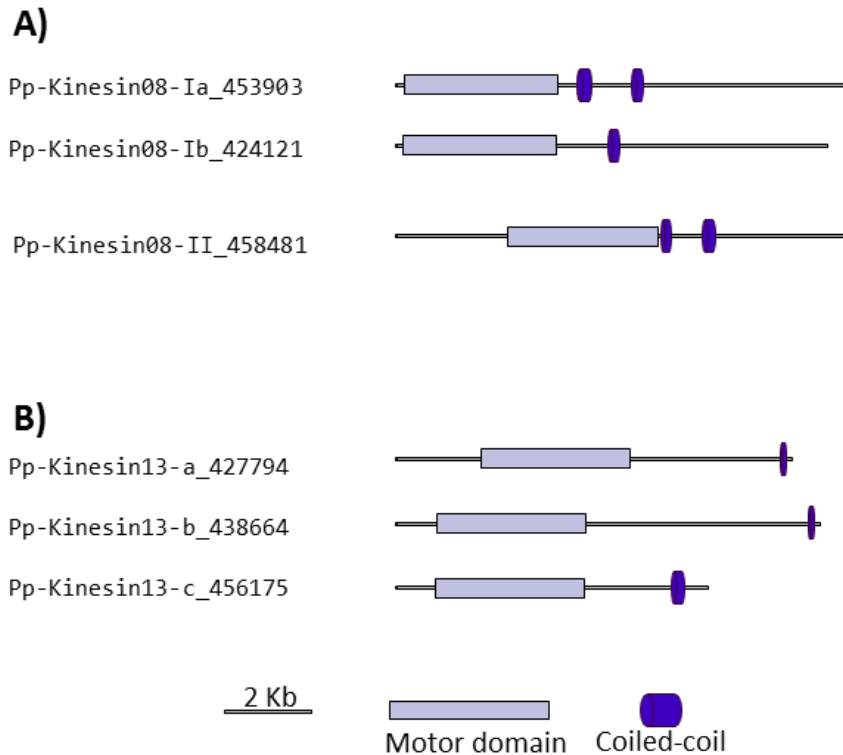


Figure 2.8: Gene models of kinesin 8s and kinesin 13s.

Gene models of **A)** kinesin 8s and **B)** kinesin 13s. Schematic diagrams showing the structure and domain architecture of kinesin 8s and 13s. Domains are indicated at the bottom of the diagrams.

Kinesin 9

Kinesin 9s have been implicated in flagella regulation, structure, and construction (Bernstein et al., 1994; Yokoyama et al., 2004; Demonchy et al., 2009), and consistent with this function, they are absent in flowering plants, yeast, and invertebrates (Richardson et al., 2006). Our phylogenetic analysis identified three kinesin 9s in *Physcomitrella* (**Figure 2.9A**). Two of the three gene models found in the cosmos.org database (Pp-Kinesin09-b and c) seem to be inaccurate because of some abnormal insertions and gaps are present when compared to other kinesin 9 sequences. The genomic sequences corresponding to the questionable regions were examined in more detailed and it was found that some exons are not present in the latest proteome version in

cosmoss.org (version 1.6) and that some introns were incorrectly spliced (Appendix File 1). We were not able to determine if additional problems exist in the gene models of the regions after the motor domain, which due to reduced conservation are harder to identify and their detailed description is beyond the scope of this manuscript. Similarly to kinesin 2 (Sloboda and Howard, 2007), we anticipate kinesin 9s will participate in the *de novo* assembly of flagella during spermatogenesis in moss.

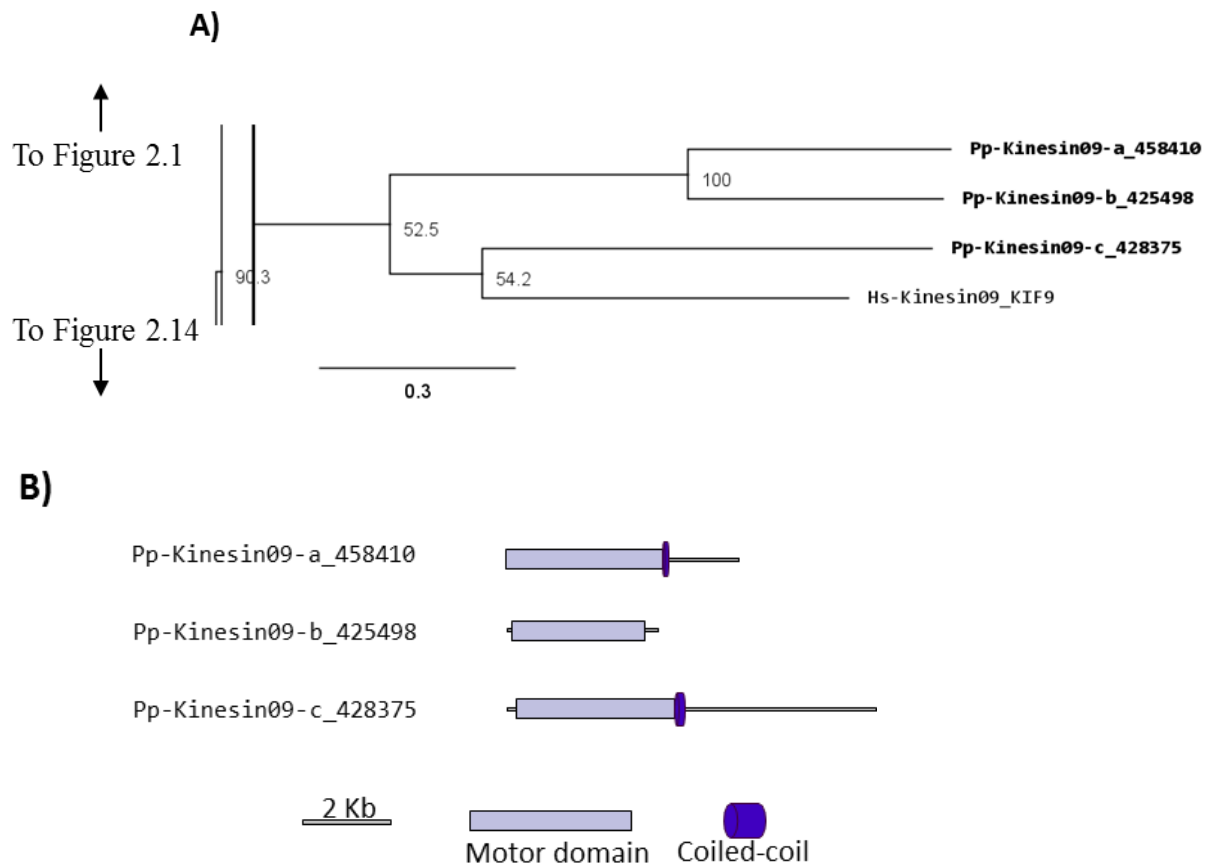


Figure 2.9: Kinesin 9s.

(A) Sub-region of the phylogenetic tree based on their motor domain showing kinesin 9s. The amino acid sequences of the motor domain were aligned using ClustalW and the phylogenetic tree was constructed using the maximum likelihood method (PhyML) and a 1000 bootstrap resampling value. Numbers on the nodes show the statistical support of values above 50%. The scale shows the estimated branch length corresponding to the number of substitutions per site. The *Physcomitrella* numbers correspond to the Phypha number uniquely associated with each gene model (version 1.6) at cosmoss.org. (B) Gene models of kinesin 9s. Schematic diagrams showing the structure and domain architecture of kinesin 9s. Domains are indicated at the bottom of the diagrams.

Kinesin 10

The kinesin 10 family members are commonly referred as “Kid” in human (Tokai et al., 1996) and “KIF 22” in mouse (Yang et al., 1997). They have been suggested to be involved in spindle formation and chromosome movement.(Miki et al., 2005). It is notable that members of the kinesin 10 family, which are present in *Arabidopsis* (2 members) are absent in *Physcomitrella* (**Figure 2.14**). Although PAKRP2 has been sometimes grouped in the kinesin 10 family (Richardson et al., 2006; Zhu and Dixit, 2011a), it is more appropriate to be classified as an orphan kinesin based on our analysis (**Figure 2.14**). A detailed discussion about this classification can be found at the section for orphan kinesins below. The presence of orthologues of the *Arabidopsis* kinesin 10s in other basal plant species may provide clues about essential developmental processes present in a common ancestor but lost in mosses.

Kinesin 12

In animals, kinesin 12s have been implicated in bipolar spindle assembly (Rogers et al., 2000; Tanenbaum et al., 2009) and neuron development and axon growth (Liu et al., 1996; Buster et al., 2003). In plants, kinesin 12s have been found to be involved in phragmoplast organization and orientation (Lee and Liu, 2000; Pan et al., 2004; Muller et al., 2006) . In general, kinesin 12s have an N-terminus head with a long C-terminus tail abundant in coiled-coils (Miki et al., 2005).

Our phylogenetic analysis shows two classes of kinesins 12s; class I kinesin 12s, which are related to the phragmoplast orienting kinesins or POKs (Muller et al., 2006), and class II kinesin 12s, which are related to the phragmoplast-associated kinesin 1s or PAKRP1s (**Figure 2.10**). We found a surprisingly large number of class I kinesin 12s in

Physcomitrella: a total of 18 genes, compared with only three in *Arabidopsis*. Some of the gene models corresponding to regions after the motor domain seem to be incomplete, but the majority of the class I sequences show long C-terminal domains with abundant coiled coils (**Figure 2.11**). The significance of this large number of kinesins is not understood and presents a challenging problem due to the likelihood of functional redundancy between its members. Nevertheless, due to their similarity to *Arabidopsis* POKs, these proteins are probably important for phragmoplast orientation. In contrast to the large number of class I kinesins 12s, there are only three class II kinesin 12s in *Physcomitrella*, forming a monophyletic group (**Figure 2.10**). The gene models for these kinesins show very similar C-terminal structures with abundant coiled coil structures, but not of the large magnitude of the ones present in class I (**Figure 2.11**). Again, we anticipate that these kinesins will play a similar role in phragmoplast organization as that of their *Arabidopsis* counterparts.

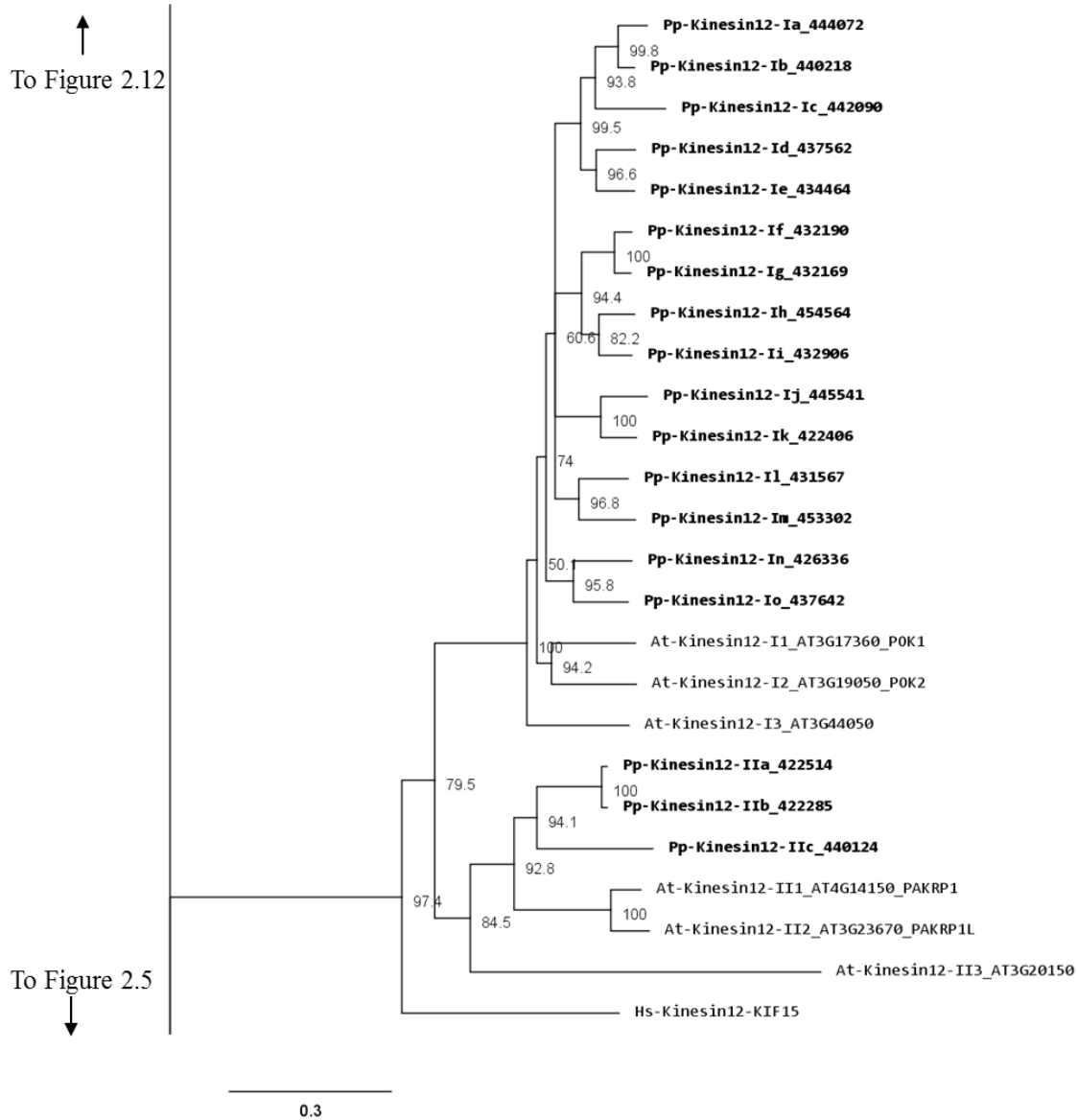


Figure 2.10: Sub-region showing kinesin 12s.

Sub-region of the phylogenetic tree based on their motor domain showing kinesin 12s. The amino acid sequences of the motor domain were aligned using ClustalW and the phylogenetic tree was constructed using the maximum likelihood method (PhyML) and a 1000 bootstrap resampling value. Numbers on the nodes show the statistical support of values above 50%. The scale shows the estimated branch length corresponding to the number of substitutions per site. The *Physcomitrella* numbers correspond to the Phypha number uniquely associated with each gene model (version 1.6) at cosmos.org.

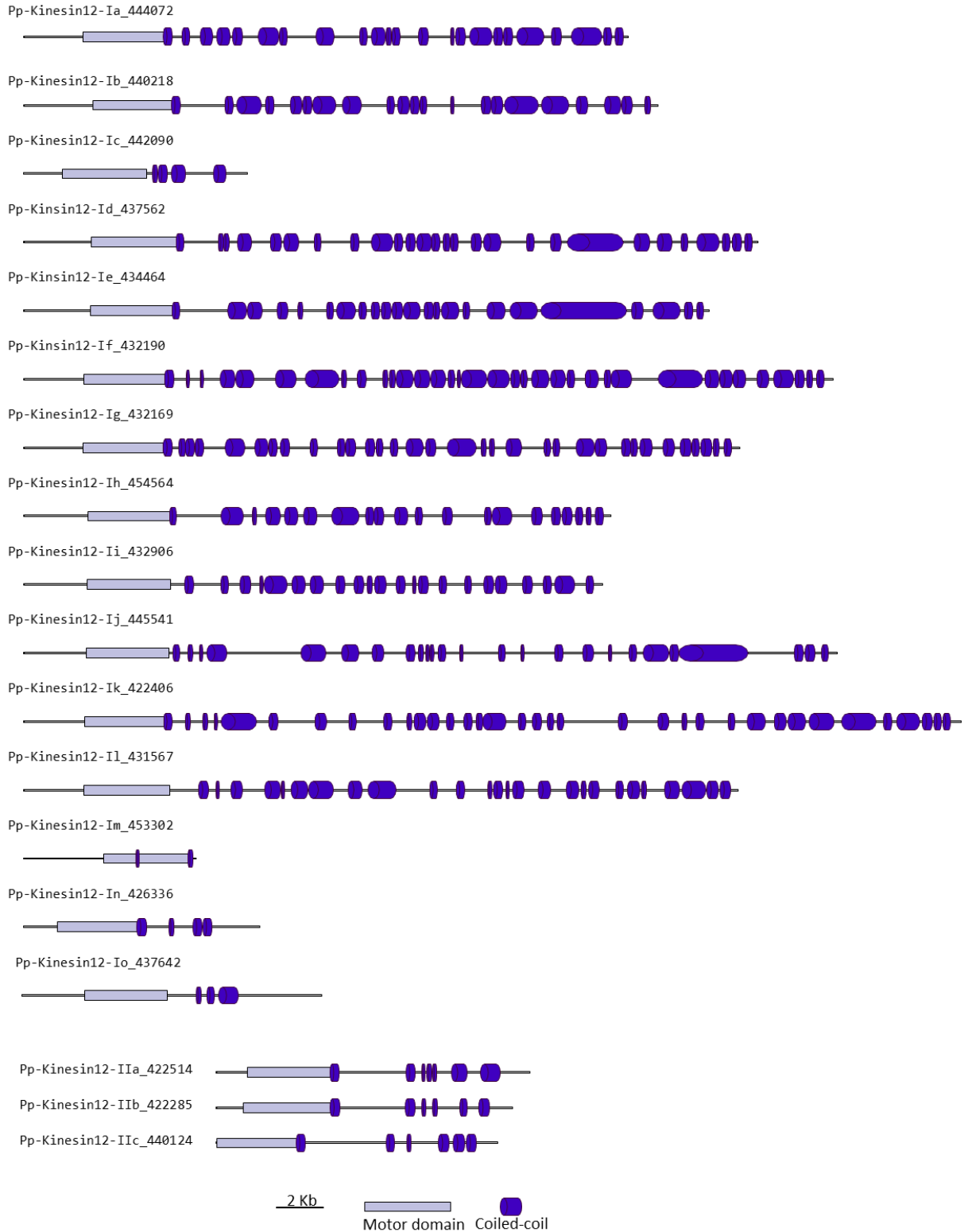


Figure 2.11: Gene models of kinesin 12s.

Schematic diagrams showing the structure and domain architecture of kinesin 12s. Domains are indicated at the bottom of the diagrams.

Kinesin 13

Similar to kinesin 8s, the animal kinesin 13s have been reported to destabilize MT and to function in intracellular transport (Miki et al., 2005). Although both plant and animal kinesin 13s share similar motor domain sequences, the kinesin 13s in plants do not have a lysine-rich neck domain present in animal kinesin 13s (Lee and Liu, 2004). The absence of this structural motif suggests that the plant kinesins may have a different function than their animal counterparts (Lee and Liu, 2004). Consistently, the *Arabidopsis* kinesin13-2, which has been shown to be associated with Golgi stacks, provides further evidence that plant kinesin 13s may differ from animal kinesin 13s in functionality (Lu et al., 2005).

Our phylogenetic analysis shows that in *Arabidopsis* there are two kinesin 13s while in *Physcomitrella*, there are three kinesin 13 members, which cluster as a monophyletic group (**Figure 2.7**). Based on their gene models, the moss kinesin 9s have a very similar structure (**Figure 2.8B**). Interestingly, for the three moss kinesin 9s, the sole coiled coil region is located at the extreme C terminus of the molecule away from the motor domain; while in most of the kinesins, the coiled-coil regions are generally closer to the motor domain (**Figure 2.8B**). It would be interesting to determine whether this structural characteristic is important for the function of these kinesins. The *Arabidopsis* kinesin-13-2 is closely related to those found in moss (**Figure 2.7**), which suggests possible functional conservation between the *Arabidopsis* kinesin13-2 and all the moss kinesin 13s.

Kinesin 14

Members of this family have been associated with functions in re-arrangement of the MT arrays at various stages of the cell cycle as well as in organelle transport (Miki et al., 2005; Richardson et al., 2006; Zhu and Dixit, 2011a). Kinesin 14s were initially divided in two groups, kinesin 14A and kinesin 14B, according to their structure and function (Miki et al., 2005). However, this family is vastly expanded in plants with 21 and 15 members in *Arabidopsis* and *Physcomitrella*, respectively, compared to 4 in humans (Richardson et al., 2006). In addition, the fact that plant kinesins 14 display some specific structural motifs prompted us to propose a new classification for the plant kinesin 14s, divided in 6 different classes (**Figure 2.12**).

Class I kinesin 14s are related to KIFC1 which is associated with the nuclear membrane in mammalian cells and is important for acrosome biogenesis and possibly for vesicle transport (Yang and Sperry, 2003; Yang et al., 2006; Nath et al., 2007), and to Kar3p which is essential for nuclear fusion during mating in *Saccharomyces cerevisiae*, by mediating MT sliding (Meluh and Rose, 1990). Among the 4 homologues present in *Arabidopsis* (**Figure 2.12**), ATK1 and ATK5 have been well studied. They share similar functions during mitosis by controlling the MT organization at the cortex, the preprophase band, the spindle and the phragmoplast, and ATK1 also play a major role in male meiosis (Liu et al., 1996; Chen et al., 2002; Marcus et al., 2003; Ambrose et al., 2005; Ambrose and Cyr, 2007). Interestingly, ATK5 possesses a second, ATP independent, MT-binding site on its N-terminal region, that could be important for bundling, a property already reported for the kinesin Ncd in *Drosophila* (Furuta and Toyoshima, 2008). Class I in *Physcomitrella* is composed of two members (**Figure 2.12**),

which contain a C-terminal motor domain (**Figure 2.13**), and therefore, similar to ATK5 (Ambrose et al., 2005), are likely to be minus-end directed motors.

Members of class II and III are related to KIFC3, which is involved in Golgi positioning and integration in mouse (Xu et al., 2002). Class II is the largest class with 8 members in *Arabidopsis* and 4 in *Physcomitrella* (**Figure 2.12**). In *Arabidopsis*, AtKP1 has been shown to organize the cortical MT array (Ni et al., 2005; Yang et al., 2011), and to regulate mitochondrial functions (Yang et al., 2011). ATK4 and homologues in cotton and rice, possess a Calponin Homology (CH) domain that mediates interaction with F-actin (Tamura et al., 1999; Preuss et al., 2004; Frey et al., 2009; Xu et al., 2009), and could be important for regulating the motor activity and coordinating the activities of MT and AFs during premitotic nuclear migration (Umezu et al., 2011). Interestingly, the 4 members of this class in *Physcomitrella* also contain the CH domain (**Figure 2.13**), strongly suggesting that the binding to actin microfilaments is conserved in moss.

Class III has 3 representatives in *Arabidopsis* and 2 in *Physcomitrella* (**Figure 12**). However, the function of these kinesins still remains unknown. Intriguingly, these kinesins possess a malectin domain (**Figure 2.13**), which allows binding to carbohydrate such as di-glucose (Schallus et al., 2008). This domain has been identified in malectins, which are conserved proteins of the endoplasmic reticulum in animals and involved in protein *N*-glycosylation (Schallus et al., 2008), as well as in plasma membrane-located leucine-rich repeat receptor kinases such as FERONIA in *Arabidopsis*, where it is thought to regulate cell growth in response to cell wall changes (Zou et al., 2011). The functional significance of the malectin domains for kinesins is unclear and further investigation will be needed to decipher the role of class III kinesin 14s in plants.

Class IV kinesin 14s are plant specific. The homologue in tobacco, TBK5, is thought to function in relocating and gathering newly formed microtubules and/or microtubules nucleating units (Goto and Asada, 2007). *Physcomitrella* possesses only one member compared to two in *Arabidopsis* (**Figure 2.12**), which makes it a great system to gain more insight into the function(s) fulfilled by these kinesins in plants.

Class V kinesin 14s KAC1 and KAC2 have been recently identified in *Arabidopsis* in a genetic screen for chloroplast movement in response to light intensity changes (Suetsugu et al., 2010b). Interestingly, they show no MT binding activity or detectable ATPase activity. Instead, they are thought to interact with AFs and mediate chloroplast movement in an actin-dependent manner. However, the precise mechanism by which they regulate chloroplast movement still needs to be determined. *Physcomitrella* also contains two members of this class (**Figure 2.12**) and whether or not they interact with MTs and/or actin filaments to move chloroplasts is not known. It will be interesting to investigate whether these two members of the class V kinesin 14 have similar functions as their *Arabidopsis* homologs. We want to note that gene model corresponding to the N-terminal sequence for kinesin 14-Vb is incorrect in Phytozome database due to an incorrect prediction of a splicing site. This does not affect the motor domain sequence that was used for our phylogenetic tree. We provide in the supplementary material what we believe is the correct protein sequence for this molecule (Appendix File 1).

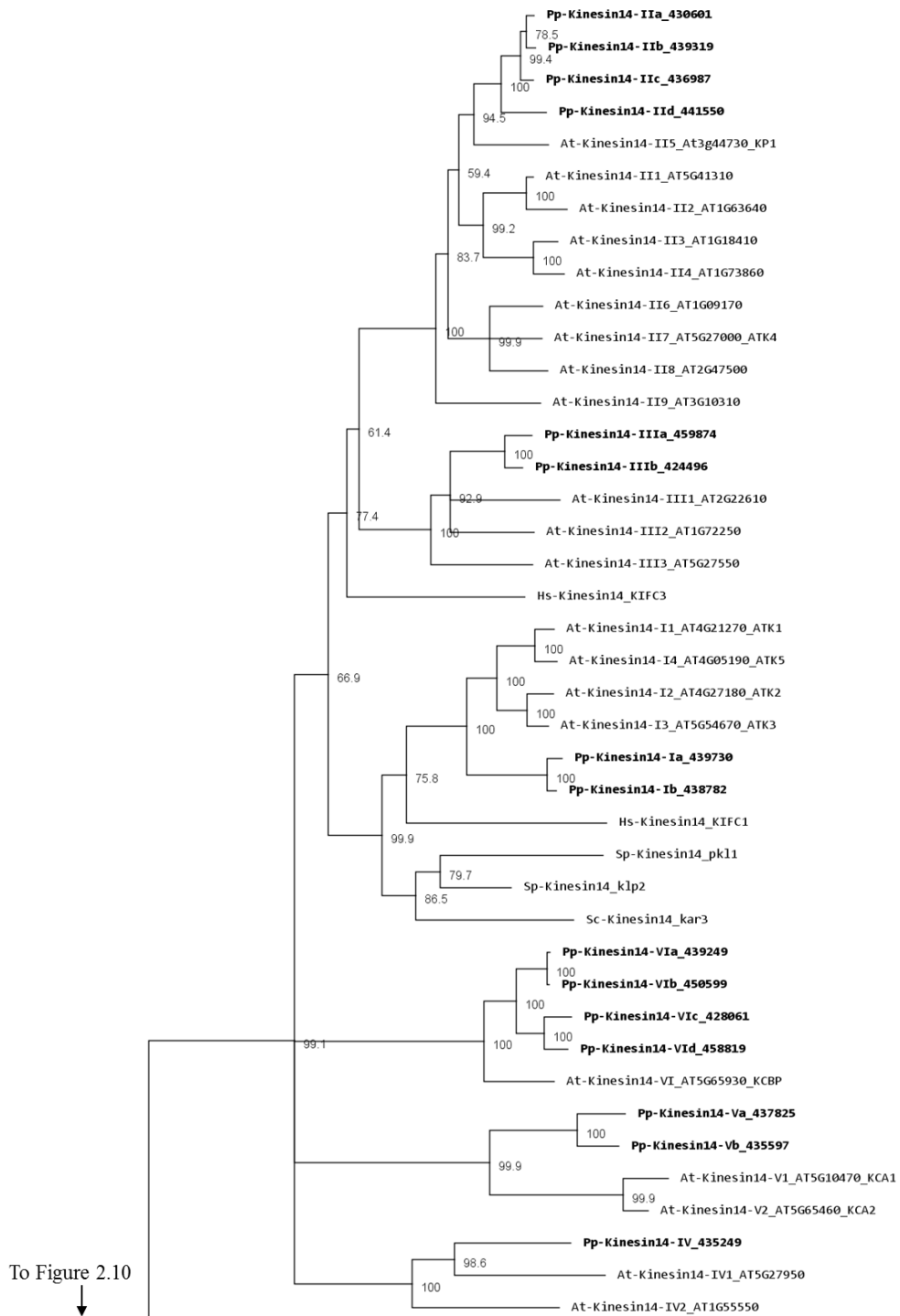


Figure 2.12: Sub-region showing kinesin 14s.

Sub-region of the phylogenetic tree based on their motor domain showing kinesin 14s. The amino acid sequences of the motor domain were aligned using ClustalW and the phylogenetic tree was constructed using the maximum likelihood method (PhyML) and a 1000 bootstrap resampling value. Numbers on the nodes show the statistical support of values above 50%. The scale shows the estimated branch length corresponding to the number of substitutions per site. The *Physcomitrella* numbers correspond to the Phypa number uniquely associated with each gene model (version 1.6) at cosmos.org.

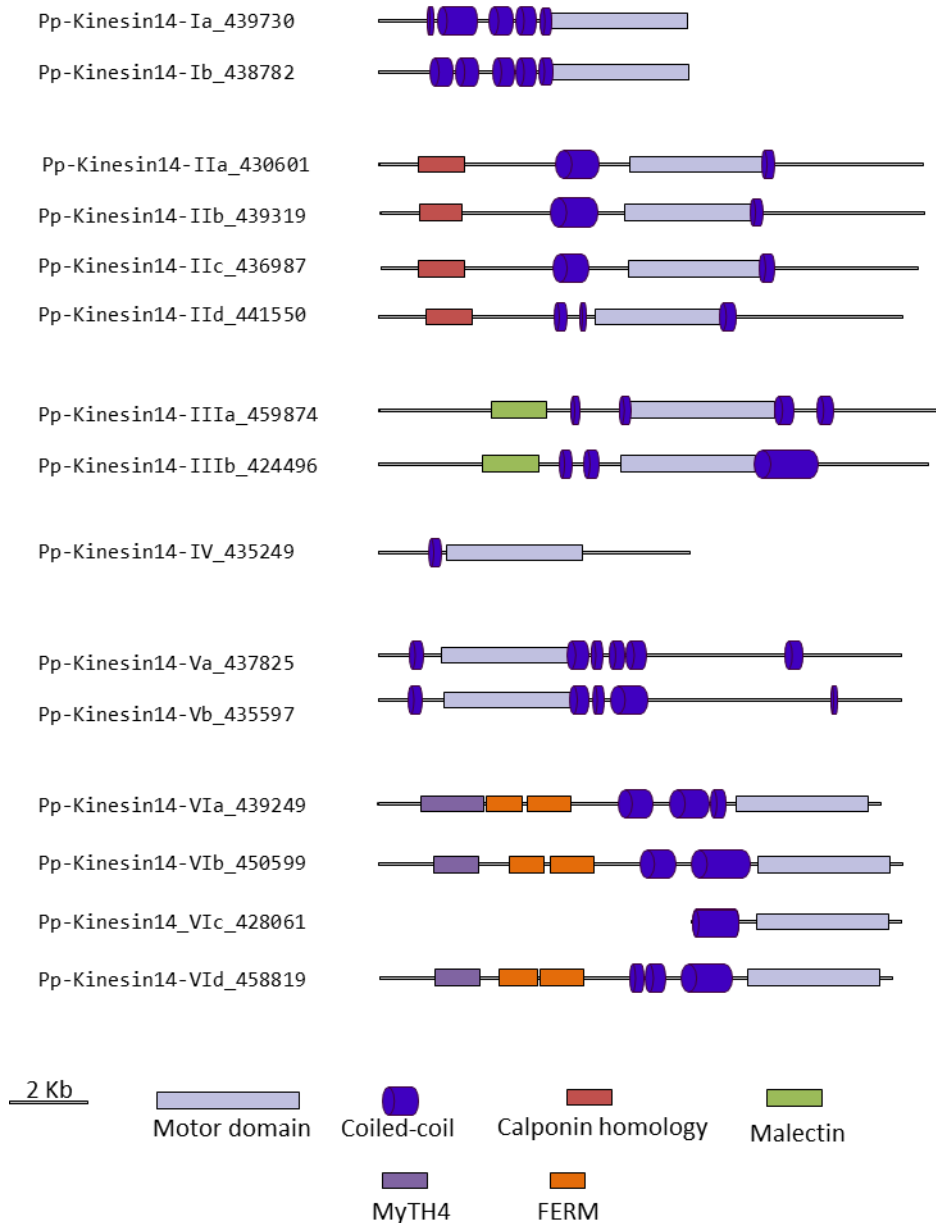


Figure 2.13: Gene models of kinesin 14s.

Schematic diagrams showing the structure and domain architecture of kinesin14s. Domains are indicated at the bottom of the diagrams. Calponin homology domains mediate interaction with F-actin; Malectin domains allow binding to carbohydrate such as di-glucose; and Myosin Tail Homology domain 4 (MyTH4) and FERM domains (motif named after proteins that contains it: 4.1 protein, Ezrin, Radixin, Moesin) also called talin-like region, are known to bind microtubules.

Surprisingly, class VI encompasses only one member in *Arabidopsis*, KCBP, compared to 4 in *Physcomitrella* (**Figure 2.12**). KCBP, which contains a calmodulin-binding domain, participates in cortical MT organization (Oppenheimer et al., 1997), and

is involved in the different stages of mitosis by regulating bundling and sliding of MT (Bowser and Reddy, 1997; Vos et al., 2000). The 4 moss homologues contain a myosin tail homology domain 4 (MyTH4) and 2 FERM domains (motif named after proteins that contains it: 4.1 protein, Ezrin, Radixin, Moesin) also called talin-like region (**Figure 2.13**), which are known to bind microtubules (Narasimhulu et al., 1997). Therefore, moss class VI kinesin 14s are likely to function in cross-linking or bundling of MTs.

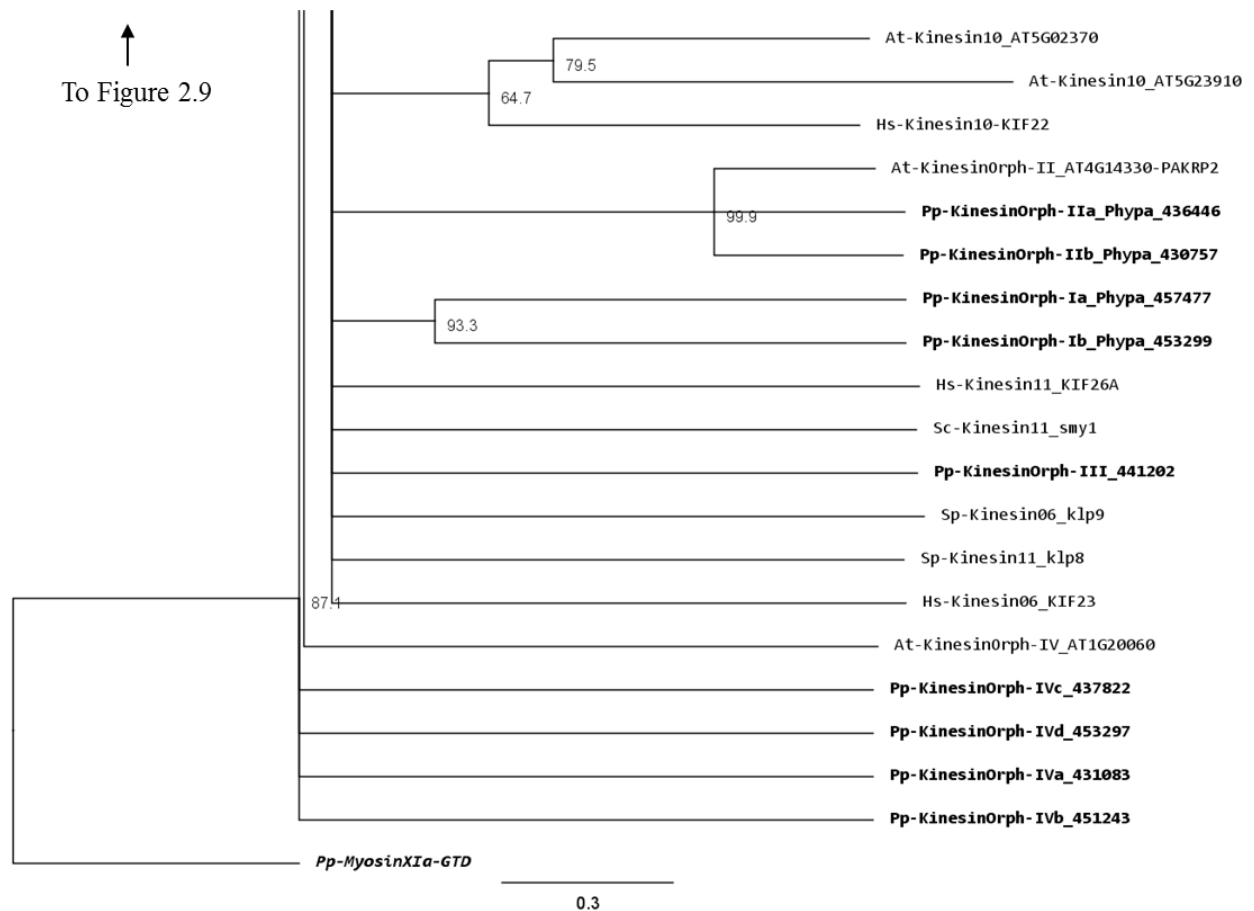


Figure 2.14: Sub-region showing kinesin 6s, 10s, 11s, and orphan kinesins.

Sub-region of the phylogenetic tree based on their motor domain showing kinesin 6s, 10s, 11s, and orphan kinesins. The amino acid sequences of the motor domain were aligned using ClustalW and the phylogenetic tree was constructed using the maximum likelihood method (PhyML) and a 1000 bootstrap resampling value. Numbers on the nodes show the statistical support of values above 50%. The scale shows the estimated branch length corresponding to the number of substitutions per site. The *Physcomitrella* numbers correspond to the Phypa number uniquely associated with each gene model (version 1.6) at cosmoss.org.

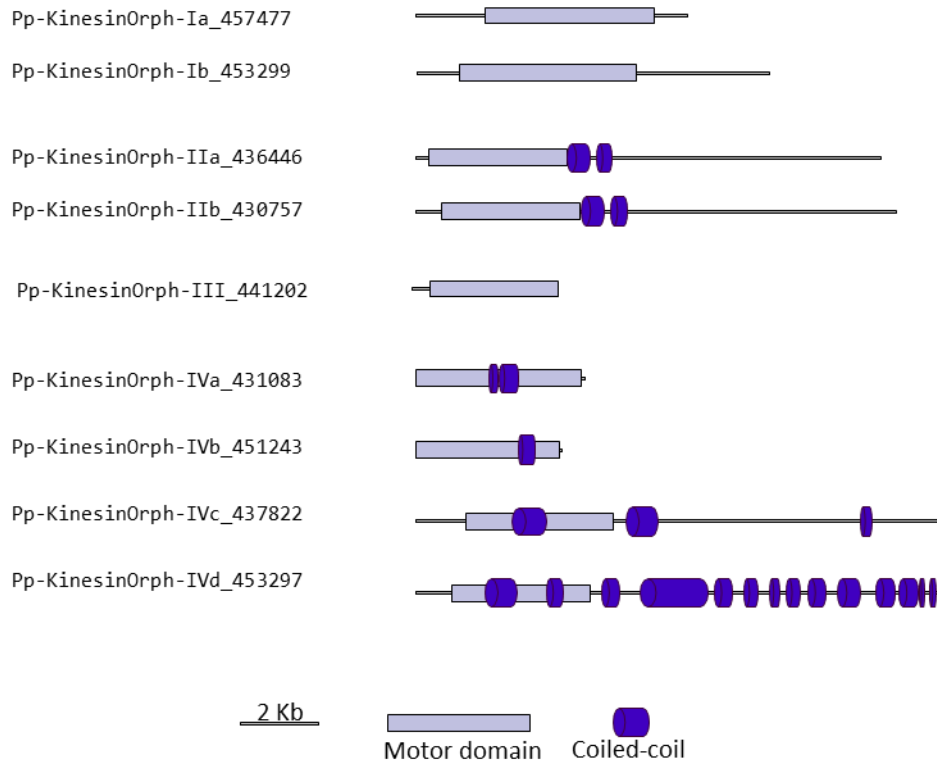


Figure 2.15: Gene models of orphan kinesins.

Schematic diagrams showing the structure and domain architecture of orphan kinesins. Domains are indicated at the bottom of the diagrams.

Orphan kinesins

We have grouped the remainder moss kinesins into four classes based on the similarity of their motor domain. Class I is composed of two related kinesins with no homologues in *Arabidopsis* or animals (**Figure 2.14**). The gene models for the region outside of the motor domain may not be well predicted due to limited transcript sequence information, so it is difficult to deduce any specific function from the available gene model sequence (**Figure 2.15**). A similar situation is present for the single member of class III (**Figures 2.14** and **2.15**). Due to the small number of members in these classes it should be relatively simple to evaluate their function using the various loss-of-function techniques

available in *Physcomitrella*. However, it is also relevant to mention that at this point it is hard to rule out the possibility that these genes might be pseudogenes.

The class II orphan kinesins are composed of a pair of kinesins (KINID1a and KINID1b) that have been shown to be important for interdigitation of phragmoplast MTs and cell plate expansion in moss (Hiwatashi et al., 2008). These kinesins are orthologues of PAKRP2 from *Arabidopsis*, which is predicted to function in the transport of Golgi-derived vesicles in the phragmoplast (Lee et al., 2001); nevertheless a conserved function between the moss and *Arabidopsis* orthologues has so far not been established (Hiwatashi et al., 2008). In previous analysis, where PAKRP2 was classified as a kinesin 10, the clade that PAKRP2 belonged to was parallel with other kinesin families as well as the second clade of Kinesin 10. In addition, that particular clade was not resolved in three of the four methods used to build the tree and had a low score in the methods that resolved the clade (Richardson et al., 2006). Based on our analysis, we suggest an orphan classification for PAKRP2 because it groups with the moss orthologues with a high bootstrap score, but not with *bona fide* kinesin 10s. Furthermore, the class II orphan kinesins have much longer C-terminal domains when compared with kinesin 10s. It is therefore more appropriate for these kinesins to be classified as orphan kinesins.

There is only one class III kinesin found in *Physcomitrella*. This kinesin is highly divergent since its relationship cannot be resolved between kinesin 6s and kinesin 11s from human and yeasts in our phylogenetic tree (**Figure 2.14**). Whether this kinesin will have conserved function to kinesin 6 or 11 is not clear from our tree, but kinesin 6s and 11s are known to be highly divergent (Miki et al., 2005). In addition, the lacking of gene

model information on the C-terminal after the motor domain casts shadow on the possibility that it might also be a pseudogene (**Figure 2.15**).

The final group of kinesins is class IV; these kinesins have the most divergent motor domains and tend to cluster with kinesin 11 members from animals and yeasts (**Figure 2.14**). In yeast, kinesin 11 or Smy1p does not bind to microtubules and it seems to regulate myosin V function (Lillie and Brown, 1998; Beningo et al., 2000). The four class IV members in *Physcomitrella* have coiled coils in their head domains (**Figure 2.15**), suggesting a non-functional motor similar to yeast. Therefore these four kinesins are classified as class IV of the orphan kinesins. Besides the relatively low homology in the motor domains, there is little additional similarity in the rest of the molecules from this class (**Figure 2.15**). Analogous to class I and III kinesins, it will be important to determine their phylogenetic distribution and conservation in other species, but a detailed loss-of-function and biochemical analyses will be required to determine their function.

Acknowledgments

I would like to thank all members from the Vidali Lab for support and discussion, in particular to Erin Agar for careful reading of the manuscript and her comments. Support was provided by WPI-startup fund and a National Science Foundation grant to L.V. (IOS-1002837).

My contribution includes screening and organizing sequences used in this paper. I also built a library of Phypa-number based kinesins in *Physcomitrella*, and helped run some initial alignments. Each member of the Vidali lab was responsible for at least one family of kinesins. I was also responsible for revision of this paper based on reviewers' suggestions before final submission.

Chapter 3 : Functional Analysis of Physcomitrella Kinesin14-Vs

Keywords:

Chloroplast photorelocation, light avoidance responses, kinesins, PpKin14-Vs, moss, cytoskeleton, actin filaments, microtubule, RNAi, intracellular transport

Abstract

Chloroplast motility in response to light signals is carefully regulated and powered by cytoskeletal elements. Specifically, chloroplasts are found to show avoidance responses to high intensity light and accumulation responses when the light intensity is low. The actin cytoskeleton has been found to mediate all chloroplast photorelocation responses in *Arabidopsis thaliana*. In contrast, in the moss *Physcomitrella patens* both actin filaments (AFs) and the microtubule (MT) cytoskeleton can transport these organelles, but the mechanism of transport for both cytoskeletal systems is not understood. It was previously shown that the kinesin-like proteins of the 14-V family are important for chloroplast photorelocation, both in vascular plants and in the moss. *Physcomitrella* has two kinesin14 class V proteins, PpKin14-Va and -Vb.

In order to elucidate the mechanism of how these two proteins function in chloroplast movement, gene-specific silencing was performed using the efficient RNA interference reporter system of *Physcomitrella patens*. Furthermore, through cytoskeleton-targeted drug studies, we were able to conclude that Ppkin14-Vs are required for chloroplast dispersion under uniform white light condition. Additionally, Ppkin14-Va and -Vb, are functionally equivalent in keeping chloroplasts dispersed throughout the cell. We also found that they mediate chloroplast light avoidance responses in an AF-dependent, rather than MT-dependent manner. Our correlation decay analysis of cytoskeletal dynamics suggests that PpKin14-Vs function by stabilization of cortical AFs. The AF-dependent chloroplast light avoidance response in the moss is slower than the MT-dependent avoidance responses, the mechanism of which is yet to be discovered.

3.1 Introduction

Organelle movements are an essential part of intracellular traffic in a functional cell. For example, chloroplast photorelocation contributes to photosynthesis and plant adaptation to the ever-changing light conditions in natural environment. This is particularly important because chloroplasts are responsible for light capture and energy conversion, which is vital for plant survival and for the rest of the eco-system. It has been shown that chloroplasts in higher plants respond to blue light in two ways: avoidance from high light and accumulation to low light (DeBlasio et al., 2005). Some alga, moss, and fern species also show responses to red light (Kasahara et al., 2004; Ichikawa et al., 2011).

Phototropins have been identified as the blue light receptor and phytochromes identified as the red light receptor (Christie, 2007). But in actuality, the functions of the two kinds of photoreceptors are not mutually exclusive. Phototropins have been indicated to mediate both blue and red light responses of chloroplasts in the moss *Physcomitrella patens* (Kasahara et al., 2004; Suetsugu and Wada, 2007b). Phytochromes are also found to modulate blue light induced chloroplast photorelocation (DeBlasio et al., 2003; Luesse et al., 2010). Chloroplasts photorelocation has been suggested to depend solely on actin filaments (AFs) in many plant species once the light stimulation signal gets transduced (Takagi, 2003; Kadota et al., 2006; Kadota et al., 2009; Yamashita et al., 2011; Usami et al., 2012). However, chloroplasts movement in *Physcomitrella patens* has been demonstrated to be microtubule-dependent (MT-dependent) as well (Sato et al., 2001). There are specific associated motors with each cytoskeletal tracks; myosins are the motors that move along AFs, and kinesins move along MTs. The fact that both cytoskeletal tracks participate in chloroplast photorelocation in moss allows searching for potential motors that are responsible for such movements. However, no direct motors

have yet been identified to facilitate chloroplast photorelocation. Recently, research on actin-dependent chloroplast photorelocation has identified short actin filaments organizing near the leading edge of the chloroplasts (Kadota et al., 2009). Since no myosins have been identified in this process, the myosin as chloroplast motor theory is less favored. On the other hand, for the MT-dependent chloroplasts movement in *Physcomitrella patens*, it will be interesting to investigate if there are kinesins involved and whether the kinesins involved act as motors. Previous studies in *Arabidopsis* identified two kinesin-like proteins but suggested that they mediate actin-dependent chloroplasts movement (Suetsugu et al., 2010a). These two proteins are also shown to be conserved in land plants including the ferns and mosses (Suetsugu et al., 2012).

Despite the protein conservation across species, the existence of MT-dependent chloroplast photorelocation in moss makes it an interesting question, whether the two proteins (highlighted in green in **Table 2.2**) function as kinesin motors in *Physcomitrella*. Here we report our research on the role of these two proteins in *Physcomitrella patens*, named Pp-Kinesin14-Va and -Vb (PpKin14-Va and -Vb for short hereafter) based on our recent phylogenetic analysis of moss kinesins (chapter 2) (Shen et al., 2012). By utilizing an efficient RNA interference system in *Physcomitrella patens* (Bezanilla et al., 2003) and further through specific drug-targeted cytoskeleton studies, we are able to pinpoint that Ppkin14-Vs are required for chloroplast dispersion within the cell under uniform white light condition. We also show that they mediate chloroplast light avoidance response in an AF-dependent, rather than MT-dependent manner. The AF-dependent chloroplast light avoidance response in the moss is slower than the MT-dependent avoidance responses, the mechanism of which remains to be discovered.

3.2 Material and Methods

Tissue culture and protoplast transformation

The moss was cultured at 25 °C under 14hr/10hr light-dark cycle. The culture medium and PEG-mediated transformation procedures were described previously (Liu and Vidali, 2011).

RNAi constructs

To create the individual UTR-RNAi constructs, we amplified ~200bp fragments immediately upstream of the start codon of each gene from genomic DNA. The fragments were cloned into pENT/D-TOPO and the inserts were transferred to RNAi construct pUGGi by LR reaction (Bezanilla et al., 2005). A BamHI site was designed in the forward and reverse primer for the 5' UTR of PpKin14 Va and Vb, respectively, and the double UTR-RNAi construct was created by ligating the BamHI digested PCR fragments before cloned into pENT/D-TOPO and transferred to pUGGi via LR reaction. The double CDS-RNAi constructs were generated using a similar strategy, except that the 200bp fragments were amplified from genomic sequences corresponding to exon 11 and exon 16 of PpKin14 Va and PpKin14 Vb, respectively.

Morphometric analysis of RNAi plants

The effect of PpKin14 Va and Vb RNAi on *Physcomitrella* was determined by observing plants seven days after transformation. The samples were observed with a Zeiss stereo-fluorescence microscope at 63X zoom. The effect on growth was determined by measuring the area of the plants: plants were placed on a thin pad of agar on PpNO₃ medium and stained with 10 µg/ml calcofluor before covered by a glass cover slip (Vidali et al., 2007). The effect of RNAi on chloroplast distribution was measured by the level of

chloroplast aggregation in the control and RNAi plants. An in-house developed ImageJ macro (available upon request) was used to determine the level of chloroplast aggregation. The macro measures the total area of chloroplast fluorescence and divides it by the number of chloroplast clusters. The voids in the cells with aggregated chloroplasts result in smaller areas occupied by chloroplasts and a larger number of clusters. Therefore, such cells would have lower average cluster area.

Cytoskeletal inhibitors and laser scanning confocal microscope analysis of chloroplast motility

After transformation, plants were placed on protoplast regenerating medium for 4 days and then transferred to PpNH₄ medium with hygromycin to select for transformed plants. On the 8th day, plants were transferred to a thin pad of agar on PpNO₃ media with, latrunculin B or oryzalin or both drugs added to reach a final drug concentration of 10 μ M immediate before the slide was placed on the Leica laser scanning confocal microscope (SP5). Ethanol was used as the drug carrier instead of DMSO because experiments with DMSO showed adverse effects on the plants while experiments with ethanol were not significantly different from the control which has neither drugs nor drug carriers added.

Images from all drug-treated cells were taken on a cell region under 5% 488nm blue light when the argon laser power was set to be 20% (final power 1%). Images stacks of 5 over 4 μ m vertical distance (z-step size of 1 μ m) were acquired at scan speed of 700Hz with a time interval of 2 seconds for 15 minutes. The objective lens was HCX PL APO lambda blue 63.0x1.40 OIL UV. The pinhole was open to the maximum, 600 μ m (6.28 airy units), at 6X zoom.

Confocal observation of cortical MTs and AFs

A moss line with Lifeact-mEGFP tagged AFs was used to observe the dynamics of AFs under the PpKin14 Va+Vb RNAi. Another moss line with GFP tagged MTs (Hiwatashi et al., 2008) was used to observe the dynamics of MTs under the PpKin14 Va+Vb RNAi. Seven-day-old plants after transformation were used to prepare PpNO₃ slides for confocal imaging as indicated above.

To observe AFs the confocal settings were as follows: time-lapse images were taken every second for 60 seconds; pinhole opened to 191.1 μm (2.00 airy units) at 16X zoom. AFs were excited with 30% of blue light at 488nm when the argon laser power was set to 20% (6% final power). A dichroic excitation beam splitter (DD 488/561) was used at the scanning speed of 200Hz. The emission bandwidth for photomultiplier (PMT) 2 was between 495nm-558nm; for PMT 4 was between 668nm and 800nm. The same oil lens described previously was used.

MT visualization settings are the same as that of actin filaments images, except that MTs were excited with 15% of blue light at 488nm when the argon laser was set to be 20% (3% final power).

Correlation coefficients decay analysis on confocal images

Pearson's product-moment correlation coefficients were calculated using the Matlab function corr2 (Vidali et al., 2010) on the confocal image stacks projected at maximum intensity. Non-linear curve fitting was carried out using GraphPad Prism version 6.02 for Windows (GraphPad Software, San Diego California USA, www.graphpad.com).

If a time-lapse image series does not change over time, each image will be perfectly correlated with the previous one, resulting in a correlation coefficient of 1 over

time. If there are constant changes over time, each image will become less correlated with the image preceding it, resulting in decays in correlation coefficients from the value 1. The range of correlation coefficient decay corresponds to the rate of changes in the process. Therefore the rate of changes in two or more processes can be compared relatively by comparing correlation decay rates when all other parameters are set unchanged.

To compare the correlation decay rates of cytoskeletons in the PpKin14_Va+Vb UTi mutants and the control RNAi plants, a global nonlinear regression approach was taken using the statistics software GraphPad Prism (version 6.02). A global model defines a set of curves, rather than one curve (Motulsky and Christopoulos, 2004). Some parameters can be shared among the curves, while some other parameters can be set individually, so that the key parameter can be compared across datasets. Parameters of a nonlinear regression can be adjusted so that the fitting curve can come as close to the data as possible. This is made possible by minimizing the sum of squared of the vertical distances between the curve and the data points. Global nonlinear regression extends this idea by fitting several datasets as once, minimizing the overall sum of squares (Motulsky and Christopoulos, 2004). It can also fit individual datasets separately. Then the sum of squares from the global fit will be compared with that of individual fit, to determine which qualifies for a better fit. This way, two or more datasets can be evaluated whether they belong to the same population or not.

One phase decay fitting model is as follows:

$$Y=(Y_0 - Plateau)*exp(-K*X) + Plateau$$

Where Y_0 is the Y value when X (time) is zero. Plateau is the Y value at infinite times. K is the rate constant, expressed in reciprocal of the X axis time units. Y_0 was set to be 1 and plateau was set as the lowest plateau from fitting each condition individually.

The correlation coefficients from cytoskeletal drug-treated chloroplast images were first fitted by this one phase model. The fitting was done by constraining Y_0 to 1 for each treatment condition and generating individual plateau values. Chloroplast numbers do not vary significantly during experimental time frame. Therefore, for the purpose of comparing the rate parameter K, it is feasible to assume that at infinity the plateaus for all treatment conditions will converge to the smallest plateau value of individual fit (**Table 3.1**). Then using fixed Y_0 and plateau values, drug-treated chloroplast motility data was fitted globally by a one phase exponential fitting model. The fitting result suggested that chloroplast motility from 8 treatment conditions does not belong to the same population. Therefore we performed individual fitting for each treatment condition and did pair-wise comparisons between each group. The 0.05 significance level was adjusted by the Bonferroni methods to avoid type-I error.

The correlation coefficients from cytoskeletal images were fitted globally by a two phase exponential fitting model. Since there are only two groups (the mutant phenotype and the control), a global nonlinear fit can tell us if the two groups belong to the same population or not. In contrast to the strong signals from chloroplast autofluorescence, signals from the cytoskeletal elements have a low signal-to-noise ratio. Therefore we tested and developed an ImageJ macro (available upon request) that applies unsharp mask, gaussian blur, subtract background, and enhance contrast subsequently on selected raw images to clean and enhance raw cytoskeletal images.

Two phase decay fitting model is the following:

$$\text{SpanFast}=(Y0-\text{Plateau})*\text{PercentFast}*.01$$

$$\text{SpanSlow}=(Y0-\text{Plateau})*(100-\text{PercentFast})*.01$$

$$Y=\text{Plateau} + \text{SpanFast}*\exp(-\text{KFast}*X) + \text{SpanSlow}*\exp(-\text{KSlow}*X)$$

Y0 is the Y value when X (time) is zero. Plateau is the Y value at infinite times. KFast and KSlow are the two rate constants, expressed in reciprocal of the X axis time units. We assume that the whole data set share the same value for the initial point Y0 (set to 1), plateau, percent fast, and KSlow; and compare the value of KFast.

To rule out nonspecific signals resulting from different background noise between experimental groups, we carefully controlled and monitored for noise levels. To estimate the noise levels, we used ImageJ built-in functions to measure the standard deviation over time for a dark corner (3 μm X 3 μm) of the time-lapse image series. Standard deviation values were compared in a two sample t-test to determine if the background noise levels belong to the same population (noise results in **Table 3.2**).

3.3 Results

***Physcomitrella* has two homologous kinesin 14 class V proteins**

Using sequence similarity to the kinesin-like proteins AtKACs (At5g10470 and At5g65460) from *Arabidopsis thaliana* (Suetsugu et al., 2010a), we identified two genes (**Figure 3.1A**), PpKin14-Va (Phypa_437825_Pp1s74_159V6.1) and PpKin14-Vb (Phypa_435597_Pp1s60_159V6.1). Their nomenclature is based on a recent systematic phylogenetic analysis of all kinesins in the moss (chapter 2) (Shen et al., 2012).

The intron exon boundaries in the coding region are highly similar between the two PpKin14-V genes (**Figure 3.1A**). We want to note that we are using a corrected version of PpKin14-Vb (1362aa) based on evidence derived from the kinesin phylogenetic analysis. The gene model corresponding to the N-terminal sequence for PpKin14-Vb was incorrect in the genomic portal (Phytozome.org) due to an incorrect prediction of a splicing site (chapter 2) (Shen et al., 2012). The sequence information for PpKin14-Va (1345aa) is consistent across databases and agrees with our sequencing results of the cDNAs of the two proteins. There are 24 exons in the coding regions in both proteins (**Figure 3.1A**). The corrected protein Vb (1362aa) prediction sequence is about the same length as protein Va (1345aa). Although the start and stop codons have been identified for both proteins, from the genomic information it is not clear where the 5'-UTR starts and where the 3'-UTR ends. Therefore the UTR upper and lower boundaries are represented by dashed lines in **Figure 3.1B**. Genomic information is based on version 1.6 (the 6th annotation of *Physcomitrella*'s first genome assembly) and our cDNA sequencing results.

The main distinguishing aspect in these two proteins is a conserved kinesin-14-

like motor domain located closer to the amino-terminus (N-terminus). Motor domains of kinesin 14s are generally documented to be closer to the C-termini or in the middle of the molecule. That is the reason why the kinesin 14 family was initially referred as the C-terminal motor proteins (Henikoff, 1996). In these two PpKin14-Vs proteins, a small region of coiled-coils and a neck domain are located N-terminal to the motor domain (Figure 3.1B). The location of these featured domains is consistent with the two proteins in *Arabidopsis thaliana* (Appendix file 2, Pp-At Kin14-V Alignment). Furthermore, this structure is shown to be conserved in the fern *Adiantum capillus-veneris* and *Ceratopteris richardii* (Suetsugu et al., 2012).

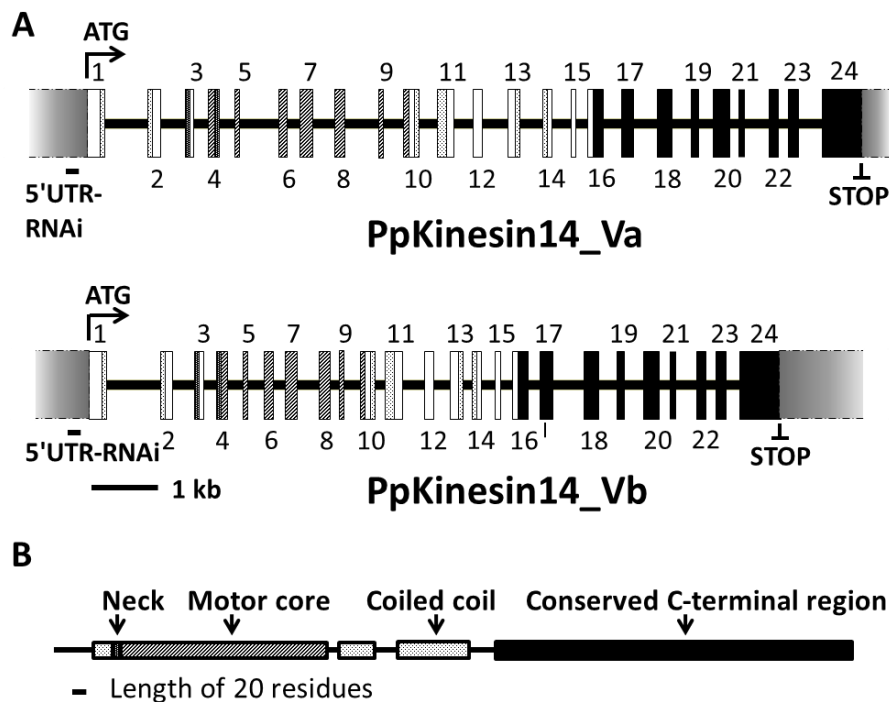


Figure 3.1: Predicted gene models and common protein domains of PpKin14-Vs

(A) The exon-intron boundary distribution shows conservation between PpKin14-Va and -Vb. RNAi sites in 5' UTR regions are indicated with black bars. Genomic information is based on version 1.6 (the 6th annotation of the *Physcomitrella* first genome assembly) and our sequencing results. (B) Common protein structures shared by PpKin14-Va and -Vb. Shown in different texture schemes are a neck domain and a motor domain between coiled coil regions followed by a long conserved C-terminal region.

The conservations in protein sequences and structures, together with evidence from phylogenetic analysis, suggest a recent common ancestor between these kinesins from several representative land plant species, but kinesin14-Vs from the moss and from *Arabidopsis* are paralogs, raising the likelihood of newly evolved functions (**chapter 2**) (Shen et al., 2012; Suetsugu et al., 2012). Interestingly, when aligning PpKin14-Vs, AtKAC1 (the dominant kin14-V in *Arabidopsis*) and a characterized yeast kinesin 14 ScKAR3, PpKin14Va, Vb and AtKAC1 showed similar amount of conservation with ScKAR3 in key amino acids from the catalytic (N-1, N-2, N3) and MT-binding sites (**Figure 3.2**).

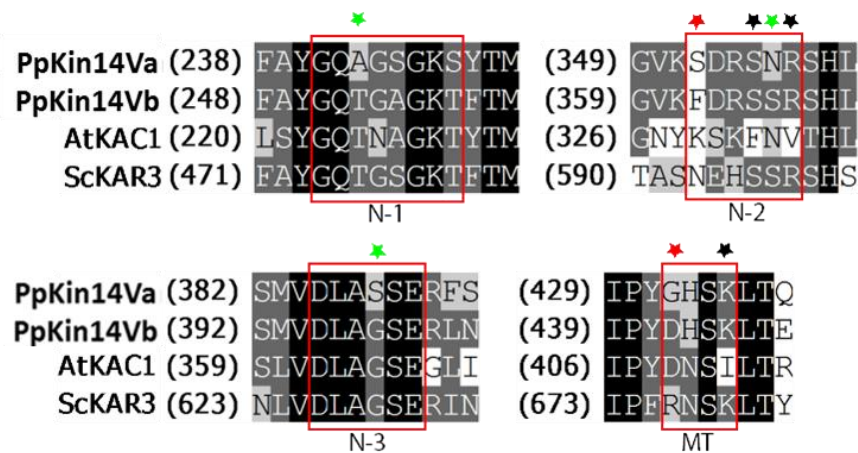


Figure 3.2: Alignment of amino acids for catalytic activities and MT-binding sites.

Alignment of amino acids important for catalytic activities and MT-binding in PpKin14-Vs, AtKAC1 and ScKAR3. Black stars denote residues conserved in moss but not in *Arabidopsis*. Red stars denote residues not conserved in moss or *Arabidopsis*. Green stars denote residues conserved only in one moss isoform. ScKAR3 is a kinesin-14 from yeast. N-1, N-2 and N-3 are three of the four conserved nucleotide binding sites; and MT stands for microtubule-binding site of the kinesin 14.

Notably PpKin14-Vs seem to be a little more conserved at the N-2 site, which is characterized by the NXXSSR, a conserved sequence in both kinesin and myosins. The asparagine in ScKAR3 was not found in either moss or *Arabidopsis*. The first serine is

believed to directly interact with nucleotides and may be involved in sensing the presence of γ -phosphate (Kull et al., 1998). PpKin14-Va has the first serine and last arginine at N-2 site; PpKin14-Vb has the entire SSR sequence. However, AtKAC1 has none of the amino acids of the SSR sequence (**Figure 3.2**). The conservation suggests that PpKin14-Vs may potentially retain more function at the N-2 catalytic site than AtKAC1. The *Arabidopsis* proteins were not capable of binding to MTs, probably due to evolutionary amino acid changes in the MT binding site (**Figure 3.2**). PpKin14-Vs do not show higher level of conservation at the MT-binding site than AtKAC1. In addition, the two kinesins contain a C-terminal domain that is conserved between members of this class; this domain is suggested to have *in vitro* actin binding activity in *Arabidopsis* (Suetsugu et al., 2010a), but is not homologous to other known actin binding sites. There is a long stretch of coiled-coils that connects the motor domain and the N-terminal domain (**Figure 3.1B**). Similar to coiled-coils in other kinesins, they are probably important for dimerization (Thormahlen et al., 1998).

PpKin14-Va and -Vb are functionally equivalent in maintaining normal chloroplast dispersion

To investigate the participation of the moss kinesin 14-Vs on chloroplast motility we designed specific RNAi constructs to silence their expression selectively. Using well-established methods (Bezanilla et al., 2003; Bezanilla et al., 2005), 5'UTR targeted RNAi constructs were designed to target the two PpKin14-Vs individually and in combination (Bezanilla et al., 2003; Bezanilla et al., 2005). While silencing either PpKin14-Va or -Vb does not generate a detectable phenotype, the expression of the RNAi construct that targets the 5'UTR of both Ppkin14-Vs leads to the accumulation of chloroplasts in the

central area of the cell where the nucleus is. In other words, Va and Vb double knockdown (Ppkin14_Va+Vb RNAi) leads to the loss of chloroplast dispersion in a steady state cell under uniform white light (**Figure 3.3A**).

In order to quantify the extent of loss in chloroplasts dispersion, we designed an ImageJ-based algorithm that, using chlorophyll autofluorescence, calculates the average area covered by the chloroplasts in one plant. In PpKin14-Vs double knockdown plants, there are many isolated chloroplast fluorescent areas (island areas or chloroplast clusters) per plant, corresponding to regions where the chloroplasts accumulate in each cell. In control plants, chloroplasts are widely dispersed, covering the entire cell length and resulting in larger average areas, most of the time comprising several cells (**Figure 3.3A**). This dispersion quantification method allows us to perform statistical comparisons between the control RNAi and the Ppkin14_Va+Vb RNAi double knockdown plants.

It is possible to obtain three different measurements from the images taken from the chloroplast autofluorescence and the cell wall staining. These are the mean island area per plant (**Figure 3.3B**), plant solidity (**Figure 3.3C**), and normalized total area (**Figure 3.3D**). When the mean island area is compared between the PpKin14-V-RNAi double knockdown plants and the control, a significant difference was observed (p-value<0.0001). However, the mean island areas measured from the Va UTi or Vb UTi single RNAi were not significantly different from each other (p-value = 0.26) and from the control RNAi at a significance level of 0.05 (**Figure 3.3B**).

This loss of chloroplast dispersion phenotype is highly reproducible and does not affect the growth of the cells or the plants, when evaluated with our well-established one-week growth assay (**Figure 3.3C and D**). We used calcofluor staining to estimate the

overall size of plants, instead of direct chlorophyll imaging, since using cell wall staining allows a more precise estimate of plant growth, in particular for plants that have highly clustered chloroplasts (**Figure 3.3A and D**). The normalized total areas from double knockdown are not significantly different from that of the control RNAi (**Figure 3.3D**). The average plant size in Va RNAi is not different from Vb RNAi, but seems to be larger than the control and the double RNAi plants, although no biological differences have been identified. These results suggest that the activity of kinesin 14-V is not essential for plant growth under optimal laboratory conditions. Growth of single knockdowns are not biologically different from the control RNAi plants, supporting the redundant role of PpKin14-Va and -Vb.

Solidity is a unitless parameter that measures the branching and polarized growth of plants. The closer to 1 the solidity value gets, the rounder and the more solid the plant is. Solidity value approaching zero indicates more branched structures in the measured plants (Vidali et al., 2010). Solidity does not vary significantly when single knock-downs and the double knock-down are compared with the control RNAi. However, the single RNAis and the double RNAi plants are slightly different in solidity (Va and double RNAi, $p=0.0346$; Vb and double RNAi, $p=0.0387$).

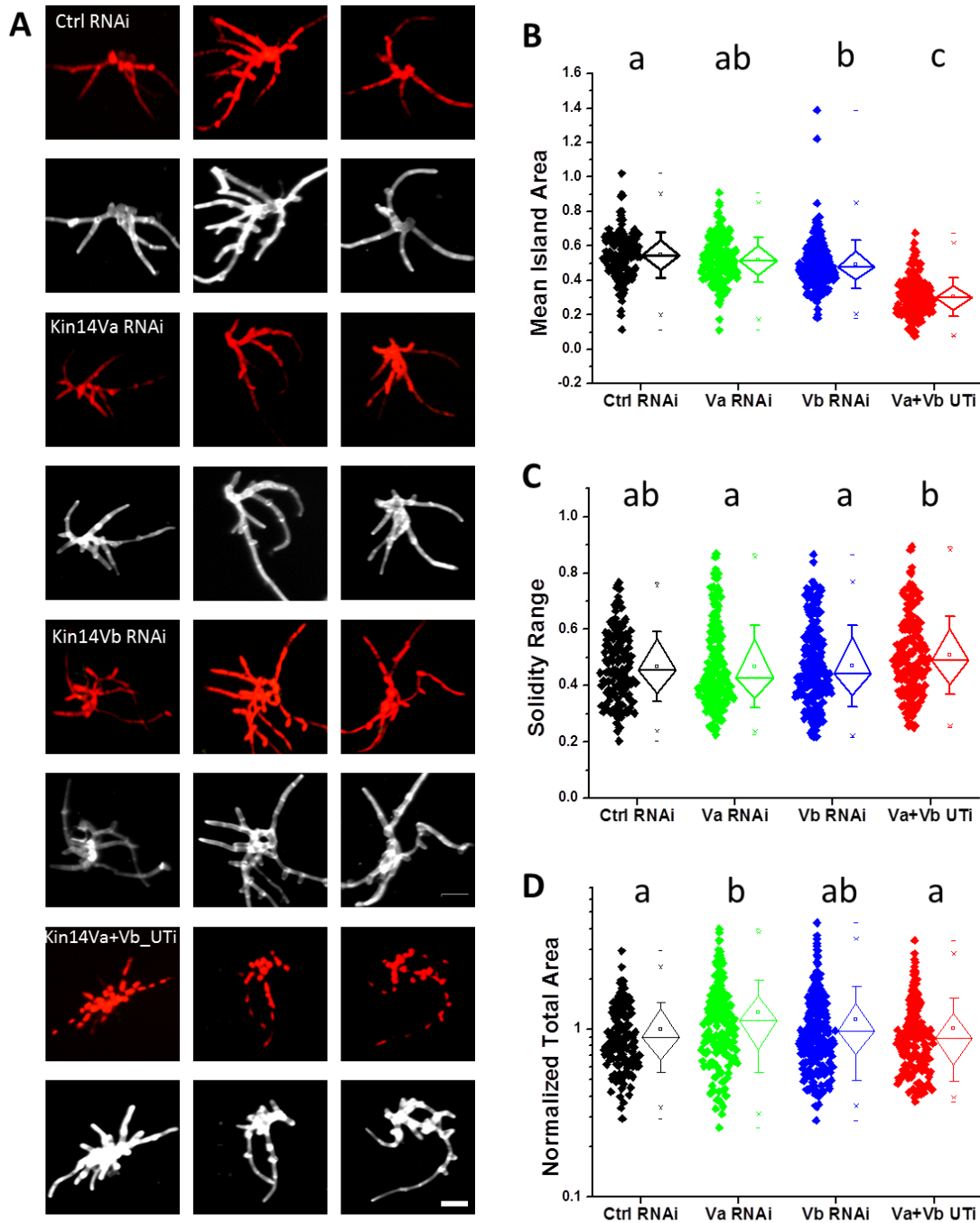


Figure 3.3: PpKin14_Va+Vb knockdown results in a loss of chloroplast dispersion phenotype.

(A) Chlorophyll and cell wall fluorescence quantitation of various RNAi plants. Three representative micrographs of the chlorophyll autofluorescence (red) and cell wall fluorescence (grey) from 1-week old transformed plants are shown. Note, lacking of nuclear GFP is a positive indication of successful RNAi. RNAi constructs added in each condition are indicated on the top left of each panel. Scale bar = 100 μ m. The numbers of plants analyzed: Ctrl RNAi, 147; Va UTi, 186; Vb UTi, 215; Va+Vb UTi, 175. (B) Data distribution and statistics for the average of the

mean island area of a plant in each condition. Range of the diamond box covers 25% to 75% of the data. The horizontal line in the box stands for group mean; the square dot in the diamond stands for population median; whiskers stand for 1 standard deviation (SD). Statistical significance is determined by $\alpha=0.05$ between two groupings. Letters on top of the columns indicate different statistical groups. The same graph settings applied for Graph C and D. **(C)** Quantification of the solidity values in the control and specific gene-targeted RNAi plants. **(D)** Total area of a plant expressed as fractions of the control RNAi. Statistics are taken from logarithmically transformed data.

The consistent and reproducible loss of chloroplast dispersion phenotype in the Va+Vb double knockdowns indicates that the two genes are functionally equivalent in relation to the observed chloroplast dispersion activity.

PpKin14-Vs mediate AF-dependent chloroplast light avoidance response

Actin filaments (AFs), rather than microtubules (MTs), are found to be responsible for chloroplast photorelocation in many plant species, including *Arabidopsis* (Yamada et al., 2007; Kadota et al., 2009; Suetsugu et al., 2010a; Kong et al., 2013), aquatic monocot *Vallisneria gigantea* Graebner, *Spinacia oleracea* L. (spinach) (Takagi, 2003; Takagi et al., 2003) and the fern (Suetsugu et al., 2012; Tsuboi and Wada, 2012). However, in the moss *Physcomitrella patens*, both MTs and actin filaments participate in chloroplast movement (Sato et al., 2001).

To evaluate the participation of specific cytoskeletal systems on generating the observed phenotype we used specific inhibitors known to depolymerize MTs (oryzalin) or AFs (latrunculin B). The cytoskeleton drugs were applied at a concentration (10 μ M) known to completely disrupt the filament networks. Ethanol was used as the solvent for drug delivery since we found a slight effect of low levels of DMSO on chloroplast dispersion (data not shown). Confocal image stacks were taken under strong blue light conditions that will produce avoidance response on illuminated cell region for 15

minutes. The treatment conditions are: ethanol (EtOH) as non-drug control, latrunculin B (LatB), oryzalin (Orz), and double drugs (LatB+Orz). Representative images at three time points from each treatment condition are displayed in red, green and blue (**Figure 3.4A**). A composite color image is then made out of the three images, to visually demonstrate motion levels of chloroplasts under each treatment condition. Less chloroplast movement will result in color overlap, thus a whiter image; and *vice versa*. The whiter the image is, the less chloroplast movement there is. This way the relative chloroplast motility can be directly visualized from the microscope time-lapse images. The confocal image stacks are analyzed using correlation coefficient decay, a previously developed method (Vidali et al., 2010) that compares correlation coefficients between frames at given time intervals. Correlation coefficient decay is a sensitive measurement of cytoskeleton dynamics including AF and MT polymerization and depolymerization, but we have adopted it here to evaluate chloroplast motility. Correlation coefficient starts with value 1, when an image is perfectly correlated to itself. As time interval increases, the correlation coefficient value decreases if it is a changing process. The faster it decreases, the more dynamic the process is. We used in-house developed Matlab codes to generate correlation coefficient decay plots from time-lapse images.

The correlation coefficients are plotted in **Figure 3.4B** for the mutant phenotype and **Figure 3.4C** for the control RNAi. When the oryzalin-treated mutant and control are compared, it is evident that PpKin14-Vs are required for AF-based chloroplast avoidance movement, but not for MT-based chloroplast avoidance response. The oryzalin treated control RNAi showed slower decay than the ethanol and latrunculin B treated control plants, but faster than oryzalin-treated mutants and double-drug treated control and

mutant plants (**Figure 3.4B**).

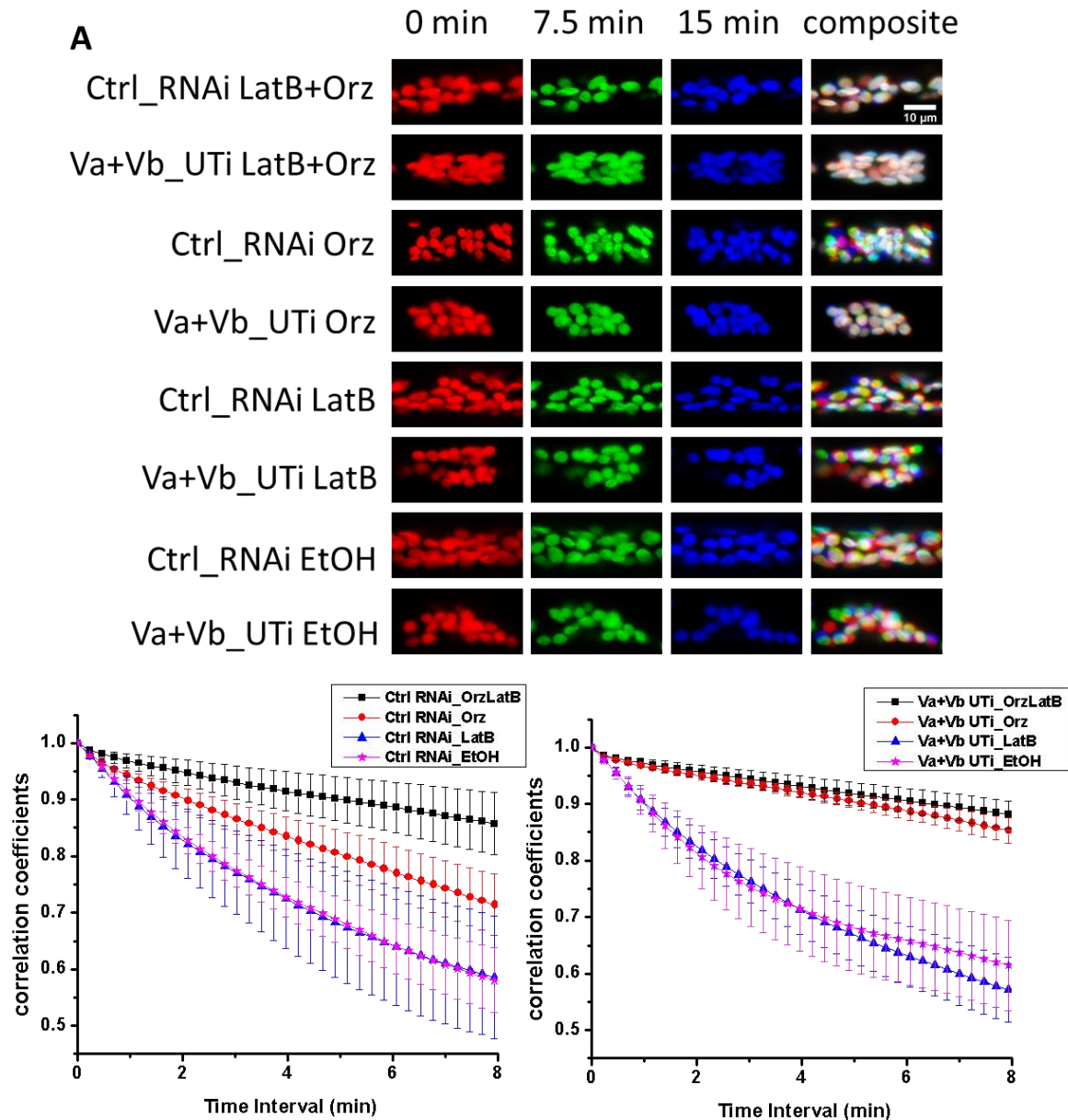


Figure 3.4: PpKin14-Vs mediate actin-dependent light avoidance response.

(A) Confocal images of chloroplast distribution in caulonema cells under different drug treatment conditions. Representative images from time 0-, 7.5-, and 15-min are shown in red, green and blue respectively. The fourth column is a color composite image of the three time points previously. Scale bar = 10 μ m. Correlation decay under four treatment conditions in the control (B) and the double knockdown mutant (C) Correlation coefficients between images within a stack of 451 images were calculated at increased frame intervals. The frame spacings were transformed to corresponding time intervals by 2s/frame. The number of plants analyzed: Va+Vb UTi (EtOH, 8; LatB, 8; Orz, 6; OrzLatB, 6); Control RNAi (EtOH, 5; LatB, 4; Orz, 4; OrzLatB, 4). Error bars stand for standard error. Statistics on the rate parameter is shown in Table 3.1.

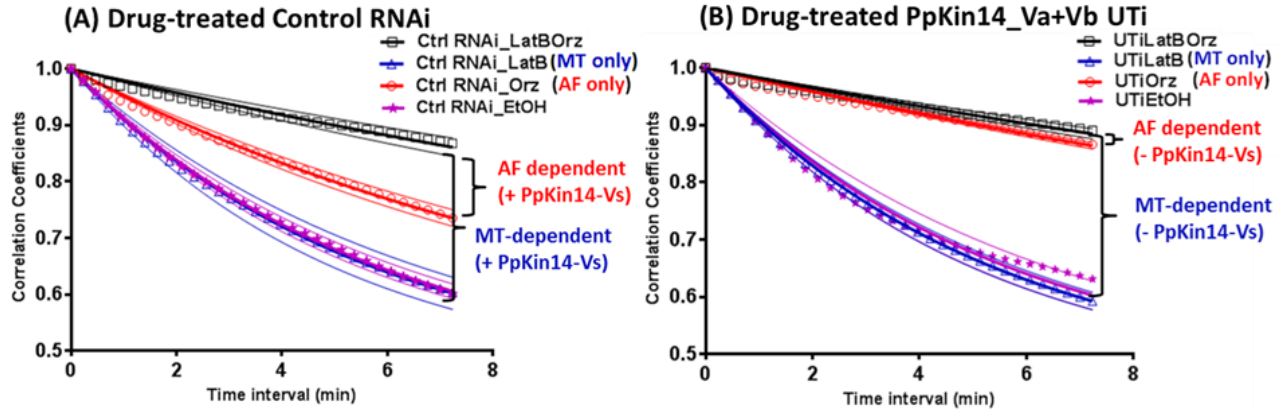


Figure 3.5: One phase exponential fit for chloroplast correlation coefficients

(A) The decays of correlation coefficients from chloroplast images in the control treated with cytoskeleton drugs are fitted by a one-phase exponential decay function in GraphPad Prism (version 6.02). Colored shapes represent actual data values of correlation coefficients of each treatment. The thicker solid line in the middle represent the best fit line, while two thinner lines represent 95% confidence intervals of the predicted best fit line. (B) The decays of correlation coefficients from chloroplast images in the mutant are fitted by a one-phase exponential decay function. The graph setting is the same as (A).

A three-parameter one phase exponential decay model was used to fit the correlation decay in chloroplasts confocal images (Figure 3.5A and B, supplementary movies 3.4). To reduce the comparisons to one parameter, the initial point was set to 1 and the plateau was set to be a shared value. This allowed us to only compare the rate parameter K (Table 3.1), which indicates differences in chloroplast dynamics between each treatment groups (see detailed explanations in material and methods). The shifts in graph from one condition to another are highlighted in Figure 3.5.

Consistent with our observations from the movies, LatB and EtOH treated plants represented in blue and pink in both ctrl and the mutant decay at about the same rate and are faster than other conditions, indicating lots of chloroplast avoidance response (Figure 3.4). The double drug treatment in black decays very slow in both the control and the mutant, indicating very little movement. Interestingly, the decay for Orz-treated ctrl in

red seems to be faster than double drug, but slower than EtOH and LatB treatment. In contrast the decay of Orz-treated mutant does not seem to differ from the double drug treatment. However these are still observations from the plots. We need to compare these decays statistically to draw conclusions.

Table 3.1 shows 28 comparisons between individual groups. A Bonferroni correction on α was applied to reduce false-positive results (type I error) when all 28 comparisons are carried out simultaneously. This table statistically supports the observation that correlation decays are different between oryzalin-treated mutant plants and oryzalin-treated control plants, supporting that PpKin14-Vs are necessary for actin-based avoidance response. Further supporting this conclusion, the correlation decay of oryzalin-treated UTi plants is not significantly different from double-drug treatment, which barely made any displacement (**Figure 3.4A** and **Table 3.1**).

Oryzalin treated ctrl RNAi and mutant are statistically different with a p-value less than 0.0001 (**Table 3.1**). Orz treated control RNAi is also different from double drug-treatment in the control and in the mutant, while the Orz-treated mutant is not different from the double drug-treatment, indicating that Pp-Kin14-Vs mediate actin-based chloroplast avoidance response (**Figure 3.5**). The EtOH and LatB groups are not different from each other, but are different from the oryzalin and double drug groups, suggesting that MTs mediate chloroplast avoidance response and that PpKin14-Vs are not required for MT-mediated avoidance response.

Table 3.1: Statistical analysis of chloroplast motility under cytoskeletal drug treatment

| p-value | Ctrl EtOH | Ctrl LatB | Ctrl Orz | Ctrl LatB+Orz | UTi EtOH | UTi LatB | UTi Orz | UTi LatB+Orz |
|--------------------------|-------------------------|------------------|------------------|--------------------|------------------|------------------|--------------------|--------------------|
| Ctrl EtOH | | 0.8062 | < 0.0001 | < 0.0001 | 0.8625 | 0.2479 | < 0.0001 | < 0.0001 |
| Ctrl LatB | | | < 0.0001 | < 0.0001 | 0.9695 | 0.5365 | < 0.0001 | < 0.0001 |
| Ctrl Orz | | | | < 0.0001 | < 0.0001 | < 0.0001 | < 0.0001 | < 0.0001 |
| Ctrl LatB+Orz | | | | | < 0.0001 | < 0.0001 | 0.6933 | 0.0067 |
| UTi EtOH | | | | | | 0.4965 | < 0.0001 | < 0.0001 |
| UTi LatB | | | | | | | < 0.0001 | < 0.0001 |
| UTi Orz | | | | | | | | 0.0001 |
| UTi LatB+Orz | | | | | | | | |
| Plateau (individual fit) | 0.4487 (minimum) | 0.4836 | 0.5633 | 0.8112 | 0.5854 | 0.4692 | 0.7841 | 0.8396 |
| Plateau (global fit) | 0.4487 | 0.4487 | 0.4487 | 0.4487 | 0.4487 | 0.4487 | 0.4487 | 0.4487 |
| K | 0.0029 | 0.0029 | 0.0015 | 0.00067 | 0.0029 | 0.0031 | 0.00065 | 0.00054 |
| 95 CI of K | 0.0027 to 0.0031 | 0.0025 to 0.0033 | 0.0014 to 0.0016 | 0.00058 to 0.00076 | 0.0026 to 0.0033 | 0.0028 to 0.0033 | 0.00062 to 0.00068 | 0.00049 to 0.00059 |
| Half-Life (sec) | 239.6 | 235.1 | 460.3 | 1034 | 236.1 | 224.1 | 1061 | 1282 |
| 95 CI of Half-Life | 224.8 to 256.4 | 205.3 to 275.1 | 426.9 to 499.5 | 911.4 to 1196 | 209.6 to 270.3 | 207.7 to 243.4 | 1012 to 1115 | 1181 to 1402 |

Note: There are 28 comparisons of the rate parameter K between individual groups; p-values for comparisons with statistical significances are marked in bold. Bonferroni adjusted $\alpha=0.05/28=0.0018$. Best fit values and 95% confidence intervals (CI) of the rate parameter K and half-life (expressed in seconds) are shown on the lower table for each condition when $Y_0=1$ and plateau=0.4487.

***Physcomitrella* chloroplast avoidance response primarily depends on MTs**

In addition, both control RNAi and the mutant plants under latrunculin B treatment which wipes out the AF cytoskeleton, showed no difference from ethanol treatment (**Figure 3.4 B and C, 3.5 A and B; Table 3.1**), indicating that MTs are primarily responsible for the observed chloroplast light avoidance response, and that MT-mediate light avoidance response does not require PpKin14-Vs. Compared with decays for ethanol-treated or latrunculin-B-treated chloroplasts, the double-drug group decays much slower (**Figure 3.4 B and C**), consistent with the observed whiter composite images which stands for less movement (**Figure 3.4A**). When AF cytoskeleton is depolymerized by latrunculin B, there are no detectable changes in chloroplast motility compared with the ethanol control (**Figure 3.5, the pink line and blue line**).

Loss of PpKin14-Vs increase actin filament dynamics but not microtubule dynamics

In addition to directly visualizing and analyzing chloroplasts movements through confocal microscopy, cytoskeletal dynamics were also visualized and recorded in the control and PpKin14-V-RNAi plants using moss lines where specific cytoskeleton elements are fluorescently tagged.

The dynamics of AFs were visualized using a lifeact-mEGFP moss line and compared between the control and the mutant phenotype. Time-lapse images were taken and processed with the correlation decay analysis described above (**Figure 3.6A, supplementary movies 3.6A**). In another moss line where the MTs are visualized through GFP-tubulin (Hiwatashi et al., 2008), confocal time-lapse images of the MT-network were collected (**Figure 3.6B, supplementary movies 3.6B**). Changes in AF dynamics are represented by correlation coefficients decays (**Figure 3.6C**). Changes in

MT dynamics are presented in the same fashion (**Figure 3.6D**). The AF correlation coefficients decay faster in the mutant than in the control, indicating increased changes in AF dynamics in the double knockdown mutant. On the other hand, MT correlation coefficients decay at the same rate between the PpKin14_Va+Vb RNAi plants and the control RNAi plants, suggesting that the two PpKin14-Vs do not affect MT dynamics. This observational comparison is statistically supported by a global nonlinear fitting analysis; we compared the correlation decays of the PpKin14_Va+Vb UTi mutant and the control RNAi using a global nonlinear regression approach in the statistics software GraphPad Prism (version 6.02) (**Figure 3.7**).

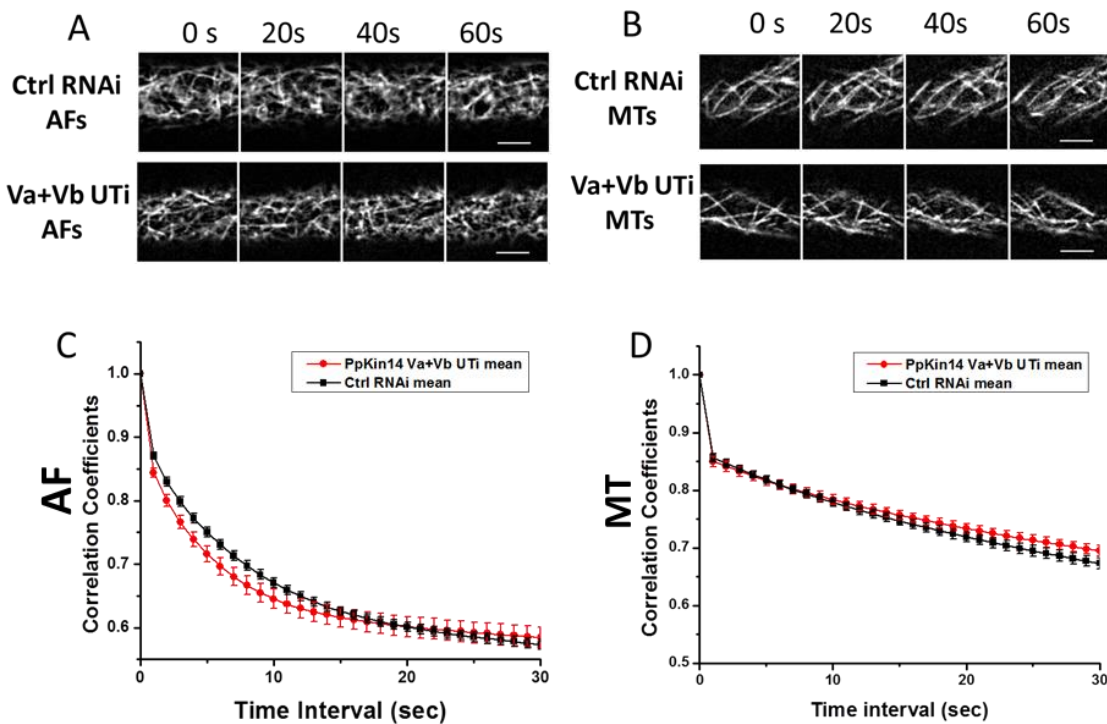


Figure 3.6: AF and MT dynamics measured by correlation coefficient decay.

(A) Cortical actin dynamics in the protonemal cells were visualized by a laser scanning confocal microscope using the F-actin marker lifeact-mEGFP. Four representative images of actin are shown at time 0-, 20-, 40- and 60-s from the control RNAi and Ppkin14 Va+Vb UTi. All images were equivalently adjusted through Gaussian blur, bandpass filter, background subtraction and contrast enhancement in ImageJ. Scale bar=5 μ m. (B) Cortical microtubule dynamics in the protonemal cells were visualized by a laser scanning confocal microscope using the GFP-labeled tubulin protein. The images are processed the same way as AF images in (A). Scale bar=5 μ m. (C)

Averaged AF correlation decay in the PpKin14 Va+Vb UTi and control RNAi plants over 60 frames of images. Correlation coefficients between images were calculated at all temporal spacings in each image stack. Lower value corresponds to higher actin dynamics. Error bars stand for SE. The number of plants analyzed: PpKin14 Va+Vb UTi, 19; Control RNAi, 17. **(D)** Averaged MT correlation decay in the PpKin14 Va+Vb UTi and control RNAi plants over 60 frames of images. Correlation coefficients are calculated the same way as in AF images. The graph is displayed in the same setting as (C). Higher value corresponds to lower MT dynamics. The number of plants analyzed: PpKin14 Va+Vb UTi, 21; Control RNAi, 18.

Table 3.2: Statistics on background noise comparison in AFs and MTs

| AF | N | Mean | SD | SEM |
|----------------------------|-------------|-------|-------------|------|
| Ctrl RNAi | 46 | 594.1 | 346.3 | 51.2 |
| PpKin14Va+Vb UTi | 53 | 662.6 | 264.6 | 36.4 |
| Difference | | 68.5 | | |
| | t Statistic | DF | Prob> t | |
| Equal Variance Assumed | 1.11 | 97 | 0.27 | |
| Equal Variance NOT Assumed | 1.09 | 83.59 | 0.28 | |

| MT | N | Mean | SD | SEM |
|----------------------------|-------------|------|--------------|-------|
| Ctrl RNAi | 44 | 1224 | 380.8 | 57.41 |
| PpKin14Va+Vb UTi | 46 | 1076 | 377.3 | 55.63 |
| Difference | | -0.3 | | |
| | t Statistic | DF | Prob> t | |
| Equal Variance Assumed | 1.85 | 88 | 0.068 | |
| Equal Variance NOT Assumed | 1.85 | 87.7 | 0.068 | |

Note: Statistics for AF noise are shown on the upper panel of in the table. Statistics for MT background noise are shown on the lower table. P-values are shown in bold indicated statistical significance at 0.05 level. (Statistics done in OriginPro 8.1 SR3)

The cytoskeletal images were filtered through an in-house developed ImageJ macro to clean the images and reduce background noises. However, due the filamentous nature of the fluorescence labeling, the level of background noise have to be evaluated before building models to make comparisons between PpKin14-Va+Vb UTi and the control RNAi. The background noises were represented by standard deviation of the background over the whole experiment time (60s). A t-test on the standard deviations demonstrates that the background noise levels are not significantly different between the mutant and the control either for AFs or for MTs (**Table 3.2**). The background noise

comparison rules out the possible effect of nonspecific signal (noise) on the analysis of cytoskeletal dynamics.

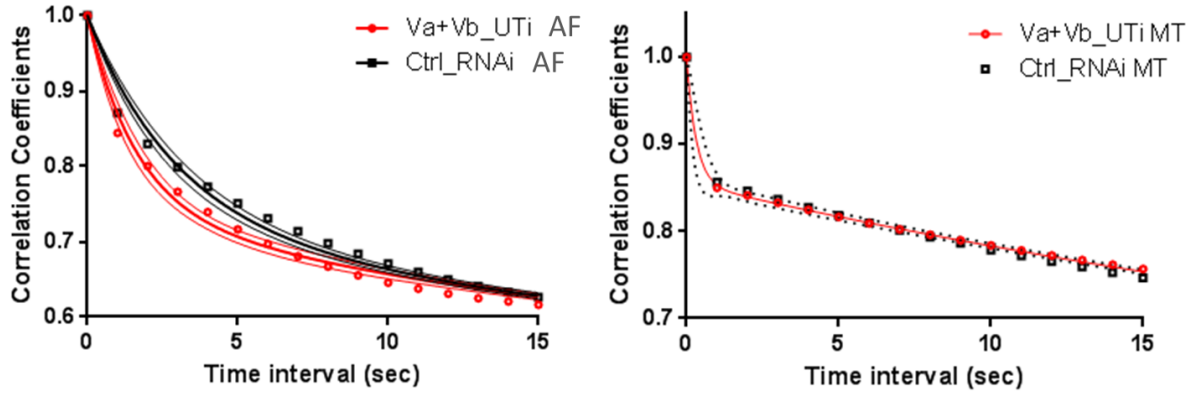


Figure 3.7: Two phase exponential fit for AF and MT correlation coefficients.

(A) The decays of correlation coefficients in cortical AFs in the mutant and in the control are fitted by two-phase exponential decays in GraphPad Prism (version 6.02). Black squares represent actual values of correlation coefficients of the control RNAi; red dots represent that of Va+Vb UTi. The thicker solid line in the middle represent the best fit line, while two thinner lines represent 95% confidence intervals of the predicted best fit line. **(B)** The decays of correlation coefficients in cortical MTs in the mutant and in the control are fitted by a global two-phase exponential decay. The red line in the middle represent the best fit line, while two dotted black lines represent 95% confidence intervals of the predicted best fit line.

Table 3.3: Statistical analysis of AF and MT correlation coefficients

| | Va+Vb_UTi AF | Ctrl_RNAi AF | | Va+Vb_UTi MT | Ctrl_RNAi MT |
|--------------------------|---------------------|---------------------|---------|-----------------|------------------|
| | | | global | | global |
| Y0 | | | 1 | | 1 |
| Plateau | | | 0.5375 | | 0.53 |
| PercentFast | | | 54.45 | | 31.16 |
| KFast | 0.6311 | 0.3597 | | | 3.165 |
| K-Slow | | | 0.05723 | | 0.02542 |
| Half-Life (Slow) | | | 12.11 | | 27.27 |
| Half-Life (Fast) | 1.098 | 1.927 | | | 0.219 |
| 95% Confidence Intervals | | | | | |
| KFast | 0.4743 to 0.7879 | 0.2974 to 0.4220 | | | 0.8024 to 5.530 |
| Half-Life (Fast) | 0.8797 to 1.462 | 1.643 to 2.331 | | | 0.1254 to 0.8641 |
| P value | < 0.0001 | | | | 0.6068 |

Note: Best fit values and 95% confidence intervals (CI) of the rate parameter KFast and half-life

(expressed in seconds) are shown for AFs and MTs when other parameters (the “global” column) are shared between the mutant and the control. P-values from are shown in bold indicated statistical significance at 0.05 level. The null hypothesis is that KFast is the same between the mutant and the control. According to the p-values from the test, two individual fittings are required for AFs ($p < 0.0001$) while one global fitting model is preferred for MTs ($p = 0.6068$).

As a nonlinear regression model, a two-phase exponential decay assumes a fast and a slow phase. There are five parameters accordingly: the initial point Y_0 , plateau, fast rate constant KFast, slow rate constant KSlow, and rate constant percentage. In the 1-minute cytoskeleton image series, we are interested comparing decays in the fast phase, which is the key parameter changing between data sets. Therefore, the decay rate parameter KFast is compared between the control RNAi and Va+Vb UTi (**Figure 3.7**), under the assumption that the whole data set share the same value for the initial point Y_0 (=1), plateau, percent fast, and KSlow.

The fitting result suggested that AF dynamics in mutant and in the control does not belong to the same population while the MT dynamics belongs to the same population. Thus we performed individual fit on the two datasets of AF dynamics. From the statistical comparisons (**Figure 3.7A**), it can be concluded that KFast for AFs in Va+Vb UTi plants differs significantly from that of the control ($p\text{-value} < 0.0001$), suggesting that actin dynamics are significantly faster in the mutant. In other words, the absence of PpKin14-Va and -Vb destabilized actin dynamics in the moss cells. On the other hand, KFast of MTs (**Figure 3.7B**) does not differ between the control and Va+Vb UTi ($p\text{-value} = 0.6068$ at significance level of 0.05), consistent with the conclusions that MTs are not required for PpKin14-Vs to function (**Figure 3.4, 3.5; Table 3.1**).

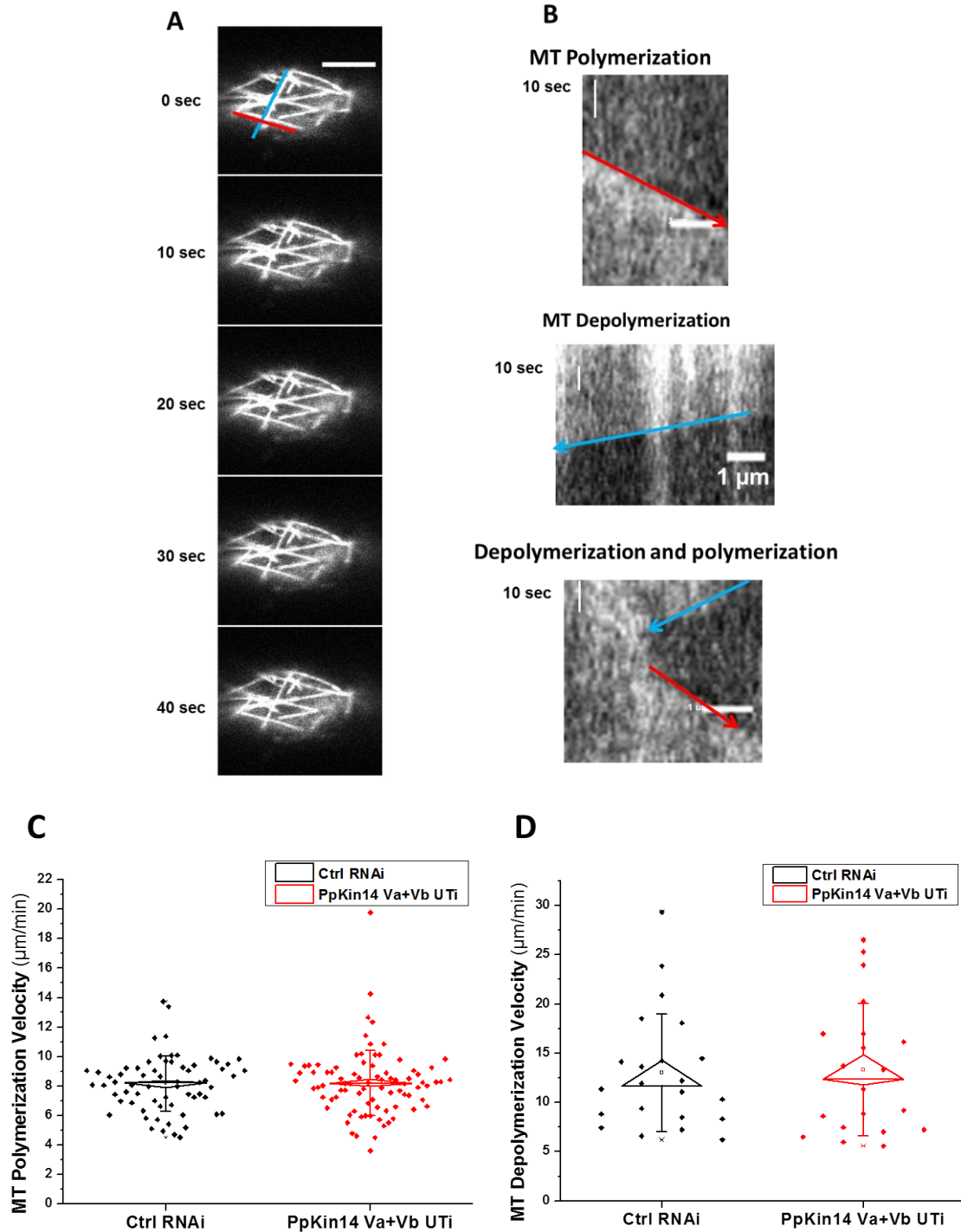


Figure 3.8: MT dynamics measured manually by kymograph analysis.

(A) Individual MTs in the mutant and in the control were identified and tracked in ImageJ to generate a kymograph over 40 seconds. Polymerization MTs are marked with red lines; depolymerization MTs are marked with blue lines. Bars = 5 μ m. (B) In the generated kymograph, the vertical direction indicates time and horizontal direction indicates distance. Vertical bars = 10sec; horizontal bars = 1 μ m. (C) Plot of microtubule polymerization rates by manual tracking the kymographs. (D) Plot of microtubule depolymerization rates by manual tracking the kymographs.

Table 3.4: Statistics on MT dynamics manually measured by kymographs

| Polymerization Rates ($\mu\text{m}/\text{min}$) | N | Mean | SD | SEM |
|---|-------------|-------|-------------|------|
| Ctrl RNAi | 65 | 8.15 | 1.87 | 0.23 |
| PpKin14Va+Vb UTi | 85 | 8.22 | 2.22 | 0.24 |
| Difference | | -0.07 | | |
| | t Statistic | DF | Prob> t | |
| Equal Variance Assumed | -0.21 | 148 | 0.84 | |
| Equal Variance NOT Assumed | -0.21 | 147 | 0.83 | |

| Depolymerization Rates($\mu\text{m}/\text{min}$) | N | Mean | SD | SEM |
|--|-------------|------|-------------|------|
| Ctrl RNAi | 22 | 13 | 5.97 | 1.27 |
| PpKin14Va+Vb UTi | 20 | 13.3 | 6.71 | 1.5 |
| Difference | | -0.3 | | |
| | t Statistic | DF | Prob> t | |
| Equal Variance Assumed | -0.15 | 40 | 0.88 | |
| Equal Variance NOT Assumed | -0.15 | 38.3 | 0.88 | |

Note: Two-sample t-test statistics on the mean, standard deviation (SD) and standard error (SEM) of MT polymerization rates are shown on the upper panel of in the table. Statistics for MT depolymerization rates are shown on the lower table. P-values are shown in bold indicated statistical significance at 0.05 level (Statistics done in OriginPro 8.1 SR3).

Further supporting the conclusions stated above we manually analyzed MTs dynamics. MT dynamics are relatively slower than that of AFs and the MT labeling is visually clearer than that of AFs, allowing us to manually track the polymerization and depolymerization of individual MTs using ImageJ (**Figure3.8A**). The growing and shrinking rates of MTs in the control and PpKin14-V-RNAi plants can be readily calculated through kymographs (**Figure3.8B**). The depolymerization rates in the mutant cells were the same as those in the control (**Figure 3.8C**). The same phenomenon was found in the polymerization rates (**Figure 3.8D**). This is the most direct measurement of the MT dynamics (**Table 3.4**), confirming that PpKin14-Vs do not affect MT dynamics; hence, PpKin14-Vs do not function through altering depolymerization and polymerization rates of the MT network.

3.4 Discussion

Chloroplast motility is carefully regulated and powered by cytoskeletal elements. In mosses, both the AF and MT cytoskeleton can transport these organelles, but the mechanism of this transport is not understood. PpKin14-Vs and ortholog genes had previously been shown to be important for chloroplast relocation, both in vascular plants and mosses (Suetsugu et al., 2010a; Suetsugu et al., 2012). Intriguingly, the original report suggested that the homologs of PpKin14-Vs in *Arabidopsis* were not associated with microtubules, but associated with actin via their C-terminal domain (Suetsugu et al., 2010a). Here we investigated the involvement of moss kinesin 14-Vs with the AFs or the MTs cytoskeletons during the blue light avoidance response. Under steady-state conditions (uniform white light) we found that loss of kinesin14-Vs function resulted in chloroplast aggregation around the nucleus, supporting a role of the two kinesins in chloroplast organization. When the role of the two kinesins in chloroplast avoidance response was evaluated, we found that it participates via the AF cytoskeleton, but not the MT cytoskeleton.

The chloroplast aggregation phenotype observed is consistent with findings of the two kinesin-like proteins, AtKAC1 and AtKAC2, in *Arabidopsis* (Suetsugu et al., 2010a; Suetsugu et al., 2012), yet there are some differences. In *Arabidopsis*, KAC1 expression is much higher than KAC2 and dominates the phenotype. KAC1 mutants were found to be partially impaired in photo-avoidance and lost their photo-accumulation response, while KAC2 mutant showed minimal deficiency in photorelocation compared with the wild type. However, the double mutant is completely deficient in both the avoidance and the accumulation response (Suetsugu et al., 2010a). Our analysis on the two PpKin14-Vs

did not show any significant difference between the Va RNAi and Vb RNAi groups in mean chloroplast island areas, solidity and normalized total area (**Figure 3.3**), indicating that the two proteins are functionally redundant in *Physcomitrella*.

While some chloroplasts accumulated to the cell center of the double mutant in *Arabidopsis* petiole cells; in *Physcomitrella*, nearly all the chloroplast aggregated to the nuclei at the cell center. KAC mutants in the fern *Adiantum capillus-veneris* also showed a phenotype where chloroplasts aggregate around the nuclei. However, nuclei were found either at the cell walls or at the upper cell surface when the *AcKAC* were mutated in the motor domain or in the conserved C-term. Thus, chloroplasts were still found to aggregate to the nucleus which is not the center of the cell in this case. This raises the possibility that kinesin14-Vs in *Adiantum capillus-veneris* interact with a cell organizing center, making it tempting to speculate that PpKin14-Vs have similar organizing function in the moss cells. It is interesting that the aggregation phenotype is stronger when the motor domain is mutated in ferns, suggesting an active functional role of the kinesin head (Suetsugu et al., 2012), but additional analyses will be required to understand how this inactive head functions. The fact that the two PpKin14-Vs show functional conservation yet some differences from their counterparts from other plant species may help further clarify this problem.

The correlation decay analysis of chloroplast motility clearly shows a dependence of PpKin14-Vs for actin-mediated chloroplast avoidance response (**Figure 3.4 - 3.7**). This result is consistent with the form of motility present in *Arabidopsis* (Suetsugu et al.), but it is puzzling that a kinesin-like molecule has adopted an actin dependent function over evolutionary time. It is tempting to speculate that this kinesin-like molecule is a

remnant of the motility mechanism present in ancestral cells, where a closer interaction between cytoskeletal elements prevailed. Although genes for kinesin14-Vs are absent in the genome of sequenced green algae (Collatos, 2012), it will be interesting to determine their presence in the streptophyta algae. Unfortunately, none of the algae that share a common ancestor with land plants has a fully sequenced genome.

We further performed correlation decay analysis of cytoskeletal elements to investigate their dynamics and a possible mechanism for the observed changes in chloroplast motility. We found a significant change in the dynamics of F-actin, but no changes were detected on MT dynamics. In the absence of PpKin14-Vs, AFs become more dynamic, suggesting that this kinesin has an AF stabilizing effect. This stability may result from a lack of polymerization-depolymerization or changes in the Brownian-motion of the filaments. Our correlation decay analysis cannot discern between the two possibilities, which will require higher temporal and spatial resolution. Nevertheless, these results provide two possible not mutually exclusive scenarios: PpKin14-Vs may modify the depolymerization, polymerization, or severing rates of F-actin (AF dynamics), alternatively they may anchor AFs to the plasma membrane, reducing their Brownian motion. The second scenario is consistent with a previous report that suggests a function of Kinesins14-Vs as an F-actin dependent chloroplast anchor to the plasma membrane (Suetsugu et al., 2012).

At steady state under white light illumination, chloroplasts of cells lacking PpKin14-Vs accumulate at the center of the cell; our preliminary experiments (data not shown) suggest this accumulation results from an actin dependent mechanism, because treating the cells with latrunculin B results in partial chloroplast dispersion. This

demonstrates that at steady state PpKin14-Vs function to maintain chloroplasts in a dispersed state; the precise mechanism for this remains to be investigated.

Here we have focused on the avoidance response because it is simpler to investigate. In a previous study in *Physcomitrella* where PpKin14Vs were deleted, the authors found impaired accumulation and avoidance responses (Suetsugu et al., 2012). Unfortunately, the authors did not report quantitative analysis or a detailed inhibitor study, as we report here. In contrast to their results, we found that the avoidance response was dominated by the microtubule cytoskeleton (**Figure 3.4** and **3.5**) and was not obviously impaired. Instead, it was necessary to disrupt the MT cytoskeleton to observe a difference between the control and the PpKin14-V-RNAi plants. The accumulation response is harder to evaluate since, in the mutant cells, the chloroplasts cluster at the center of the cell and it is more difficult to assess their accumulation at one end of the cell. Unfortunately this control is missing from the published report using knockouts (Suetsugu et al., 2012); in our hands it was difficult to consistently accumulate chloroplasts to one side of the cell using the small one week old plants needed for the transient RNAi assay. Some of the discrepancies observed may be the result of the residual levels of PpKin14-Vs present in the RNAi, but also on the lack of quantitative analysis of the knockout plants.

The UTR-based individual-gene RNAi knockdown experiments allowed us to assess the function of those two proteins independently and rapidly and demonstrated the functional redundancy of these two proteins. This analysis also tested the specificity of our silencing approach, because it was not until we combined the individual RNAi constructs that we observed the chloroplast aggregation phenotype (**Figure 3.3**).

Furthermore, this phenotype can also be observed with a CDS-RNAi that silences both genes (data not shown). It is important to note that compared with gene knockouts, our transient RNAi approach is much faster.

The phenotype we observed is similar to the CHUP1 phenotype in the moss and in *Arabidopsis* (Oikawa et al., 2008; Usami et al., 2012). CHUP1 was found to be an actin regulator on the chloroplast outer envelope. It is likely that PpKin14 Va and Vb work closely with CHUP1 to regulate the position of chloroplasts in the cell.

This report also shows how changes in correlation coefficient decay can be used to evaluate dynamics that are hard to quantify otherwise. For example, when chloroplasts are clustered, it is difficult to identify individual chloroplasts using automated computer-based algorithms. Using correlation coefficient decay analysis, changes in dynamics can quickly be evaluated. Furthermore, the analysis can be optimized to evaluate a variety of structures and dynamics at different spatial and temporal scales, as is evident from the analysis of chloroplasts (**Figure 3.4**) and cytoskeletal elements (**Figure 3.6**). In this report we also show that a detailed analysis of MTs dynamics is possible in the one week old protonemal cells (**Figure 3.8**), and that the high resolution analysis is consistent with the simpler correlation decay analysis. In the future, these different approaches could be combined as needed to quickly evaluate global dynamics or to determine specific changes in polymerization and depolymerization rates.

In a bigger picture, the chloroplast red-light receptor phytochrome and blue light receptor phototropin initiate the chloroplast photorelocation pathway upon light reception. The chloroplast responses to light are so fast that it is less likely to be controlled by changes in gene expression due to time constraints. Phototropins are not

only responsible for blue-light response pathway, but also are shown to participate in the signal transduction in the red-light response pathway (Kasahara et al., 2004). In the moss, chloroplasts use both AFs and MTs for photorelocation. While red-light responses depend on MTs, blue-light induced chloroplast photorelocation depends on actin filaments for short moves and on MTs for fast and long moves. Therefore PpKin14-Va and -Vb will fit in the actin-dependent blue-light response pathway of chloroplasts (Suetsugu and Wada, 2009). The chloroplast avoidance to blue light pathways with PpKin14-Va and -Vb incorporated are summarized in **Figure 3.9**.

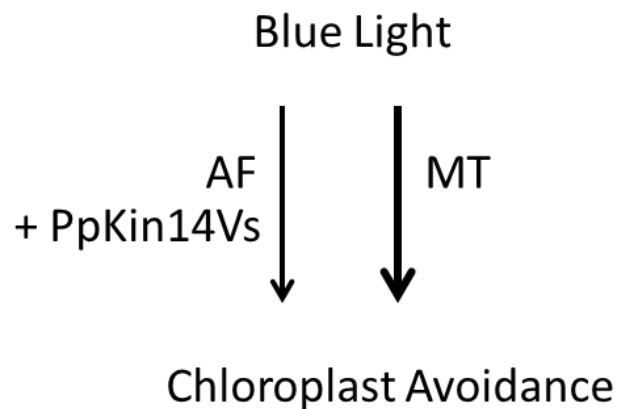


Figure 3.9: Ppkin14-Vs in blue light response pathway

Ppkin14-Vs mediate AF-based chloroplast avoidance response to blue light in the moss *Physcomitrella patens*. (Adapted from Figure 4 by Suetsugu., N. and M. Wada. (2009). Chloroplast Photorelocation Movement. The Chloroplast: Interactions with the Environment. A. S. S. H. Aronsson. Heidelberg, Germany, Springer. 13).

Both cytoplasmic and membrane bound kinesin14-Vs from *Arabidopsis* (AtKACs) were found by immunoblotting experiments (Suetsugu et al., 2010a). Furthermore, there was evidence that the AtKAC1, the predominant isoform, localized to the plasma membrane from immunolocalization assays in *Arabidopsis* root tips and from over-expressed GFP-tagged proteins in tobacco BY-2 cells. Noticeably, GFP-KAC1 was found on the plasma membrane as well as the cell plate during cell division, indicating

that the participation of the AtKAC1 in chloroplast dispersion as well as in cell division (Suetsugu and Wada, 2009). Nevertheless, although chloroplasts were observed to lose their regular dispersion in the PpKin14-Va and -Vb double knockdown, there was no observed abnormality in cell division, cell sizes, or plant growth under lab conditions.

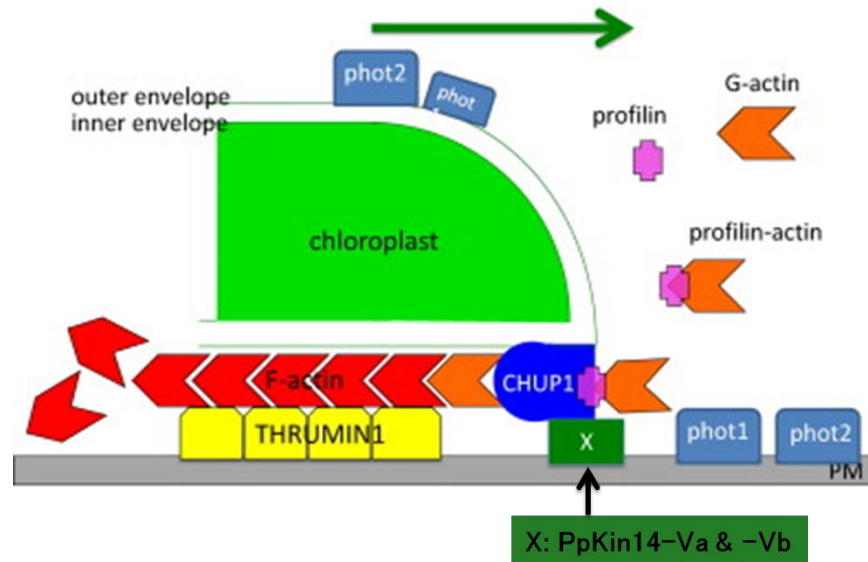


Figure 3.10: Ppkin14-Vs in the latest working model.

PpKin14-Vs might work with CHUP1 to mediate AF-based chloroplast movement. Model adapted from the latest chloroplast movement model in *Arabidopsis* (Wada, 2013). This graph adapted from **Figure 1.2** so that protein X is hypothesized as PpKin14-Va and Vb.

In the latest model for chloroplast movement in *Arabidopsis* shown in **Figure 3.10** (Wada, 2013), there is a proposed protein X that potentially works closely with CHUP1 and functions to anchor chloroplasts to the membrane. The PpKin14_Va+Vb double knockout phenotype is very similar to that of the CHUP1 mutant in *Physcomitrella* and in *Arabidopsis*. Thus it is reasonable to speculate the moss PpKin14-Vs function is conserved with the *Arabidopsis* model, which was built based on all the information we have so far on chloroplast photorelocation. Although the detailed mechanism of protein X-CHUP1 interaction, or how protein X interacts with the plasma membrane are not

known yet, it is highly likely that PpKin14-Vs fits the proposed function of the proposed protein X.

The fact the PpKin14-Va and -Vb result in a similar phenotype as CHUP1 mutants suggests that those two proteins are acting on the same pathway. PpKin14-Vs can potentially work closely with a complex of proteins that regulate the position of chloroplasts in the cell. Since Va and Vb are functionally redundant, either one of them can fulfill this function. CHUP1 connects to the chloroplasts through their N-term and functions to add profilin-actin complexes to the F-actin that is anchored to the plasma membrane (PM) by THRUMIN. Silencing protein X will result in loss of chloroplast anchorage to the PM, which agrees with the observed phenotype.

Chloroplast photorelocation in *Arabidopsis* is purely dependent on AFs, hence MTs are not present in the model (**Figure 3.10**). However, our finding confirmed that MTs participate in chloroplast movement in *Physcomitrella patens*. Furthermore, we even prove that MTs play a major role in chloroplast avoidance responses. The mechanism for the MT-mediated chloroplast avoidance response is yet to be discovered. Our systematic phylogenetic analysis (chapter 2) (Shen et al., 2012) can be used a guide in identifying kinesins that are directly as motors or indirectly involved in this process.

Acknowledgements

I would like to thank all members from the Vidali Lab for support and discussion, in particular to Dr. Yen-Chun Liu who introduced me to this project. Dr. Liu and I work cooperatively on the phenotype measurements. I performed the confocal imaging and statistical analysis. Special thanks to Jeff Bibeau who helped with nonlinear regression statistical analysis.

Chapter 4 : Concluding Remarks



The phylogenetic characterization and classification of the kinesin superfamily in the moss *Physcomitrella patens* has added to the limited knowledge and resources on kinesins in this model organism. We now know that kinesins from the majority of 14 families are present in *Physcomitrella patens*, except for family 1, 3, 6, 10 and 11. Although there is no identifiable member from kinesin 1 family in the moss, kinesins containing the armadillo repeat motifs are in close proximity with kinesin 1's from human, yeasts, and *Arabidopsis*. Because of their presence in all plants so far investigated, we classified them as a Kinesin-ARK family that is separated from the orphan kinesins. The moss *Physcomitrella patens* also contains other plant-specific kinesins such as class IV kinesin 14 and the orphan kinesins.

Based on comparisons with *Arabidopsis*, each family is subdivided into classes identified with roman numerals. Individuals from each class are designated with letters in *Physcomitrella patens* and numbers in *Arabidopsis* to avoid confusions in future comparison studies. The nomenclature proposed here is based on an established nomenclature for the kinesin superfamily in general (Lawrence et al., 2004) and has been further adapted to situations in plant kinesins. It can also be adapted to systematically characterize kinesins in other organisms where genomic and proteomic information for kinesins is available (Collatos, 2012). Deduced from research on similar kinesins in other species, the functional summaries for each family not only contribute to our understanding of kinesins in the moss, but also provide outlined guidance to future functional studies on kinesins in *Physcomitrella* and in other species.

As one example of functional analysis on specific kinesins from the phylogenetic study, the role of two moss kinesins in chloroplast photorelocation has been studied using gene-targeted knockdowns, phenotypic quantification, and chloroplasts and cytoskeletal dynamic analysis. The two kinesins are named PpKin14-Va and -Vb based on their relations in the phylogenetic tree and our proposed nomenclature. These proteins are found to be essential in maintaining chloroplast normal dispersion within the *Physcomitrella* cell. Similar to their homologs in *Arabidopsis*, they mediate AF-based chloroplast avoidance response.

In summary (**Table 4.1**), *Physcomitrella* PpKin14-Va and -Vb are functionally equivalent in keeping chloroplasts dispersed throughout the cell in the white light condition. PpKin14-Vs mediate AF-dependent, not MT-dependent, chloroplast light avoidance response. In addition, AF dynamics are lower in the presence of PpKin14-Vs, suggesting that PpKin14-Vs may function directly or indirectly through stabilizing AFs. Interestingly PpKin14-Vs are not necessary for MT-dependent chloroplast avoidance response. In contrast to chloroplast avoidance response in *Arabidopsis* which solely depends on AFs, MTs play a major role in the chloroplast avoidance response in *Physcomitrella*; this MT dependent response does not require the participation of either of the two PpKin14-Vs. The identified roles of PpKin14-Vs have added to our knowledge for chloroplast light avoidance response in moss, which is part of the complicated process of chloroplast photorelocation.

Table 4.1: PpKin14-Va &-Vb function summary

| | WT | Mutant |
|--|---|---|
| PpKin14Va & Vb | ✓ | X |
| Under white light |  |  |
| Changes in AF dynamics | X | ✓ increased |
| Changes in MT dynamics | X | X |
| AF-mediated chloroplast avoidance response | ✓ | X |
| MT-mediated chloroplast avoidance response | ✓ | ✓ |

The research methods used in this study can be readily applied to similar studies. For instance, RNAi silencing can be used to address the function of one or more genes rapidly. Our phenotypic quantification method can be used to quantify and compare phenotypes where cells differ in shape, size and/or internal area. The correlation coefficient decay analysis is a sensitive measure for changing dynamics of a process, especially useful for those processes where direct measurements are difficult to acquire. Using similar approaches and novel methods such as biochemical analysis, the role of PpKin14-Vs in chloroplast positioning and relocation can be further clarified to build a more detailed description of how chloroplasts response to light stimuli.

References

- Ambrose, J.C., and Cyr, R. (2007). The kinesin ATK5 functions in early spindle assembly in *Arabidopsis*. *Plant Cell* 19, 226-236.
- Ambrose, J.C., Li, W., Marcus, A., Ma, H., and Cyr, R. (2005). A minus-end-directed kinesin with plus-end tracking protein activity is involved in spindle morphogenesis. *Mol Biol Cell* 16, 1584-1592.
- Bannigan, A., Lizotte-Waniewski, M., Riley, M., and Baskin, T.I. (2008). Emerging molecular mechanisms that power and regulate the anastral mitotic spindle of flowering plants. *Cell Motil Cytoskeleton* 65, 1-11.
- Bannigan, A., Scheible, W.R., Lukowitz, W., Fagerstrom, C., Wadsworth, P., Somerville, C., and Baskin, T.I. (2007). A conserved role for kinesin-5 in plant mitosis. *J Cell Sci* 120, 2819-2827.
- Beningo, K.A., Lillie, S.H., and Brown, S.S. (2000). The yeast kinesin-related protein Smy1p exerts its effects on the class V myosin Myo2p via a physical interaction. *Mol Biol Cell* 11, 691-702.
- Bernstein, M., Beech, P.L., Katz, S.G., and Rosenbaum, J.L. (1994). A new kinesin-like protein (Klp1) localized to a single microtubule of the *Chlamydomonas* flagellum. *J Cell Biol* 125, 1313-1326.
- Bezanilla, M., Pan, A., and Quatrano, R.S. (2003). RNA interference in the moss *Physcomitrella patens*. *Plant Physiol* 133, 470-474.
- Bezanilla, M., Perroud, P.F., Pan, A., Klueh, P., and Quatrano, R.S. (2005). An RNAi system in *Physcomitrella patens* with an internal marker for silencing allows for rapid identification of loss of function phenotypes. *Plant Biol (Stuttg)* 7, 251-257.
- Bouquin, T., Mattsson, O., Naested, H., Foster, R., and Mundy, J. (2003). The *Arabidopsis* lue1 mutant defines a katanin p60 ortholog involved in hormonal control of microtubule orientation during cell growth. *J Cell Sci* 116, 791-801.
- Bowser, J., and Reddy, A.S. (1997). Localization of a kinesin-like calmodulin-binding protein in dividing cells of *Arabidopsis* and tobacco. *Plant J* 12, 1429-1437.
- Buster, D.W., Baird, D.H., Yu, W.Q., Solowska, J.M., Chauviere, M., Mazurek, A., Kress, M., and Baas, P.W. (2003). Expression of the mitotic kinesin Kif15 in postmitotic neurons: Implications for neuronal migration and development. *Journal of Neurocytology* 32, 79-96.
- Cai, G., and Cresti, M. (2010). Microtubule motors and pollen tube growth--still an open question. *Protoplasma* 247, 131-143.

- Chen, C., Marcus, A., Li, W., Hu, Y., Calzada, J.P., Grossniklaus, U., Cyr, R.J., and Ma, H. (2002). The *Arabidopsis* ATK1 gene is required for spindle morphogenesis in male meiosis. *Development* 129, 2401-2409.
- Christie, J.M. (2007). Phototropin blue-light receptors. *Annu Rev Plant Biol* 58, 21-45.
- Coates, J.C. (2003). Armadillo repeat proteins: beyond the animal kingdom. *Trends in Cell Biology* 13, 463-471.
- Collatos, A.R. (2012). *Transformation, Growth, and the Cytoskeleton: Tools to Study Oil Producing Algae*. Master's thesis Master's thesis, Worcester Polytechnic Institute.
- Cove, D. (2005). The moss *Physcomitrella patens*. *Annu Rev Genet* 39, 339-358.
- Cove, D.J., Perroud, P.F., Charron, A.J., Mcdaniel, S.F., Khandelwal, A., and Quatrano, R.S. (2009). The moss *Physcomitrella patens*: a novel model system for plant development and genomic studies. *Cold Spring Harb Protoc* 2009, pdb emo115.
- Dagenbach, E.M., and Endow, S.A. (2004). A new kinesin tree. *J Cell Sci* 117, 3-7.
- Deblasio, S.L., Luesse, D.L., and Hangarter, R.P. (2005). A plant-specific protein essential for blue-light-induced chloroplast movements. *Plant Physiol* 139, 101-114.
- Deblasio, S.L., Mullen, J.L., Luesse, D.R., and Hangarter, R.P. (2003). Phytochrome modulation of blue light-induced chloroplast movements in *Arabidopsis*. *Plant Physiol* 133, 1471-1479.
- Demonchy, R., Blisnick, T., Deprez, C., Toutirais, G., Loussert, C., Marande, W., Grellier, P., Bastin, P., and Kohl, L. (2009). Kinesin 9 family members perform separate functions in the trypanosome flagellum. *J Cell Biol* 187, 615-622.
- Doi, M., Shigenaga, A., Emi, T., Kinoshita, T., and Shimazaki, K. (2004). A transgene encoding a blue-light receptor, phot1, restores blue-light responses in the *Arabidopsis* phot1 phot2 double mutant. *J Exp Bot* 55, 517-523.
- Doi, M., Wada, M., and Shimazaki, K. (2006). The fern *Adiantum capillus-veneris* lacks stomatal responses to blue light. *Plant and Cell Physiology* 47, 748-755.
- Ferenz, N.P., Gable, A., and Wadsworth, P. (2010). Mitotic functions of kinesin-5. *Semin Cell Dev Biol* 21, 255-259.
- Frey, N., Klotz, J., and Nick, P. (2009). Dynamic bridges--a calponin-domain kinesin from rice links actin filaments and microtubules in both cycling and non-cycling cells. *Plant Cell Physiol* 50, 1493-1506.

- Furuta, K., and Toyoshima, Y.Y. (2008). Minus-end-directed motor Ncd exhibits processive movement that is enhanced by microtubule bundling in vitro. *Curr Biol* 18, 152-157.
- Geelen, D.N., and Inze, D.G. (2001). A bright future for the bright yellow-2 cell culture. *Plant Physiol* 127, 1375-1379.
- Goto, Y., and Asada, T. (2007). Excessive expression of the plant kinesin TBK5 converts cortical and perinuclear microtubules into a radial array emanating from a single focus. *Plant Cell Physiol* 48, 753-761.
- Guindon, S., Dufayard, J.F., Lefort, V., Anisimova, M., Hordijk, W., and Gascuel, O. (2010). New algorithms and methods to estimate maximum-likelihood phylogenies: assessing the performance of PhyML 3.0. *Syst Biol* 59, 307-321.
- Hagan, I., and Yanagida, M. (1992). Kinesin-related cut7 protein associates with mitotic and meiotic spindles in fission yeast. *Nature* 356, 74-76.
- Henikoff, L.G.S. (1996). *The KinesinHomePage-The Kinesin-14 Family* [Online]. Available: http://www.proweb.org/kinesin/BE4_Cterm.html [Accessed September-2 2013].
- Hiwatashi, Y., Obara, M., Sato, Y., Fujita, T., Murata, T., and Hasebe, M. (2008). Kinesins are indispensable for interdigitation of phragmoplast microtubules in the moss *Physcomitrella patens*. *Plant Cell* 20, 3094-3106.
- Ichikawa, S., Yamada, N., Suetsugu, N., Wada, M., and Kadota, A. (2011). Red Light, Phot1 and JAC1 Modulate Phot2-Dependent Reorganization of Chloroplast Actin Filaments and Chloroplast Avoidance Movement. *Plant and Cell Physiology* 52, 1422-1432.
- Itoh, R., Fujiwara, M., and Yoshida, S. (2001). Kinesin-related proteins with a mitochondrial targeting signal. *Plant Physiol* 127, 724-726.
- Kadota, A., Yamada, N., Sato, Y., Oikawa, K., Nakai, M., Ogura, Y., Kasahara, M., Kagawa, T., Suetsugu, N., and Wada, M. (2006). Role of actin in the chloroplast photorelocation movement of Arabidopsis. *Plant and Cell Physiology* 47, S40-S40.
- Kadota, A., Yamada, N., Suetsugu, N., Hirose, M., Saito, C., Shoda, K., Ichikawa, S., Kagawa, T., Nakano, A., and Wada, M. (2009). Short actin-based mechanism for light-directed chloroplast movement in Arabidopsis. *Proceedings of the National Academy of Sciences of the United States of America* 106, 13106-13111.
- Kagawa, T., Kasahara, M., Abe, T., Yoshida, S., and Wada, M. (2004). Function analysis of phototropin2 using fern mutants deficient in blue light-induced chloroplast

- avoidance movement. *Plant Cell Physiol* 45, 416-426.
- Kagawa, T., and Wada, M. (1999). Chloroplast-avoidance response induced by high-fluence blue light in prothallial cells of the fern *Adiantum capillus-veneris* as analyzed by microbeam irradiation. *Plant Physiol* 119, 917-924.
- Kandasamy, M.K., and Meagher, R.B. (1999). Actin-organelle interaction: association with chloroplast in *Arabidopsis* leaf mesophyll cells. *Cell Motil Cytoskeleton* 44, 110-118.
- Kasahara, M., Kagawa, T., Oikawa, K., Suetsugu, N., Miyao, M., and Wada, M. (2002). Chloroplast avoidance movement reduces photodamage in plants. *Nature* 420, 829-832.
- Kasahara, M., Kagawa, T., Sato, Y., Kiyosue, T., and Wada, M. (2004). Phototropins mediate blue and red light-induced chloroplast movements in *Physcomitrella patens*. *Plant Physiology* 135, 1388-1397.
- Knight, C.D., and Perroud, P.-F. (2001). "*Physcomitrella patens*: A Model Bryophyte," in *eLS*. John Wiley & Sons, Ltd).
- Kodama, Y., Tsuboi, H., Kagawa, T., and Wada, M. (2008). Low temperature-induced chloroplast relocation mediated by a blue light receptor, phototropin 2, in fern gametophytes. *Journal of Plant Research* 121, 441-448.
- Kong, L.J., and Hanley-Bowdoin, L. (2002). A geminivirus replication protein interacts with a protein kinase and a motor protein that display different expression patterns during plant development and infection. *Plant Cell* 14, 1817-1832.
- Kong, S.G., Arai, Y., Suetsugu, N., Yanagida, T., and Wada, M. (2013). Rapid Severing and Motility of Chloroplast-Actin Filaments Are Required for the Chloroplast Avoidance Response in *Arabidopsis*. *Plant Cell* 25, 572-590.
- Kull, F.J., Vale, R.D., and Fletterick, R.J. (1998). The case for a common ancestor: kinesin and myosin motor proteins and G proteins. *J Muscle Res Cell Motil* 19, 877-886.
- Lawrence, C.J., Dawe, R.K., Christie, K.R., Cleveland, D.W., Dawson, S.C., Endow, S.A., Goldstein, L.S., Goodson, H.V., Hirokawa, N., Howard, J., Malmberg, R.L., McIntosh, J.R., Miki, H., Mitchison, T.J., Okada, Y., Reddy, A.S., Saxton, W.M., Schliwa, M., Scholey, J.M., Vale, R.D., Walczak, C.E., and Wordeman, L. (2004). A standardized kinesin nomenclature. *J Cell Biol* 167, 19-22.
- Lee, Y.R., Giang, H.M., and Liu, B. (2001). A novel plant kinesin-related protein specifically associates with the phragmoplast organelles. *Plant Cell* 13, 2427-2439.

- Lee, Y.R., and Liu, B. (2000). Identification of a phragmoplast-associated kinesin-related protein in higher plants. *Curr Biol* 10, 797-800.
- Lee, Y.R., and Liu, B. (2004). Cytoskeletal motors in *Arabidopsis*. Sixty-one kinesins and seventeen myosins. *Plant Physiol* 136, 3877-3883.
- Li, J., Jiang, J., Qian, Q., Xu, Y., Zhang, C., Xiao, J., Du, C., Luo, W., Zou, G., Chen, M., Huang, Y., Feng, Y., Cheng, Z., Yuan, M., and Chong, K. (2011). Mutation of rice BC12/GDD1, which encodes a kinesin-like protein that binds to a GA biosynthesis gene promoter, leads to dwarfism with impaired cell elongation. *Plant Cell* 23, 628-640.
- Lillie, S.H., and Brown, S.S. (1998). Smy1p, a kinesin-related protein that does not require microtubules. *J Cell Biol* 140, 873-883.
- Liu, B., Cyr, R.J., and Palevitz, B.A. (1996). A kinesin-like protein, KatAp, in the cells of *Arabidopsis* and other plants. *Plant Cell* 8, 119-132.
- Liu, Y.C., and Vidali, L. (2011). Efficient polyethylene glycol (PEG) mediated transformation of the moss *Physcomitrella patens*. *J Vis Exp*.
- Lu, L., Lee, Y.R., Pan, R., Maloof, J.N., and Liu, B. (2005). An internal motor kinesin is associated with the Golgi apparatus and plays a role in trichome morphogenesis in *Arabidopsis*. *Mol Biol Cell* 16, 811-823.
- Luesse, D.R., Deblasio, S.L., and Hangarter, R.P. (2010). Integration of Phot1, Phot2, and PhyB signalling in light-induced chloroplast movements. *J Exp Bot* 61, 4387-4397.
- Ma, Y.Z., and Taylor, E.W. (1995). Mechanism of microtubule kinesin ATPase. *Biochemistry* 34, 13242-13251.
- Marcus, A.I., Li, W., Ma, H., and Cyr, R.J. (2003). A kinesin mutant with an atypical bipolar spindle undergoes normal mitosis. *Mol Biol Cell* 14, 1717-1726.
- Meluh, P.B., and Rose, M.D. (1990). KAR3, a kinesin-related gene required for yeast nuclear fusion. *Cell* 60, 1029-1041.
- Menzel, D., and Schliwa, M. (1986). Motility in the siphonous green alga *Bryopsis*. II. Chloroplast movement requires organized arrays of both microtubules and actin filaments. *European journal of cell biology* 40, 286-295.
- Miki, H., Okada, Y., and Hirokawa, N. (2005). Analysis of the kinesin superfamily: insights into structure and function. *Trends Cell Biol* 15, 467-476.
- Miki, H., Setou, M., Kaneshiro, K., and Hirokawa, N. (2001). All kinesin superfamily

- protein, KIF, genes in mouse and human. *Proc Natl Acad Sci U S A* 98, 7004-7011.
- Motulsky, H., and Christopoulos, A. (2004). *Fitting models to biological data using linear and nonlinear regression : a practical guide to curve fitting*. Oxford ; New York: Oxford University Press.
- Muller, S., Han, S., and Smith, L.G. (2006). Two kinesins are involved in the spatial control of cytokinesis in *Arabidopsis thaliana*. *Curr Biol* 16, 888-894.
- Narasimhulu, S.B., Kao, Y.L., and Reddy, A.S.N. (1997). Interaction of *Arabidopsis* kinesin-like calmodulin binding protein with tubulin subunits: modulation by Ca²⁺-calmodulin. *Plant Journal* 12, 1139-1149.
- Nath, S., Bananis, E., Sarkar, S., Stockert, R.J., Sperry, A.O., Murray, J.W., and Wolkoff, A.W. (2007). Kif5B and Kifc1 interact and are required for motility and fission of early endocytic vesicles in mouse liver. *Mol Biol Cell* 18, 1839-1849.
- Ni, C.Z., Wang, H.Q., Xu, T., Qu, Z., and Liu, G.Q. (2005). AtKP1, a kinesin-like protein, mainly localizes to mitochondria in *Arabidopsis thaliana*. *Cell Res* 15, 725-733.
- Nozue, K., Kanegae, T., Imaizumi, T., Fukuda, S., Okamoto, H., Yeh, K.C., Lagarias, J.C., and Wada, M. (1998). A phytochrome from the fern *Adiantum* with features of the putative photoreceptor NPH1. *Proc Natl Acad Sci U S A* 95, 15826-15830.
- Oikawa, K., Kasahara, M., Kiyosue, T., Kagawa, T., Suetsugu, N., Takahashi, F., Kanegae, T., Niwa, Y., Kadota, A., and Wada, M. (2003). CHLOROPLAST UNUSUAL POSITIONING1 is essential for proper chloroplast positioning. *Plant Cell* 15, 2805-2815.
- Oikawa, K., Yamasato, A., Kong, S.G., Kasahara, M., Nakai, M., Takahashi, F., Ogura, Y., Kagawa, T., and Wada, M. (2008). Chloroplast outer envelope protein CHUP1 is essential for chloroplast anchorage to the plasma membrane and chloroplast movement. *Plant Physiology* 148, 829-842.
- Oppenheimer, D.G., Pollock, M.A., Vacik, J., Szymanski, D.B., Ericson, B., Feldmann, K., and Marks, M.D. (1997). Essential role of a kinesin-like protein in *Arabidopsis* trichome morphogenesis. *Proc Natl Acad Sci U S A* 94, 6261-6266.
- Pan, R.Q., Lee, Y.R., and Liu, B. (2004). Localization of two homologous *Arabidopsis* kinesin-related proteins in the phragmoplast. *Planta* 220, 156-164.
- Peters, C., Brejc, K., Belmont, L., Bodey, A.J., Lee, Y., Yu, M., Guo, J., Sakowicz, R., Hartman, J., and Moores, C.A. (2010). Insight into the molecular mechanism of the multitasking kinesin-8 motor. *Embo Journal* 29, 3437-3447.

- Preuss, M.L., Kovar, D.R., Lee, Y.R., Staiger, C.J., Delmer, D.P., and Liu, B. (2004). A plant-specific kinesin binds to actin microfilaments and interacts with cortical microtubules in cotton fibers. *Plant Physiol* 136, 3945-3955.
- Rashid, D.J., Wedaman, K.P., and Scholey, J.M. (1995). Heterodimerization of the two motor subunits of the heterotrimeric kinesin, KRP85/95. *J Mol Biol* 252, 157-162.
- Reddy, A.S., and Day, I.S. (2001). Kinesins in the Arabidopsis genome: a comparative analysis among eukaryotes. *BMC Genomics* 2, 2.
- Rensing, S.A., Lang, D., Zimmer, A.D., Terry, A., Salamov, A., Shapiro, H., Nishiyama, T., Perroud, P.F., Lindquist, E.A., Kamisugi, Y., Tanahashi, T., Sakakibara, K., Fujita, T., Oishi, K., Shin, I.T., Kuroki, Y., Toyoda, A., Suzuki, Y., Hashimoto, S., Yamaguchi, K., Sugano, S., Kohara, Y., Fujiyama, A., Anterola, A., Aoki, S., Ashton, N., Barbazuk, W.B., Barker, E., Bennetzen, J.L., Blankenship, R., Cho, S.H., Dutcher, S.K., Estelle, M., Fawcett, J.A., Gundlach, H., Hanada, K., Heyl, A., Hicks, K.A., Hughes, J., Lohr, M., Mayer, K., Melkozernov, A., Murata, T., Nelson, D.R., Pils, B., Prigge, M., Reiss, B., Renner, T., Rombauts, S., Rushton, P.J., Sanderfoot, A., Schween, G., Shiu, S.H., Stueber, K., Theodoulou, F.L., Tu, H., Van De Peer, Y., Verrier, P.J., Waters, E., Wood, A., Yang, L., Cove, D., Cuming, A.C., Hasebe, M., Lucas, S., Mishler, B.D., Reski, R., Grigoriev, I.V., Quatrano, R.S., and Boore, J.L. (2008). The *Physcomitrella* genome reveals evolutionary insights into the conquest of land by plants. *Science* 319, 64-69.
- Richardson, D.N., Simmons, M.P., and Reddy, A.S. (2006). Comprehensive comparative analysis of kinesins in photosynthetic eukaryotes. *BMC Genomics* 7, 18.
- Robertson, E.J., and Leech, R.M. (1995). Significant Changes in Cell and Chloroplast Development in Young Wheat Leaves (*Triticum aestivum* cv Hereward) Grown in Elevated CO₂. *Plant Physiol* 107, 63-71.
- Rogers, G.C., Chui, K.K., Lee, E.W., Wedaman, K.P., Sharp, D.J., Holland, G., Morris, R.L., and Scholey, J.M. (2000). A kinesin-related protein, KRP(180), positions prometaphase spindle poles during early sea urchin embryonic cell division. *J Cell Biol* 150, 499-512.
- Sakai, T., Honing, H., Nishioka, M., Uehara, Y., Takahashi, M., Fujisawa, N., Saji, K., Seki, M., Shinozaki, K., Jones, M.A., Smirnov, N., Okada, K., and Wasteneys, G.O. (2008). Armadillo repeat-containing kinesins and a NIMA-related kinase are required for epidermal-cell morphogenesis in *Arabidopsis*. *Plant J* 53, 157-171.
- Sakamoto, W., Miyagishima, S.Y., and Jarvis, P. (2008). Chloroplast biogenesis: control of plastid development, protein import, division and inheritance. *Arabidopsis Book* 6, e0110.
- Sasabe, M., Boudolf, V., De Veylder, L., Inze, D., Genschik, P., and Machida, Y. (2011).

- Phosphorylation of a mitotic kinesin-like protein and a MAPKKK by cyclin-dependent kinases (CDKs) is involved in the transition to cytokinesis in plants. *Proc Natl Acad Sci U S A* 108, 17844-17849.
- Sato, Y., and Kadota, A. (2006). "Chloroplast Movements in Response to Environmental Signals," in *The Structure and Function of Plastids*, eds. R. Wise & J.K. Hooper. Springer Netherlands), 527-537.
- Sato, Y., Wada, M., and Kadota, A. (2001). Choice of tracks, microtubules and/or actin filaments for chloroplast photo-movement is differentially controlled by phytochrome and a blue light receptor. *Journal of Cell Science* 114, 269-279.
- Sazuka, T., Aichi, I., Kawai, T., Matsuo, N., Kitano, H., and Matsuoka, M. (2005). The rice mutant dwarf bamboo shoot 1: a leaky mutant of the NACK-type kinesin-like gene can initiate organ primordia but not organ development. *Plant Cell Physiol* 46, 1934-1943.
- Schallus, T., Jaech, C., Feher, K., Palma, A.S., Liu, Y., Simpson, J.C., Mackeen, M., Stier, G., Gibson, T.J., Feizi, T., Pieler, T., and Muhle-Goll, C. (2008). Malectin: a novel carbohydrate-binding protein of the endoplasmic reticulum and a candidate player in the early steps of protein N-glycosylation. *Mol Biol Cell* 19, 3404-3414.
- Senn, G. (1908). Die Gestalts- und Lageveränderung der Pflanzen-Chromatophoren
- Setou, M., Nakagawa, T., Seog, D.H., and Hirokawa, N. (2000). Kinesin superfamily motor protein KIF17 and mLin-10 in NMDA receptor-containing vesicle transport. *Science* 288, 1796-1802.
- Shen, Z., Collatos, A.R., Bibeau, J.P., Furt, F., and Vidali, L. (2012). Phylogenetic analysis of the Kinesin superfamily from physcomitrella. *Front Plant Sci* 3, 230.
- Sloboda, R.D., and Howard, L. (2007). Localization of EB1, IFT polypeptides, and kinesin-2 in *Chlamydomonas* flagellar axonemes via immunogold scanning electron microscopy. *Cell Motil Cytoskeleton* 64, 446-460.
- Straight, A.F., Sedat, J.W., and Murray, A.W. (1998). Time-lapse microscopy reveals unique roles for kinesins during anaphase in budding yeast. *J Cell Biol* 143, 687-694.
- Suetsugu, N., Sato, Y., Tsuboi, H., Kasahara, M., Imaizumi, T., Kagawa, T., Hiwatashi, Y., Hasebe, M., and Wada, M. (2012). The KAC Family of Kinesin-Like Proteins is Essential for the Association of Chloroplasts with the Plasma Membrane in Land Plants. *Plant and Cell Physiology* 53, 1854-1865.

- Suetsugu, N., and Wada, M. (2007a). Chloroplast photorelocation movement mediated by phototropin family proteins in green plants. *Biological Chemistry* 388, 927-935.
- Suetsugu, N., and Wada, M. (2007b). Phytochrome-dependent photomovement responses mediated by phototropin family proteins in cryptogam plants. *Photochemistry and Photobiology* 83, 87-93.
- Suetsugu, N., and Wada, M. (2009). "Chloroplast Photorelocation Movement," in *The Chloroplast*, eds. A. Sandelius & H. Aronsson. Springer Berlin Heidelberg), 235-266.
- Suetsugu, N., Yamada, N., Kagawa, T., Yonekura, H., Uyeda, T., Kadota, A., and Wada, M. (2010a). Two kinesin-like proteins mediate actin-based chloroplast movement in *Arabidopsis thaliana*. *Proceedings of the National Academy of Sciences of the United States of America* 107, 8860-8865.
- Suetsugu, N., Yamada, N., Kagawa, T., Yonekura, H., Uyeda, T.Q., Kadota, A., and Wada, M. (2010b). Two kinesin-like proteins mediate actin-based chloroplast movement in *Arabidopsis thaliana*. *Proc Natl Acad Sci U S A* 107, 8860-8865.
- Takagi, S. (2003). Actin-based photo-orientation movement of chloroplasts in plant cells. *J Exp Biol* 206, 1963-1969.
- Takagi, S., Kong, S.G., Mineyuki, Y., and Furuya, M. (2003). Regulation of actin-dependent cytoplasmic motility by type II phytochrome occurs within seconds in *Vallisneria spiralis* epidermal cells. *Plant Cell* 15, 331-345.
- Takahashi, Y., Soyano, T., Kosetsu, K., Sasabe, M., and Machida, Y. (2010). HINKEL kinesin, ANP MAPKKs and MKK6/ANQ MAPKK, which phosphorylates and activates MPK4 MAPK, constitute a pathway that is required for cytokinesis in *Arabidopsis thaliana*. *Plant Cell Physiol* 51, 1766-1776.
- Tamura, K., Nakatani, K., Mitsui, H., Ohashi, Y., and Takahashi, H. (1999). Characterization of katD, a kinesin-like protein gene specifically expressed in floral tissues of *Arabidopsis thaliana*. *Gene* 230, 23-32.
- Tanaka, H., Ishikawa, M., Kitamura, S., Takahashi, Y., Soyano, T., Machida, C., and Machida, Y. (2004). The AtNACK1/HINKEL and STUD/TETRASPORE/AtNACK2 genes, which encode functionally redundant kinesins, are essential for cytokinesis in *Arabidopsis*. *Genes Cells* 9, 1199-1211.
- Tanenbaum, M.E., Macurek, L., Janssen, A., Geers, E.F., Alvarez-Fernandez, M., and Medema, R.H. (2009). Kif15 cooperates with eg5 to promote bipolar spindle assembly. *Curr Biol* 19, 1703-1711.
- Taylor, E.W. (1979). Mechanism of actomyosin ATPase and the problem of muscle

- contraction. *CRC Crit Rev Biochem* 6, 103-164.
- Thormahlen, M., Marx, A., Sack, S., and Mandelkow, E. (1998). The coiled-coil helix in the neck of kinesin. *J Struct Biol* 122, 30-41.
- Thornton, L.E., Keren, N., Ohad, I., and Pakrasi, H.B. (2005). *Physcomitrella patens* and *Ceratodon purpureus*, mosses as model organisms in photosynthesis studies. *Photosynth Res* 83, 87-96.
- Tokai, N., Fujimoto-Nishiyama, A., Toyoshima, Y., Yonemura, S., Tsukita, S., Inoue, J., and Yamamota, T. (1996). Kid, a novel kinesin-like DNA binding protein, is localized to chromosomes and the mitotic spindle. *EMBO J* 15, 457-467.
- Tsuboi, H., Suetsugu, N., Kawai-Toyooka, H., and Wada, M. (2007). Phototropins and neochromel mediate nuclear movement in the fern *Adiantum capillus-veneris*. *Plant and Cell Physiology* 48, 892-896.
- Tsuboi, H., and Wada, M. (2012). Distribution pattern changes of actin filaments during chloroplast movement in *Adiantum capillus-veneris*. *Journal of Plant Research* 125, 417-428.
- Umezu, N., Umeki, N., Mitsui, T., Kondo, K., and Maruta, S. (2011). Characterization of a novel rice kinesin O12 with a calponin homology domain. *J Biochem* 149, 91-101.
- Usami, H., Maeda, T., Fujii, Y., Oikawa, K., Takahashi, F., Kagawa, T., Wada, M., and Kasahara, M. (2012). CHUP1 mediates actin-based light-induced chloroplast avoidance movement in the moss *Physcomitrella patens*. *Planta* 236, 1889-1897.
- Vale, R.D. (2003). The molecular motor toolbox for intracellular transport. *Cell* 112, 467-480.
- Vanstraelen, M., Torres Acosta, J.A., De Veylder, L., Inze, D., and Geelen, D. (2004). A plant-specific subclass of C-terminal kinesins contains a conserved a-type cyclin-dependent kinase site implicated in folding and dimerization. *Plant Physiol* 135, 1417-1429.
- Vidali, L., Augustine, R.C., Kleinman, K.P., and Bezanilla, M. (2007). Profilin is essential for tip growth in the moss *Physcomitrella patens*. *Plant Cell* 19, 3705-3722.
- Vidali, L., and Bezanilla, M. (2012). *Physcomitrella patens*: a model for tip cell growth and differentiation. *Curr Opin Plant Biol* 15, 625-631.
- Vidali, L., Burkart, G.M., Augustine, R.C., Kerdavid, E., Tuzel, E., and Bezanilla, M. (2010). Myosin XI is essential for tip growth in *Physcomitrella patens*. *Plant Cell* 22, 1868-1882.

- Vidali, L., Rounds, C.M., Hepler, P.K., and Bezanilla, M. (2009). Lifeact-mEGFP reveals a dynamic apical F-actin network in tip growing plant cells. *PLoS One* 4, e5744.
- Vos, J.W., Safadi, F., Reddy, A.S.N., and Hepler, P.K. (2000). The kinesin-like calmodulin binding protein is differentially involved in cell division. *Plant Cell* 12, 979-990.
- Wada, M. (2013). Chloroplast movement. *Plant Sci* 210, 177-182.
- Wang, W., Dang, R., Zhu, J.Q., and Yang, W.X. (2010). Identification and dynamic transcription of KIF3A homologue gene in spermiogenesis of *Octopus tankahkeei*. *Comp Biochem Physiol A Mol Integr Physiol* 157, 237-245.
- Weaver, B.A., Bonday, Z.Q., Putkey, F.R., Kops, G.J., Silk, A.D., and Cleveland, D.W. (2003). Centromere-associated protein-E is essential for the mammalian mitotic checkpoint to prevent aneuploidy due to single chromosome loss. *J Cell Biol* 162, 551-563.
- Whippo, C.W., Khurana, P., Davis, P.A., Deblasio, S.L., Desloover, D., Staiger, C.J., and Hangarter, R.P. (2011). THRUMIN1 is a light-regulated actin-bundling protein involved in chloroplast motility. *Curr Biol* 21, 59-64.
- Wickstead, B., and Gull, K. (2007). Dyneins across eukaryotes: a comparative genomic analysis. *Traffic* 8, 1708-1721.
- Xu, T., Qu, Z., Yang, X., Qin, X., Xiong, J., Wang, Y., Ren, D., and Liu, G. (2009). A cotton kinesin GhKCH2 interacts with both microtubules and microfilaments. *Biochem J* 421, 171-180.
- Xu, Y., Takeda, S., Nakata, T., Noda, Y., Tanaka, Y., and Hirokawa, N. (2002). Role of KIFC3 motor protein in Golgi positioning and integration. *J Cell Biol* 158, 293-303.
- Yamada, N., Suetsugu, N., Wada, M., and Kadota, A. (2007). Role of short chloroplast actin filaments in the chloroplast photorelocation movement of Arabidopsis. *Plant and Cell Physiology* 48, S55-S55.
- Yamashita, H., Sato, Y., Kanegae, T., Kagawa, T., Wada, M., and Kadota, A. (2011). Chloroplast actin filaments organize meshwork on the photorelocated chloroplasts in the moss *Physcomitrella patens*. *Planta* 233, 357-368.
- Yamazaki, H., Nakata, T., Okada, Y., and Hirokawa, N. (1995). Kif3a/B - a heterodimeric kinesin superfamily protein that works as a microtubule plus end-directed motor for membrane organelle transport. *J Cell Biol* 130, 1387-1399.
- Yang, G., Gao, P., Zhang, H., Huang, S., and Zheng, Z.L. (2007). A mutation in MRH2 kinesin enhances the root hair tip growth defect caused by constitutively activated

- ROP2 small GTPase in *Arabidopsis*. *PLoS One* 2, e1074.
- Yang, W.X., Jefferson, H., and Sperry, A.O. (2006). The molecular motor KIFC1 associates with a complex containing nucleoporin NUP62 that is regulated during development and by the small GTPase RAN. *Biol Reprod* 74, 684-690.
- Yang, W.X., and Sperry, A.O. (2003). C-terminal kinesin motor KIFC1 participates in acrosome biogenesis and vesicle transport. *Biol Reprod* 69, 1719-1729.
- Yang, X.Y., Chen, Z.W., Xu, T., Qu, Z., Pan, X.D., Qin, X.H., Ren, D.T., and Liu, G.Q. (2011). *Arabidopsis* kinesin KP1 specifically interacts with VDAC3, a mitochondrial protein, and regulates respiration during seed germination at low temperature. *Plant Cell* 23, 1093-1106.
- Yang, Z., Hanlon, D.W., Marszalek, J.R., and Goldstein, L.S. (1997). Identification, partial characterization, and genetic mapping of kinesin-like protein genes in mouse. *Genomics* 45, 123-131.
- Yokoyama, R., O'toole, E., Ghosh, S., and Mitchell, D.R. (2004). Regulation of flagellar dynein activity by a central pair kinesin. *Proc Natl Acad Sci U S A* 101, 17398-17403.
- Zhang, M., Zhang, B., Qian, Q., Yu, Y., Li, R., Zhang, J., Liu, X., Zeng, D., Li, J., and Zhou, Y. (2010). Brittle Culm 12, a dual-targeting kinesin-4 protein, controls cell-cycle progression and wall properties in rice. *Plant J* 63, 312-328.
- Zhong, R., Burk, D.H., Morrison, W.H., 3rd, and Ye, Z.H. (2002). A kinesin-like protein is essential for oriented deposition of cellulose microfibrils and cell wall strength. *Plant Cell* 14, 3101-3117.
- Zhu, C., and Dixit, R. (2011a). Functions of the *Arabidopsis* kinesin superfamily of microtubule-based motor proteins. *Protoplasma* DOI:10.1007/s00709-011-0343-9.
- Zhu, C., and Dixit, R. (2011b). Single molecule analysis of the *Arabidopsis* FRA1 kinesin shows that it is a functional motor protein with unusually high processivity. *Mol Plant* 4, 879-885.
- Zou, Y., Aggarwal, M., Zheng, W.G., Wu, H.M., and Cheung, A.Y. (2011). Receptor-like kinases as surface regulators for RAC/ROP-mediated pollen tube growth and interaction with the pistil. *Arabidopsis Plants* 2011, plr017.

Appendix

Appendix File 1

Note: Updated sequences for Pp-Kinesin09-b, Pp-Kinesin09-c and Pp-Kinesin14-Vb. The bold sequences indicate exons absent from the Phytozome database. These sequences were updated from the genomic sequence information available on JGI (www.jgi.doe.gov) by aligning representative kinesins from multiple species.

>Pp-Kinesin09-b_425498_Motor_Domain

SRIRVYLRLRPSVKPSPAINIESETHRVLIDVEKSIGGGPPKAYVNQIVFNVDNIVQTTNQQ
TMYELCAKASVDEFLKGYNSTIMSYGQVGAGKFTTMTGDMKVYVHRGIIPRAIQQIF
EEKEAKPEAGIVVHMSYMEIYQEGLYDLLQKRRDDLMIIEDNQLLNVRGLAKVRVETET
EALKWFQEGEKSRSGFNHFLNSLSSRSHTILTFYMERRVARVSTQLALQVAKLNLVDLA
GVERLKKTKGDTGSLMRKEACINNKTLFLEQTIFALRLKKAHIPFRHSKVTLLKESLG
NNHKTVMVCAWPEEYFLDETIGALRFAQRVKYLKIFQVTHKKPDCADTT

>Pp-Kinesin09-c_428375_Motor_Domain

MQLFVSSTKFSAMGAGFDSTIDIYLRVRPISSGAKAVLELNQEEGRVTWTIPRHVSLGLA
NHQREHFTFKFTGLFDMESKQDEVFQKVAHKVVIGSLDGYNGTIFAYGQTGSGKTYTIT
GGSERYVDRGIIPRTISLIFSEIAERSEYAYTLHFSYMEVYNETGYDLLNPDHETKALEDLP
KDFILANEPIIANYQFANAFRVATEEEALNLVFGDTNRIISSTPMNMASSRSHCIFTAHIL
ACKVGEETVRKSKLHLVDLAGSERVWKTGVDG**QILREAKYINLSLHYLEQ**VIVALQEK
FQGKMRTHIPYRNSMMSVLRDSIGGNCLTVMIAVTIAQDQLPETISTCRFAQRVAMIS
NQVTLNEEVDPNLLI

>Pp-Kinesin14-Vb_435597_Full_Length

MGDAKGVRNSWGGGLPSYRQFDADDEPRVREAPVYV**PQSPSLTGRVPQSPSLAGR**
VPQSPSLAGRRHSISAVQFPDTPKQKSLQSP**TFVSKVLKVKDRLSSAREECIELRQEA**
SDLQEYSNAKIERVTRYLGVLAEKARRLDEVALDSESRVTPLKKEKKKLFNELVSAKG
NVRVYCRARPQFEDEGPSSTTYPDFTLRLNSNVTAAPNKDFELDRIYGP**PHISQADIFQDL**
QPLVQSALDGFNV**SIFAYGQTGAGKFTTMEG**PSHDRGLYYRVLEELFDLVN**SEATPTSST**
SFFVTMFELYNEQVRDLLKAPDNRGASTVLFGE**PGRGVELVDERLDSPSGFARIFKFGKQ**
MRANVDGVK**FDRSSRSHLVVTIHIHSSDSL**TGEEHYSKLSMVDLAGSERLN**KAANGDR**
L**TESLHINKSLSALGDVLSALTTKKDYIPYDHSKL**TELLYDSLGGDSKAVLIANVN**PSNAE**
VQETIATLN**FASRARS**AEISLGNRDTIKKWRDMASEARKELYEKEKEATEALGEVMQLK
RAL**KESDDQCLLLFGEVQKAWKLASSLQADLT**SHESYINKLQLENDRLSEQSIRDKEQYT
NVLTQLTTFTTREEQYQS**QIKERSARNEALEVRVQVLEQQL**NEARVAAARTL**PARPDNS**
AELQRLREETENALDMNQKLEEELSKRDELIERLHQENEKLFERLTDRSM**TTISSPRVSST**
PKIPRAESRGMDDFNL**DGGFVSATAVPGSPDMR**SSSSMRESAGPPSSPGGSGALLKYGSG
ESVKSTPAGEYLTAALMDFNPAQ**YESDAAIADGANKLLMLVLA**AVIKAGASREHEMLA
EIQGA**VFGFLHKMENLLVMDTMLVSRVRILYIRSLLSRAPEL**QSLK**VPPVERFLEKAGSG**
SATGSGSGR**SSRNSSLGSSPQRSPAHRNKGADDY**GP**GFKVSLRQEKR**SKFSSLVSKLMGN
GDQDNGRPHVTEGKLKETTEE**ARAF**AIGNKGLASLFVHT**PAGELQRQIRG**WLAENFDL
SLTGEESIGGV**TSHLELLSTAILDGWMSG**LG**VPAQPSTDALGQLLSDY**TS**MVYTRQLQHL**
TDVAATLATEEAEDAAQ**VTKLRS**AL**ESVEHKRRK**VLMQ**MRTN**VALLSKDDATSP**TRSS**
SMDTEN**VRIASLMSLDDFFKQ**AEIYRDAP**HGTTTTVN**KKMTYL**RRLDALEERM**STLLSID
QPCANKC**IMDARKF**VESLEE**QQVVSGGRHSR**SRT**MDELDASGNIGQWDEAM**NNG**VESE**
VVQWSVLQ**FNNGSATPFVIKCGATS**NLELVVKAQAK**MQE**KNGKEIVAV**VPVPSVLDGL**
SVETIRQT**ISHLPESFLQLAMARTADG**TRARY**TRLYKTLAIR**VPGLKH**VVEE**EETS**MSK**

Appendix File 2

Pp-At Kin14-V Alignment

| | Section 1 | | | | | |
|------------------------|---------------------------------------|--------|---------------|-------------|--------------------|------------------------|
| | (1) 1 | 10 | 20 | 30 | 47 | |
| PpKin14Va_Phypa_437825 | (1) MGDAAE | RYW | GWGVPSYRE | GI | DEPSRREAPVFVPPSP | |
| PpKin14Vb_Phypa_435597 | (1) MGDAGV | RNSW | GGGLPSYRQFDAL | DEPRV | REAPVYVPPSPSLTGRVP | |
| AtKAC1_At5g10470.2 | (1) MADQSK | LRN | WNEVSGFE | PKSSNAS | ----- | |
| AtKAC2_At5g65460.1 | (1) MAFQKS | LRN | WNEVTGFE | ESKKS | SPS----- | |
| Consensus | (1) MADQKSLTNSWNWGVPSFR | | RKSDSEPS | REAPVFVPPSP | | |
| | Section 2 | | | | | |
| | (48) 48 | 60 | 70 | 80 | 94 | |
| PpKin14Va_Phypa_437825 | (41) --- | SRAGR | VHQSPSLA | GRRHS | MSAHYFDTPKQGPSQSP | SKALR |
| PpKin14Vb_Phypa_435597 | (48) QSP | SLAGRV | PQSPSLA | GRRHS | ISAVQFPDTPKQKSLQSP | TFVSKVLK |
| AtKAC1_At5g10470.2 | (29) --- | FAESTG | HRTTGPL | LRNSI | STPSP | LPKQ-----AIFSKVNG |
| AtKAC2_At5g65460.1 | (25) --- | SEEGV | HRTTSP | SM | LRYSI | PKNSLPHSS-----ELFSKVQS |
| Consensus | (48) SAEGRVHRSPSLALRRHSISAMSLPPTPKQ | | QSPSFV | SKVLK | | |
| | Section 3 | | | | | |
| | (95) 95 | 100 | 110 | 120 | 141 | |
| PpKin14Va_Phypa_437825 | (85) V | LRISRA | EECIE | LRQEAS | DLQEYSNAK | TERVTRYLGVLA |
| PpKin14Vb_Phypa_435597 | (95) V | KDRLSS | AREECIE | LRQEAS | DLQEYSNAK | TERVTRYLGVLA |
| AtKAC1_At5g10470.2 | (65) L | KEKVKL | AREFDY | LELRQEAT | DLQEYSNAK | TERVTRYLGVLA |
| AtKAC2_At5g65460.1 | (61) L | KDKVQL | AKDDYV | GLRQEAT | DLQEYSNAK | TERVTRYLGVLA |
| Consensus | (95) LKDKVSLAKEDYIELRQEASDLQEYSNAK | | TERVTRYLGVLA | EA | KAR | KL |
| | Section 4 | | | | | |
| | (142) 142 | 150 | 160 | 170 | 188 | |
| PpKin14Va_Phypa_437825 | (132) D | VALESE | SRV | IPLK | EKKKLFN | DLVSA |
| PpKin14Vb_Phypa_435597 | (142) D | VALDSE | SRVTPL | K | EKKKLFN | ELVSA |
| AtKAC1_At5g10470.2 | (112) D | FVLETE | ARISPL | IN | EKKKLFN | DLTAV |
| AtKAC2_At5g65460.1 | (108) D | YALETE | ARISPL | IN | EKKKLFN | DLTAV |
| Consensus | (142) DQVALESEARISPLKNEKKKLFNDLLSAK | | GNIKVFCRARP | Q | FEDE | GP |
| | Section 5 | | | | | |
| | (189) 189 | 200 | 210 | 220 | 235 | |
| PpKin14Va_Phypa_437825 | (179) S | FISYP | DDFTLR | IN | NS | TAPS-- |
| PpKin14Vb_Phypa_435597 | (189) S | STTYP | DDFTLR | IN | NS | TAAP-- |
| AtKAC1_At5g10470.2 | (159) S | VIEFP | GCTIC | VNTS | DDTL | SNPK |
| AtKAC2_At5g65460.1 | (155) S | VIEFP | NCTIR | VNTS | DDTL | SNPK |
| Consensus | (189) SIEFPDDFTIRVNSVDTLSNPKDFELDRYGP | | HISQADIF | SD | LQ | |
| | Section 6 | | | | | |
| | (236) 236 | 250 | N-1 | 260 | 282 | |
| PpKin14Va_Phypa_437825 | (224) P | LVQSAL | DGYNVSI | FAYGQ | AGSGKSY | TMEG |
| PpKin14Vb_Phypa_435597 | (234) P | LVQSAL | DGFNVSI | FAYGQ | TGAGK | ETMEG |
| AtKAC1_At5g10470.2 | (206) P | FVQSAL | DGSNVSI | L | FAYGQ | TNAGK |
| AtKAC2_At5g65460.1 | (202) P | FVQSAL | DGSNVSI | FAYGQ | TNAGK | TYTMEG |
| Consensus | (236) PLVQSALDGSNVSI | FAYGQ | TGAGK | TYTMEG | SSH | DRGLYRC |

Coiled coil (CC)

Motor head

| | Section 7 | | | | | | | | | | | | | | | | | | | | | | | | | | | | | | | | | | | | | | | | | | | | | | | |
|------------------------|------------|-----|-----|-----|-----|-----|-----|---|---|---|---|---|---|---|---|---|---|---|---|---|---|---|---|---|---|---|---|---|---|---|---|---|---|---|---|---|---|---|---|---|---|---|---|---|---|---|---|---|
| | (283) | 283 | 290 | 300 | 310 | 329 | | | | | | | | | | | | | | | | | | | | | | | | | | | | | | | | | | | | | | | | | | |
| PpKin14Va_Phypa_437825 | (271) | L | V | N | A | E | N | S | P | S | S | T | A | Y | V | T | M | F | E | L | H | N | E | Q | V | R | D | L | L | K | T | S | D | S | S | G | A | S | T | V | M | M | G | L | G | | | |
| PpKin14Vb_Phypa_435597 | (281) | L | V | N | S | E | A | T | P | T | S | S | T | S | F | F | V | T | M | F | E | L | N | E | Q | V | R | D | L | L | K | P | D | N | R | G | A | S | T | V | L | F | E | E | E | G | | |
| AtKAC1_At5g10470.2 | (253) | L | A | N | S | D | S | T | S | T | S | R | F | S | F | S | L | S | V | F | E | L | N | E | Q | V | R | D | L | L | E | F | R | C | S | N | - | F | P | N | I | N | M | D | L | H | E | |
| AtKAC2_At5g65460.1 | (249) | L | A | N | S | D | S | T | S | A | S | Q | F | S | F | S | V | S | V | F | E | L | N | E | Q | V | R | D | L | L | S | G | C | S | N | - | P | K | I | N | M | G | L | R | E | | | |
| Consensus | (283) | L | V | N | S | D | S | T | S | T | S | R | T | S | F | S | V | S | M | F | E | L | N | E | Q | V | R | D | L | L | S | A | S | Q | S | N | G | L | S | T | I | N | M | G | L | G | | |
| | Section 8 | | | | | | | | | | | | | | | | | | | | | | | | | | | | | | | | | | | | | | | | | | | | | | | |
| | (330) | 330 | 340 | 350 | 360 | 376 | | | | | | | | | | | | | | | | | | | | | | | | | | | | | | | | | | | | | | | | | | |
| PpKin14Va_Phypa_437825 | (318) | H | G | V | E | L | V | D | E | R | I | D | S | P | S | G | F | T | R | V | F | K | F | S | Q | M | R | R | A | N | V | D | G | V | K | S | D | R | S | N | R | S | H | L | V | V | I | |
| PpKin14Vb_Phypa_435597 | (328) | R | G | V | E | L | V | D | E | R | I | D | S | P | S | G | F | A | I | F | K | F | K | Q | M | R | R | A | N | V | D | G | V | K | F | D | R | S | S | R | S | H | L | V | V | I | | |
| AtKAC1_At5g10470.2 | (299) | S | V | I | E | L | G | Q | E | K | V | D | N | P | L | E | F | F | G | V | L | K | S | A | L | N | R | G | N | Y | K | - | - | - | - | S | K | F | N | V | T | H | L | I | V | S | I | |
| AtKAC2_At5g65460.1 | (295) | S | V | I | E | L | S | Q | E | K | V | D | N | P | S | E | F | M | R | V | L | N | S | A | F | Q | N | R | G | N | K | - | - | - | - | S | K | S | T | V | T | H | L | I | V | S | I | |
| Consensus | (330) | S | V | I | E | L | V | O | E | K | V | D | N | P | S | G | F | L | R | V | L | K | S | A | F | Q | N | R | A | N | V | K | G | V | K | S | K | N | V | S | H | L | I | V | S | I | | |
| | Section 9 | | | | | | | | | | | | | | | | | | | | | | | | | | | | | | | | | | | | | | | | | | | | | | | |
| | (377) | 377 | 390 | 400 | 410 | 423 | | | | | | | | | | | | | | | | | | | | | | | | | | | | | | | | | | | | | | | | | | |
| PpKin14Va_Phypa_437825 | (365) | H | I | Y | S | N | T | I | T | R | E | N | V | I | S | K | L | S | L | V | D | L | A | G | S | E | R | L | S | K | E | E | D | N | G | D | R | L | T | D | S | L | H | I | N | N | S | |
| PpKin14Vb_Phypa_435597 | (375) | H | I | Y | S | N | T | I | T | R | E | N | V | I | S | K | L | S | L | V | D | L | A | G | S | E | R | L | S | K | E | E | D | N | G | D | R | L | T | D | S | L | H | I | N | N | S | |
| AtKAC1_At5g10470.2 | (342) | H | I | Y | S | N | T | I | T | R | E | N | V | I | S | K | L | S | L | V | D | L | A | G | S | E | R | L | S | K | E | E | D | N | G | D | R | L | T | D | S | L | H | I | N | N | S | |
| AtKAC2_At5g65460.1 | (338) | H | I | Y | S | N | T | I | T | R | E | N | V | I | S | K | L | S | L | V | D | L | A | G | S | E | R | L | S | K | E | E | D | N | G | D | R | L | T | D | S | L | H | I | N | N | S | |
| Consensus | (377) | H | I | Y | S | N | T | I | T | R | E | N | V | I | S | K | L | S | L | V | D | L | A | G | S | E | R | L | S | K | E | E | D | N | G | D | R | L | T | D | S | L | H | I | N | N | S | |
| | Section 10 | | | | | | | | | | | | | | | | | | | | | | | | | | | | | | | | | | | | | | | | | | | | | | | |
| | (424) | 424 | 430 | 440 | 450 | 460 | 470 | | | | | | | | | | | | | | | | | | | | | | | | | | | | | | | | | | | | | | | | | |
| PpKin14Va_Phypa_437825 | (412) | L | S | A | L | G | D | V | L | S | A | L | T | S | K | K | D | Y | I | P | Y | D | N | S | K | L | R | L | L | A | D | S | L | G | G | S | S | K | L | M | I | V | N | I | C | P | | |
| PpKin14Vb_Phypa_435597 | (422) | L | S | A | L | G | D | V | L | S | A | L | T | S | K | K | D | Y | I | P | Y | D | N | S | K | L | R | L | L | A | D | S | L | G | G | S | S | K | L | M | I | V | N | I | C | P | | |
| AtKAC1_At5g10470.2 | (389) | L | S | A | L | G | D | V | L | S | A | L | T | S | K | K | D | Y | I | P | Y | D | N | S | K | L | R | L | L | A | D | S | L | G | G | S | S | K | L | M | I | V | N | I | C | P | | |
| AtKAC2_At5g65460.1 | (385) | L | S | A | L | G | D | V | L | S | A | L | T | S | K | K | D | Y | I | P | Y | D | N | S | K | L | R | L | L | A | D | S | L | G | G | S | S | K | L | M | I | V | N | I | C | P | | |
| Consensus | (424) | L | S | A | L | G | D | V | L | S | A | L | T | S | K | K | D | Y | I | P | Y | D | N | S | K | L | R | L | L | A | D | S | L | G | G | S | S | K | L | M | I | V | N | I | C | P | | |
| | Section 11 | | | | | | | | | | | | | | | | | | | | | | | | | | | | | | | | | | | | | | | | | | | | | | | |
| | (471) | 471 | 480 | 490 | 500 | 517 | | | | | | | | | | | | | | | | | | | | | | | | | | | | | | | | | | | | | | | | | | |
| PpKin14Va_Phypa_437825 | (459) | S | N | A | E | V | Q | E | T | I | A | T | L | N | F | A | R | A | R | N | T | V | P | S | L | G | N | R | D | I | K | K | W | R | D | V | A | S | D | A | R | K | E | L | Y | E | | |
| PpKin14Vb_Phypa_435597 | (469) | S | N | A | E | V | Q | E | T | I | A | T | L | N | F | A | R | A | R | N | T | V | P | S | L | G | N | R | D | I | K | K | W | R | D | V | A | S | D | A | R | K | E | L | Y | E | | |
| AtKAC1_At5g10470.2 | (436) | S | V | Q | T | L | S | E | T | I | A | T | L | N | F | A | A | R | A | R | N | T | V | P | S | L | G | N | R | D | I | K | K | W | R | D | V | A | S | D | A | R | K | E | L | Y | E | |
| AtKAC2_At5g65460.1 | (432) | S | A | R | N | L | S | E | T | I | A | T | L | N | F | A | A | R | A | R | N | T | V | P | S | L | G | N | R | D | I | K | K | W | R | D | V | A | S | D | A | R | K | E | L | Y | E | |
| Consensus | (471) | S | N | A | D | L | S | E | T | I | A | T | L | N | F | A | A | R | A | R | N | T | V | P | S | L | G | N | R | D | I | K | K | W | R | D | V | A | S | D | A | R | K | E | L | Y | E | |
| | Section 12 | | | | | | | | | | | | | | | | | | | | | | | | | | | | | | | | | | | | | | | | | | | | | | | |
| | (518) | 518 | 530 | 540 | 550 | 564 | | | | | | | | | | | | | | | | | | | | | | | | | | | | | | | | | | | | | | | | | | |
| PpKin14Va_Phypa_437825 | (506) | K | E | K | E | A | T | E | A | Q | G | E | V | M | Q | L | K | R | A | L | K | E | A | D | A | Q | C | L | L | L | F | D | E | V | Q | K | A | W | K | L | A | S | S | L | Q | A | D | L |
| PpKin14Vb_Phypa_435597 | (516) | K | E | K | E | A | T | E | A | Q | G | E | V | M | Q | L | K | R | A | L | K | E | S | D | T | Q | C | L | L | L | F | D | E | V | Q | K | A | W | K | L | A | S | S | L | Q | A | D | L |
| AtKAC1_At5g10470.2 | (483) | K | E | R | E | N | Q | N | L | K | Q | E | V | T | G | L | K | Q | A | L | K | E | A | N | D | Q | C | V | L | L | S | E | V | Q | R | A | W | K | V | S | F | T | L | Q | S | D | L | |
| AtKAC2_At5g65460.1 | (479) | K | E | R | E | N | Q | R | L | K | Q | E | V | T | G | L | K | Q | A | L | K | E | A | N | D | Q | C | V | L | L | S | E | V | Q | R | A | W | K | V | S | F | T | L | Q | S | D | L | |
| Consensus | (518) | K | E | K | E | N | T | E | L | K | Q | E | V | M | Q | L | K | R | A | L | K | E | A | N | D | Q | C | L | L | L | F | D | E | V | Q | K | A | W | K | L | A | S | S | L | Q | A | D | L |

Motor head

Coiled coil (CC)

| | | Section 13 | | | | | |
|------------------------|-------|-------------------------|-------------|-------------|-----------|----------------|-------------------|
| | (565) | 565 | 570 | 580 | 590 | 600 | 611 |
| PpKin14Va_Phypa_437825 | (553) | ESHESYINKLQVENHRLSEFKSR | QIQYAVM | QLSMF | ML | EEQYQS | |
| PpKin14Vb_Phypa_435597 | (563) | ESHESYINKLQLENDRLSEQSI | ROKEQYTNVLE | QLTTFT | TR | EEQYQS | |
| AtKAC1_At5g10470.2 | (530) | KS----- | ENIMLYDKHFL | KEQNSQL | NCIAQEL | LDQEQKI | |
| AtKAC2_At5g65460.1 | (526) | KS----- | ENAMVVDKHL | IKENFQ | LRNGLAQLL | LEEQEKI | |
| Consensus | (565) | TSHESYINKLQLEN | RLVDQHKR | DKEQYSQLR | TQIAQFTQ | REQQYQS | |
| | | Section 14 | | | | | |
| | (612) | 612 | 620 | 630 | 640 | 652 | |
| PpKin14Va_Phypa_437825 | (600) | QIKERGAR | EAL | LEVRVQVLEQQ | LHFA | RSAAASTLPAGQDN | ---LAEI |
| PpKin14Vb_Phypa_435597 | (610) | QIKERSAR | NEALE | LEVRVQVLEQQ | LNFA | RVAAARTLPARP | DN---SAEI |
| AtKAC1_At5g10470.2 | (567) | MQQQDSAL | QNLAK | TDLESQV | SEAV | RSAT | TRTGDAQSQDIFSEI |
| AtKAC2_At5g65460.1 | (563) | QAQQDST | IQNL | SKVKDLESQ | LSKAL | KSPM | TRSRPLP |
| Consensus | (612) | QIQORDAR | IQNLQV | KVQVLESQ | LSEARKAD | ATTLPDAL | DN API |
| | | Section 15 | | | | | |
| | (659) | 659 | 670 | 680 | 690 | 705 | |
| PpKin14Va_Phypa_437825 | (644) | QMLREETENAV | SLNQKLE | EELTKRDE | LIERLH | ENEKLF | FDRLTER |
| PpKin14Vb_Phypa_435597 | (654) | QLREETENAL | DMNQKLE | EELTKRDE | LIERLH | ENEKLF | FDRLTRSM |
| AtKAC1_At5g10470.2 | (614) | PFAVEGT | TDSSVT | KKLE | EELKKRD | ALIERLH | ENEKLF |
| AtKAC2_At5g65460.1 | (604) | PLAAENT | LDSAVT | KKLE | EELKKRD | ALIERLH | ENEKLF |
| Consensus | (659) | QRLREETENASSVT | QKLE | EELKKRDE | LIERLH | ENEKLF | FDRLTERSM |
| | | Section 16 | | | | | |
| | (706) | 706 | 720 | 730 | 740 | 752 | |
| PpKin14Va_Phypa_437825 | (691) | ILGS-PR | IVSPKI | PHLEQ | RAVD | DFNLDGS | TYSSTAPASFD |
| PpKin14Vb_Phypa_435597 | (701) | LTISSP | VSSTPKI | PRAES | RGMD | DFNLDG | GFVSATAVPGSPDMRSS |
| AtKAC1_At5g10470.2 | (661) | AVSTQV | LSPLRAS | PNIQ | PANV | NRGEGY | SAEVALPST |
| AtKAC2_At5g65460.1 | (651) | ASSTQV | SPSSKAS | PTVCP | ADV | VSAG | -----TLPSSVDKNE |
| Consensus | (706) | TTSSQVKSSSSPKSP | IQ | PRAVDS | FNLDGS | SATLPSS | PKDN SS |
| | | Section 17 | | | | | |
| | (753) | 753 | 760 | 770 | 780 | 799 | |
| PpKin14Va_Phypa_437825 | (737) | MKSSSV | QPPSSPR | GAV | ELLKYGS | DEQLKST | PAGEYLTAAL |
| PpKin14Vb_Phypa_435597 | (748) | SMRES | SAGPPSSPG | GGG | GALLKYGS | GSV | KSTPAGEYLTAAL |
| AtKAC1_At5g10470.2 | (705) | ----- | GAITL | VKSGT | -ELV | KTT | PAGEYLTAAL |
| AtKAC2_At5g65460.1 | (687) | ----- | GTLT | VKSSS | -ELV | KTT | PAGEYLTAAL |
| Consensus | (753) | S G | PSSP | GAITL | LKYGS | ELV | KSTPAGEYLTAAL |
| | | Section 18 | | | | | |
| | (800) | 800 | 810 | 820 | 830 | 846 | |
| PpKin14Va_Phypa_437825 | (784) | YESDA | AADI | AGANKLL | MVL | LAAVIK | KAGASREHE |
| PpKin14Vb_Phypa_435597 | (795) | YESDA | AADI | AGANKLL | MVL | LAAVIK | KAGASREHE |
| AtKAC1_At5g10470.2 | (738) | YEGLA | AADI | AGANKLL | MVL | LAAVIK | KAGASREHE |
| AtKAC2_At5g65460.1 | (720) | YEGLA | AADI | AGANKLL | MVL | LAAVIK | KAGASREHE |
| Consensus | (800) | YESLA | AADI | AGANKLL | MVL | LAAVIK | KAGASREHE |

Coiled coil (CC)

| | | Section 19 | | | | | | | | | | | | | | | | | | | | | | | | | | | | | |
|------------------------|--------|------------|-------------|----------|--------------|--------------|--------|---------|-----|------|--------|--------|-------------|----|-----|-----|---|---|---|---|---|---|---|---|---|---|---|---|---|---|---|
| | | 847 | 860 | 870 | 880 | 893 | | | | | | | | | | | | | | | | | | | | | | | | | |
| PpKin14Va_Phypa_437825 | (831) | LENRTAM | MDTMLVSRVRI | LYIRSLLS | SRAPELQSLKVP | PLVERFLEKAGS | | | | | | | | | | | | | | | | | | | | | | | | | |
| PpKin14Vb_Phypa_435597 | (842) | MENLLV | MDTMLVSRVRI | LYIRSLLS | SRAPELQSLKVP | PLVERFLEKAGS | | | | | | | | | | | | | | | | | | | | | | | | | |
| AtKAC1_At5g10470.2 | (785) | MEPRRV | MDTMLVSRVRI | LYIRSLLS | ARSPELQSLKVP | PLVERFLEKAGS | | | | | | | | | | | | | | | | | | | | | | | | | |
| AtKAC2_At5g65460.1 | (767) | MEPRRV | MDTMLVSRVRI | LYIRSLLS | ARSPELQSLKVP | PLVERFLEKAGS | | | | | | | | | | | | | | | | | | | | | | | | | |
| Consensus | (847) | MEPRRV | MDTMLVSRVRI | LYIRSLLS | ARSPELQSLKVP | PLVERFLEKAGS | | | | | | | | | | | | | | | | | | | | | | | | | |
| | | Section 20 | | | | | | | | | | | | | | | | | | | | | | | | | | | | | |
| | | 894 | 900 | 910 | 920 | 930 | 940 | | | | | | | | | | | | | | | | | | | | | | | | |
| PpKin14Va_Phypa_437825 | (878) | GFI | SG--- | RSSRNS | SLGSSP | QRSPN | SLK | DGYDYL | HGF | RVNL | RQEK | | | | | | | | | | | | | | | | | | | | |
| PpKin14Vb_Phypa_435597 | (889) | GSAT | GSGSG | RSSRNS | SLGSSP | QRSP | PAHRNK | GADDY | GP | GFKV | SLRQEK | | | | | | | | | | | | | | | | | | | | |
| AtKAC1_At5g10470.2 | (832) | GRSK | ----- | SRGSSP | GRSP | --- | VR | YLD | TQ | HGF | KVNL | RAEK | | | | | | | | | | | | | | | | | | | |
| AtKAC2_At5g65460.1 | (814) | GRTR | ----- | SRGSSP | GRSP | --- | VR | YDE | Q | HGF | KVNL | RAEK | | | | | | | | | | | | | | | | | | | |
| Consensus | (894) | GRSS | | RSSRNS | SLGSSP | QRSP | H | VKYADDY | I | HGF | KVNL | RQEK | | | | | | | | | | | | | | | | | | | |
| | | Section 21 | | | | | | | | | | | | | | | | | | | | | | | | | | | | | |
| | | 941 | 950 | 960 | 970 | 987 | | | | | | | | | | | | | | | | | | | | | | | | | |
| PpKin14Va_Phypa_437825 | (921) | RSKF | SSNF | FSKLRGN | -DQDS | SRQH | VSER | KLK | ET | SE | DARA | FAIGNK | SLA | | | | | | | | | | | | | | | | | | |
| PpKin14Vb_Phypa_435597 | (936) | RSKF | SSLV | SKLMGN | -DQDN | GRPH | VTEG | KLK | ET | TE | EARA | FAIGNK | SLA | | | | | | | | | | | | | | | | | | |
| AtKAC1_At5g10470.2 | (867) | RNKL | ASV | SRMRGL | -EQD | AGRQ | QVTG | VKLR | EM | Q | DEAK | FAIGNK | SLA | | | | | | | | | | | | | | | | | | |
| AtKAC2_At5g65460.1 | (849) | RSKL | LV | SVSRIRGH | -DQD | TRG | QVTG | GKLR | E | Q | DEAK | FAIGNK | SLA | | | | | | | | | | | | | | | | | | |
| Consensus | (941) | RSKLS | SVVSKLRGN | | DQDS | GRQ | QVTG | GKLR | ET | Q | DEAK | FAIGNK | SLA | | | | | | | | | | | | | | | | | | |
| | | Section 22 | | | | | | | | | | | | | | | | | | | | | | | | | | | | | |
| | | 988 | 1000 | 1010 | 1020 | 1034 | | | | | | | | | | | | | | | | | | | | | | | | | |
| PpKin14Va_Phypa_437825 | (967) | SLFV | HTPAGEL | RRQIR | GWLAEN | FD | FLS | LT | GG | E | TIS | GVSS | HLELLSTA | | | | | | | | | | | | | | | | | | |
| PpKin14Vb_Phypa_435597 | (983) | SLFV | HTPAGEL | RRQIR | GWLAEN | FD | FLS | LT | GG | E | SI | GGVT | HLELLSTA | | | | | | | | | | | | | | | | | | |
| AtKAC1_At5g10470.2 | (913) | ALFV | HTPAGEL | RRQIR | LWLAEN | FE | FLS | VT | SD | V | SGG | NGG | QLELLSTA | | | | | | | | | | | | | | | | | | |
| AtKAC2_At5g65460.1 | (895) | ALFV | HTPAGEL | RRQIR | SWLAEN | SE | FLS | VT | AD | D | V | SVT | TGQLELLSTA | | | | | | | | | | | | | | | | | | |
| Consensus | (988) | ALFV | HTPAGEL | RRQIR | GWLAEN | FD | FLS | LT | GG | D | V | SGG | VTSQLELLSTA | | | | | | | | | | | | | | | | | | |
| | | Section 23 | | | | | | | | | | | | | | | | | | | | | | | | | | | | | |
| | | 1035 | 1040 | 1050 | 1060 | 1070 | 1081 | | | | | | | | | | | | | | | | | | | | | | | | |
| PpKin14Va_Phypa_437825 | (1014) | ILDG | WMSGL | GVF | QYF | STD | ALG | QLLS | DY | T | M | YNR | QLQ | QD | VGA | ALA | | | | | | | | | | | | | | | |
| PpKin14Vb_Phypa_435597 | (1030) | ILDG | WMSGL | GVFA | QF | STD | ALG | QLLS | DY | T | S | M | Y | T | R | Q | H | L | D | V | A | A | T | L | | | | | | | |
| AtKAC1_At5g10470.2 | (960) | IMDG | WMA | GLGAA | VPH | TD | ALG | QLLS | EY | A | K | R | V | T | S | Q | M | Q | H | M | K | D | I | A | G | T | L | | | | |
| AtKAC2_At5g65460.1 | (942) | IMDG | WMA | GLGAA | VPH | TD | ALG | QLLS | EY | A | K | R | V | T | S | Q | M | Q | H | M | K | D | I | A | G | T | L | | | | |
| Consensus | (1035) | ILDG | WMA | GLGVP | VPP | STD | ALG | QLLS | DY | T | K | R | V | T | S | Q | M | Q | H | L | K | D | I | A | G | T | L | | | | |
| | | Section 24 | | | | | | | | | | | | | | | | | | | | | | | | | | | | | |
| | | 1082 | 1090 | 1100 | 1110 | 1128 | | | | | | | | | | | | | | | | | | | | | | | | | |
| PpKin14Va_Phypa_437825 | (1061) | AEEA | EDAG | QVTK | LRSA | LES | V | D | H | K | R | K | V | L | Q | M | F | S | N | A | A | L | L | T | L | E | D | G | S | S | P |
| PpKin14Vb_Phypa_435597 | (1077) | TEEA | EDAG | QVTK | LRSA | LES | V | D | H | K | R | K | V | L | Q | M | F | S | N | A | A | L | L | T | L | E | D | G | S | S | P |
| AtKAC1_At5g10470.2 | (1007) | AEEA | EDAG | QVTK | LRSA | LES | V | D | H | K | R | K | V | L | Q | M | F | S | N | A | A | L | L | T | L | E | D | G | S | S | P |
| AtKAC2_At5g65460.1 | (989) | SEEA | EDAG | QVTK | LRSA | LES | V | D | H | K | R | K | V | L | Q | M | F | S | N | A | A | L | L | T | L | E | D | G | S | S | P |
| Consensus | (1082) | AEEA | EDAG | QVTK | LRSA | LES | V | D | H | K | R | K | V | L | Q | M | F | S | N | A | A | L | L | T | L | E | D | G | S | S | P |

Coiled coil (CC)

Section 25

(1129) 1129 1140 1150 1160 1175

PpKin14Va_Phypa_437825 (1108) RNP FMDAMNARVASTSLEDYKQAGEPRKDAPEGRSTANKKLSYLK

PpKin14Vb_Phypa_435597 (1124) RSSMTEVRIASLMSLDDFFKQAEELYRDAPHGTTVNNKMTYLR

AtKAC1_At5g10470.2 (1054) PNPSTAAEDSRILASLISLDGILKQVKELTRQASVHVLSSKSKKALLE

AtKAC2_At5g65460.1 (1036) QNPSTAAEDSRILASLISLDAILKQVKELTRQASVHVLSSKSKKALLE

Consensus (1129) RNPSTDAENSRLASLISLDDILKQVKELTRQASVHVLSSKSKKAYLE

Section 26

(1176) 1176 1190 1200 1210 1222

PpKin14Va_Phypa_437825 (1155) HLDALFERMSTLLSIDYPCAQRCTDARRFVELLVHQLVETIPEQEDTN-----

PpKin14Vb_Phypa_435597 (1171) RLDALFERMSTLLSIDYPCAQRCTMDARKFVESLEQQVVSQGRHSR

AtKAC1_At5g10470.2 (1101) SLDELTERMPSLLDIDYPCAQRREIATAHQDLVETIPEQEDTN-----

AtKAC2_At5g65460.1 (1083) SLDELNERMPSLLDIDYPCAQRREIATAHQDLVETIPEQEDTN-----

Consensus (1176) SLDELEERMSSLLSIDHPCAQRREI TARQLVETIPEQQDV G RHSR

Section 27

(1223) 1223 1230 1240 1250 1269

PpKin14Va_Phypa_437825 (1202) SRTL DGVNRSLEFVHLDERMNNRVESEVIQWSVLQFNNG-SATPFVI

PpKin14Vb_Phypa_435597 (1218) SRTLDELDAEGNIGQWDEAMNNGVESEVVQWSVLQFNNG-SATPFVI

AtKAC1_At5g10470.2 (1142) -----LLEQLHRRRFSLESISGETDVSQWNVLQFNNTG-SAPFFII

AtKAC2_At5g65460.1 (1123) -----IQLEKRPSIDSISATELDVQWNVLQFNNTGSSAPFFII

Consensus (1223) SRTL D I SADDKRPSEDSNSSVESDVSQWSVLQFNNTG SATPFII

Section 28

(1270) 1270 1280 1290 1300 1316

PpKin14Va_Phypa_437825 (1248) KCGATSNLELVVKAQAKMQEKTKKEIIVAVVPVPSALAGLSISGIAQT

PpKin14Vb_Phypa_435597 (1264) KCGATSNLELVVKAQAKMQEKTKKEIIVAVVPVPSVLDGLSVEITRQT

AtKAC1_At5g10470.2 (1182) KCGENNSSELVVKADARVQEPKGGIIVVVPVPSVLDNMSISEMKQM

AtKAC2_At5g65460.1 (1161) KCGATSNSELVVKADARVQEPKGGIIVVVPVPSVLDNMSISEMKQV

Consensus (1270) KCGATSNSELVKAQAKMQEPKKEIIVRVPVPSVLDNLSLEEIKQT

Section 29

(1317) 1317 1330 1340 1350 1363

PpKin14Va_Phypa_437825 (1295) ISHLPESEFYQLAMARTADGTRARYTRLYKTLAIRVPSLKHVLESEEE

PpKin14Vb_Phypa_435597 (1311) ISHLPESEFLQLAMARTADGTRARYTRLYKTLAIRVPSGLKHVVEELEEE

AtKAC1_At5g10470.2 (1229) FVQLPEALSLLALARTADGTRARYSRLYKTLAMKVPVSLKDLVSELE-

AtKAC2_At5g65460.1 (1208) FVQLPEALSLLALARTADGTRARYSRLYKTLAMKVPVSLKDLVGELEK

Consensus (1317) ISQLPEALSQLALARTADGTRARYSRLYKTLAIKVPVSLKHLVVEELEEE

Section 30

(1364) 1364 1373

PpKin14Va_Phypa_437825 (1342) SALR-----

PpKin14Vb_Phypa_435597 (1358) TSMSE-----

AtKAC1_At5g10470.2 (1275) -----

AtKAC2_At5g65460.1 (1255) GGLKDTKST

Consensus (1364) SAL K